

RICE UNIVERSITY

**Mitral Valve Organ Culture Provides a Novel Experimental
Paradigm**

by
Nikhil Gheewala

A THESIS SUBMITTED
IN PARTIAL FULFILLMENT OF THE
REQUIREMENTS FOR THE DEGREE

Doctor of Philosophy

APPROVED, THESIS COMMITTEE:



K. Jane Grande-Allen, Chair,
Associate Professor
Bioengineering



Jun Lou
Assistant Professor
Mechanical Engineering and
Materials Science



Antonios G. Mikos
Louis Calder Professor
Bioengineering



Jennifer West
Isabel C. Cameron Professor
Bioengineering

Houston, TX
May, 2011

ABSTRACT

Mitral Valve Organ Culture Provides a Novel Experimental Paradigm

by

Nikhil Gheewala

Mitral valve diseases and disorders affect tens of thousands of Americans each year, but understanding of the disease processes has yet to be fully developed. The behavior and characteristics of valve cells and tissue are highly dependent on their surrounding environment, including neighboring cells, extracellular matrix composition and 3D structure, mechanical forces, and signaling molecules both in the tissue and the circulation. In order to study native valve behavior and responses, an *ex vivo* bioreactor system was developed to culture whole mitral valves. The organ culture system simulated a physiologically relevant mechanical environment and provided nutrients and gas exchange. Valves cultured in this dynamic system retained more native cell and tissue characteristics than valves cultured in a static environment. To utilize this novel tool, a study was conducted to determine the effects of Angiotensin II on mitral valves, alone and in combination with the statin drug, Simvastatin. Angiotensin II was found to alter the native valve composition. Simvastatin inhibited some of these alterations, but accentuated others and also affected separate valve characteristics. In conclusion, an organ culture system for mitral valves has been designed, characterized, validated, and effectively put to use in a novel study.

ACKNOWLEDGMENTS

This dissertation is a culmination of several years of work and is a work of great pride for myself. I cannot fathom how I could have gotten to this point without the encouragement of my family and friends, of whom the most significant is my wife, Tanvi. Your love and support helped keep me working through to the end.

Dr. Jane Grande-Allen deserves my very sincere thanks for her guidance and mentorship. Jane is truly dedicated to the education and development of all of her students. Under her guidance, I have learned much and matured as a researcher during the last six years. I must also recognize the assistance from our entire lab group, particularly my fellow grad students and the talented students I have been lucky to mentor.

I would also like to express that Rice University has a wonderful community of faculty, staff, and students that I have greatly enjoyed being a part of.

TABLE OF CONTENTS

Abstract	ii
Acknowledgments	iii
Table of Contents	iv
List of Figures	vii
List of Tables	ix
Chapter 1 Dissertation Overview	1
Chapter 2 Background	3
Gross Anatomy	3
Tissue Structure	5
Valvular Cells	6
Mechanical Signaling	7
Methods of Studying Valve Biology	11
Prior and Current Relevant Work	13
Chapter 3 Design and Mechanical Evaluation of a Physiological Mitral Valve Organ Culture System	17
Introduction.....	17
Methods	17
Design Criteria	17
Design Overview	19
Flow Control and Measurement.....	21
Flow Loop Components.....	22
Results.....	26
Mechanical Evaluation.....	26
Sterility.....	30
Discussion.....	31
Chapter 4 Organ Culture of Mitral Valves as a Novel Experimental Paradigm	33
Introduction.....	33
Materials & Methods	34
Organ Culture System.....	34
Harvest, Preparation, and Culture of Valves.....	34

Biochemical Analyses.....	37
Materials Testing	38
Histological Staining.....	40
Statistical Analysis.....	44
Results.....	45
Flow Through the Mitral Valve	45
Macroscale Anatomy	46
Biochemical Assays	46
Materials Testing	48
Histology and Immunohistochemistry.....	50
Discussion.....	63
Chapter 5 Simvastatin Inhibits Angiotensin-II Induced Mitral Valve Remodeling in an <i>Ex Vivo</i> Organ Culture Model.....	68
Introduction.....	68
Background.....	68
Materials and Methods.....	70
Organ Culture System.....	70
Harvest, Preparation, and Culture of Valves.....	71
Biochemical Analyses.....	72
Materials Testing	72
Histological and Immunohistochemical Staining	73
Statistical Analysis.....	76
Results.....	77
Flow Measurements	77
Macroscale Anatomy	79
Biochemical Analyses.....	79
Materials Testing	81
Histology and Immunohistochemistry.....	83
Discussion.....	90
Chapter 6 Conclusions, Discussion, and Future Directions.....	94
Aim 1 Conclusions.....	94
Aim 2 Conclusions.....	95
Aim 3 Conclusions.....	96

Impact/Importance of Work as a Whole.....	96
Limitations	97
Wide Scope of Possible Future Research	100
Conclusion	101
Appendix A Design Process	102
Functions, Objectives, Constraints	102
Major Design Elements	103
Pumping mechanism	103
Ventricular Chamber.....	105
Chordal Anchoring.....	107
Appendix B Flow Loop Operating Manual.....	109
Preparatory Steps	109
Two days prior to harvest and start of culture:	109
One day prior to harvest and start of culture:.....	110
Pre-Dissection	111
Heart Dissection.....	112
Suturing.....	113
Assembly	115
Filling.....	117
Putting the System in the Incubator, Connecting Cables, and Starting it up.....	118
Operation	119
Medium Exchange	119
Draining the System.....	120
Refilling and Restarting	120
Stopping and Disassembly.....	121
Stopping the system:	121
Disassembly	121
Valve Dissection	122
Clean-Up.....	124
References.....	125

LIST OF FIGURES

Figure 2.1. Top view of a mitral valve during systole and diastole.	4
Figure 2.2. Layered structure of the mitral valve leaflets	5
Figure 3.1. Pumping schematic	20
Figure 3.2. Ventricular Chamber.....	23
Figure 3.3. Outflow port with mechanical aortic valve.....	24
Figure 3.4. Mitral Valve Attachment.....	25
Figure 3.5. Flow Waveforms.....	27
Figure 3.6. Average flow rate vs. control signal peak pressure in organ culture system	28
Figure 3.7. Flow waveforms produced from a physiologic pressure control signal.....	29
Figure 4.1. Static culture environment	36
Figure 4.2. Mitral valve sections	37
Figure 4.3. Material testing data analysis.....	39
Figure 4.4. A typical radially oriented section of the mitral valve	42
Figure 4.5. Picosirius Red Grading	43
Figure 4.6. Average flow characteristics through the mitral valve	45
Figure 4.7. Tissue hydration by weight.....	47
Figure 4.8. DNA measurement by tissue weight	47
Figure 4.9. Collagen concentration by weight.....	47
Figure 4.10. GAG concentration by weight.....	47
Figure 4.11. Tensile elastic moduli.....	49
Figure 4.12. Extensibility among all sections and treatment groups.	49
Figure 4.13. Delineation grading of Movat stained tissue sections.....	51
Figure 4.14. Movat stained AC tissue sections	51
Figure 4.15. Collagen intensity grading of Movat stained tissue sections.....	52
Figure 4.16. GAG intensity grading of Movat stained tissue sections.....	52

Figure 4.17. Picrosirius Red staining results.....	54
Figure 4.18. CD-31 staining by IHC	55
Figure 4.19. Hematoxylin staining intensity.....	56
Figure 4.20. PCNA staining intensity by IHC.....	56
Figure 4.21. Caspase 3 staining intensity by IHC.....	57
Figure 4.22. Smooth Muscle α -Actin staining intensity by IHC.....	57
Figure 4.23. Prolyl-4-Hydroxylase staining intensity by IHC	59
Figure 4.24. Decorin staining intensity by IHC	60
Figure 4.25. Versican staining intensity by IHC.....	61
Figure 4.26. Hyaluronan staining intensity by histochemistry	62
Figure 5.1. Flow Characteristics	78
Figure 5.2. Biochemical Assay Results.....	80
Figure 5.3. Tensile modulus measurements	82
Figure 5.4. Extensibility across experimental groups.....	82
Figure 5.5. Movat Grading Results.....	83
Figure 5.6 Picrosirius Red staining results.....	85
Figure 5.7. Collagen III IHC staining intensity	87
Figure 5.8. IHC staining of Angiotensin II Receptor I and TGF- β	87
Figure 5.9. Hyaluronan Staining Intensity	88
Figure 5.10. IHC Versican Staining Intensity	89
Figure 5.11. Hematoxylin staining intensity across experimental groups	89
Figure 6.1. First iteration of A) Complete ventricular chamber assembly, B) Ventricular chamber only, and C) Mitral valve holder.	106
Figure 6.2. Early implementation of chordal anchoring	108

LIST OF TABLES

Table 4.1. Materials Testing Regimens.....	39
Table 4.2. Immunohistochemistry Markers.....	42
Table 4.3. Thickness (mm) of Valve Sections in Different Groups.	46
Table 5.1. Immunohistochemistry Markers.....	74
Table 5.2. Thickness (mm) of Valve Sections in Different Groups.	79
Table 5.3. ECM Composition and DNA Content by Treatment Group	81

Chapter 1 DISSERTATION OVERVIEW

Mitral valve diseases are responsible for over 40,000 hospitalizations each year in just the United States. Treatment options are almost entirely surgical, and the disease progression often involves a deterioration of broader cardiovascular health. Most studies of valve biology and pathogenesis are conducted *in vitro*, but these conditions are unnatural and strongly influence the behavior of cultured valve cells

This dissertation is centered on the hypothesis that a physiological mechanical environment will help maintain the native characteristics of mitral valves in organ culture and serve as a novel experimental paradigm. Such a system offers a new model to study heart valve biology by observing the behavior of the entire tissue structure. Studying the mitral valve at the organ level will lead to a better understanding of various valvular disorders, especially when accompanied by an altered mechanical environment, such as in heart failure. An *ex vivo* organ culture bioreactor that can mimic the mitral valve's mechanical environment was developed; this document describes its purpose, design, characterization, and use and discusses the implications of the results.

The research project was organized into the following three Aims:

1. Design and mechanically characterize a mitral valve organ culture system capable of reproducing the valve's physiologic mechanical environment.
2. Further develop the organ culture system to integrate a porcine mitral valve in a sterile environment with adequate oxygen and nutrients. Evaluate the cultured valves to determine the effect of the dynamic mechanical environment.

3. Employ the organ culture system to study the *ex vivo* effects of Angiotensin II, alone and in combination with Simvastatin, on mitral valve tissue.

Chapter 2 describes further details about the motivation for this research, basic biology of mitral valves, and the concept of mechanotransduction, in which mechanical strains lead to biochemical responses. The chapter also summarizes prior literature that has led to the current work. The following three chapters will each describe the methods, results, and conclusions of the three research Aims. The chapter on Aim 1 focuses on the mechanical aspects of the organ culture system, whereas the chapter on Aim 2 focuses on its biological aspects. Aim 3 is distinct from the previous aims in that it does not address the development of the organ culture system, but rather utilizes it as a novel experimental model. An explanation of the specific study and its background will be reserved for the beginning of that chapter. The final chapter discusses the implications of the entire body of research. Additionally, appendices have been included to document the design process of the organ culture system and its detailed experimental protocol.

Chapter 2 BACKGROUND

The ability of the mammalian heart to provide blood flow throughout the circulatory system depends greatly on its four valves. Without the unidirectional flow created by the tricuspid, pulmonic, mitral, and aortic valves, the heart would be profoundly inefficient. Because of this important role, it is of concern whenever any of the valves becomes dysfunctional; in the United States valve disease caused over 21,000 deaths in 2009 and contributed to an additional 22,000 deaths (1).

All but a hundred of these deaths involved valves of the left heart. The left side of the heart powers the systemic circulation and is stronger than the right side, creating much higher pressure differentials across the left side valves, the aortic valve and the mitral valve. Disorders are found more often in these valves and have more deleterious effects. Aortic valves were found to be sclerotic or stenotic in 30% of women and men above 65 years-old; these conditions indicate a 50% greater risk of cardiovascular-related death (2, 3). Mitral valve prolapse was found in over 2% of middle-aged study subjects (3) and results in minor regurgitation. The causes of these disorders are unclear. Current treatments for severe mitral valve prolapse include valve repair or a complete valve replacement, both involving open-heart surgery. A better understanding of mitral valve physiology and pathogenesis can lead to improved options for treatment, early diagnosis, and prevention of valve diseases.

Gross Anatomy

The mitral valve controls flow between the left atrium and ventricle. The mitral valve's complex structure begins at the atrioventricular junction with the roughly 'D'-shaped

annulus and extends inwards, forming the leaflets and commissures. The anterior and posterior leaflets comprise the majority of the valve, while the commissures are relatively small and less important to proper valve function. Extending from the ventricular surface of the leaflets and commissures are the chordae tendineae, which are anchored by the papillary muscles in the ventricular wall.

The normal physiological behavior of the mitral valve is demonstrated in Figure 2.1. During diastole the chordae are relaxed and the leaflets are pressed against the ventricular wall as blood flows into the ventricle. As the ventricle contracts during systole, blood is pushed towards the atrium. The leaflets fill with blood, billow into the atrium, and press against each other to block the passageway into the atrium. The commissures participate similarly, but to a smaller extent because of their size. The papillary muscles contract synchronously, pulling the chordae taut and preventing the leaflets from prolapsing into the atrium. During each cardiac cycle, various regions of the mitral valve experience large cyclic strains, both in compression (-0.51 m/m) and in tension (0.25 m/m) (4, 5).

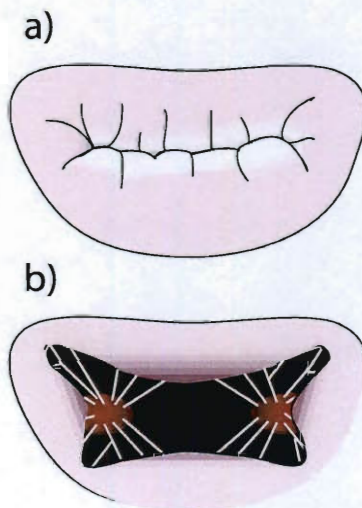


Figure 2.1. A) Top view of a mitral valve during systole, with the leaflets coapting to prevent regurgitant flow. B) Top view of a mitral valve during diastole, where the valve leaflets move aside to allow blood to fill the ventricle. The chordae tendineae and papillary muscles, which contract during systole to hold back the valve leaflets and prevent prolapse, are seen beyond.

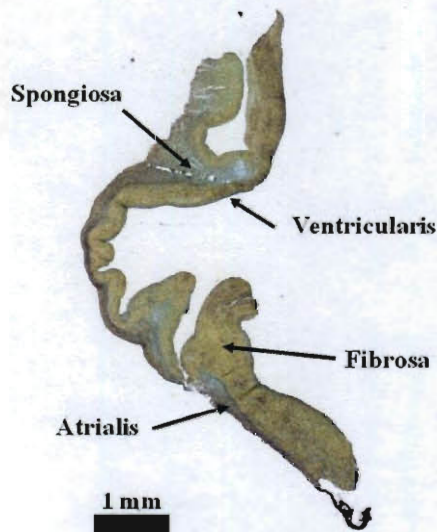


Figure 2.2. Layered structure of the mitral valve leaflets. The left atrium is at the left side of the image and the left ventricle is to the right. Yellow saffron staining indicates collagen, blue staining indicates proteoglycans (PGs), and black indicates elastin or cell nuclei.

Tissue Structure

A healthy mitral valve exhibits a laminar structure made up of the atrialis, spongiosa, fibrosa, and ventricularis layers (6-9). While the transitions between these layers are continuous, they are clearly distinguished from one another when tissue sections are stained for extracellular matrix (ECM) components (Figure 2.2). These layers are similar between the leaflets and vary in thickness, most notably radially from the annulus to the end of the leaflets, known as the free edge. On the atrial surface is the atrialis, a layer of mostly randomly oriented elastic fibers. The atrialis is thin at the annulus and disappears towards the valve free edge. Below the atrialis is the proteoglycan (PG)-rich spongiosa, which conversely dominates the valve free edge but shrinks as it approaches the annulus. The fibrosa is composed mainly of radially aligned collagen fibers. It is thick at the annulus and thins toward the free edge. The final layer is the ventricularis, at the ventricular surface. The ventricularis is composed of randomly oriented elastic fibers, similar to the atrialis, but is even thinner.

Because the layers vary in ECM composition, regions of the valve leaflets exhibit varying local ECM compositions depending on the relative contribution of each layer. For example, the fibrosa-dominated annulus is represented by a large proportion of collagen, some elastin, and little PGs. The chordae tendineae consist of a collagen core surrounded by an elastic fiber sheath. The core and sheath extend from and are continuous with the fibrosa and ventricularis, respectively.

Following the idiom that "Form Follows Function" (Davis' Law) in soft tissues, one can compare the regional ECM composition with corresponding regional mechanical loading characteristics. The valve undergoes the most significant strains during systole, so those characteristics will be discussed. As explained above, during this phase the leaflet free edges press against each other to form a seal. This pressing together involves a significant level of transvalvular compressive stress (4, 5). So, it is not surprising that the free edge has a thickened spongiosa, filled with high compressive modulus PGs. Likewise, the chordae and the central and annular leaflet regions experience high radial and circumferential tensile strains (4, 5), and have a higher concentration of collagen aligned in the direction of these strains (7).

Valvular Cells

Valvular endothelial cells (VECs) of the mitral valve are part of the endothelial cell monolayer that coats the entire inner surface of the cardiovascular system. The valvular and vascular endothelial cells are very similar, but are known to be morphologically distinct (10-13). The VECs appear in a layer of polygonal or elongated cells aligned circumferentially on the leaflets and along the length of the chordae tendineae. VECs are

believed to function both to produce ECM components and hormones and also to regulate inflammatory responses, reacting to various agents found in the circulation.

Valvular interstitial cells (VICs) are found throughout all layers of the valve tissue (14-18). They are found in up to five sub-populations including both a quiescent, fibroblast-type morphology and an activated, myofibroblast-type morphology. VICs are responsible for the regular ongoing maintenance and remodeling of valvular tissues, as well as remodeling in response to changes in environment. They are known to produce collagen and PGs, as well as molecules that regulate ECM. Various signals are known to modulate these functions, including norepinephrine, paracrine signals from VECs, and mechanical stresses (17-25).

VECs and VICs are often studied separately, however this method does not allow for the normal signaling between the two cell types. In a layered hydrogel co-culture under shear flow, seeding VECs atop VICs was found to encourage more physiological VIC behavior (25). These cells showed a more native phenotype; they had decreased proliferation, increased protein synthesis and a reduced loss of GAGs when compared to those cultured without a layer of endothelial cells. Attempts to recreate physiological behavior in these cells necessitates cell signaling between both VECs and VICs.

Mechanical Signaling

Heart valves, like many other tissues in the body, react to their mechanical environment not only through deformation, but also through cellular stimulation. The compressive, tensile, and shear stresses in the tissue are transferred to VECs and VICs via the ECM and can provoke responses ranging from ECM remodeling to phenotypic modulation.

This type of mechanical-to-biochemical signaling is known as mechanotransduction. Integrins, transmembrane proteins that connect an individual cell's cytoskeleton to adjacent ECM molecules, convey the strains of the surrounding tissue to the cell. Within the cell, these integrins bind to anchor proteins, which attach to cytoskeletal actin or intermediate filaments and interact with Focal Adhesion Kinase (FAK) molecules (26) to transduce the mechanical signal into a biochemical one.

As explained above, each region of the the mitral valve experiences dynamic mechanical conditions throughout the cardiac cycle; these strains are transferred to the cells and have been shown to be important in modulating cellular behavior and synthesis of ECM components (22, 27, 28). Dynamic strains can also lead to changes in valvular cellular function (23, 29, 30). Our research group has previously demonstrated the increased synthesis, but reduced retention, of various classes of PGs (23, 29, 30) in cyclically stretched VICs seeded in collagen gels. Cyclic tensile strains have been linked to increased collagen production in VICs (23). VICs from porcine aortic valves were seeded onto flexible collagen-coated plates and subjected to cyclic strains of 10%, 14%, and 20% tension. The cells stretched at 14% showed both an increased uptake of hydroxyproline, a collagen component, as well as an increase in collagen III mRNA expression, though without increase in collagen I expression. Mesenchymal stem cells treated identically also showed increases in hydroxyproline uptake and in mRNA expression for both collagen types I and III. Other studies corroborate this effect of mechanical strains on valve cells (28, 31).

Valves also experience shear strains associated with blood flow through the valve and along valve leaflets and chordae. While the interstitial cells do not directly experience

shear flow, the VECs are affected and communicate to them through cell-ECM-cell mechanical connections, cytokines, ECM production and growth factor secretion (10), resulting in modulation of VIC behavior (25). Like normal strains, physiological levels of dynamic shear strain are believed to contribute to normal maintenance of cell functions and tissue structure (13). Porcine aortic valve leaflets exposed to various levels of shear stress up to 22 dyne/cm² reversed increases in synthesis of proteins, GAGs, and DNA that appeared in static controls, indicating that valve cells cultured without shear stress would overproduce these ECM components and over-proliferate (27). Shear strains can also lead to types of pathologic remodeling, such as the development of calcific aortic stenosis (32). Two groups of human VECs were exposed to shear stresses modeled to mimic the stresses experienced on the ventricular and aortic surfaces of the aortic valve. The cells exposed to ventricular shear stresses expressed genes linked to the inhibition of inflammation. This finding potentially explains the development of calcific plaques on the aortic side of aortic valve leaflets and not the ventricular side. It also demonstrates that the magnitude of shear stresses is an important factor in mechanotransduction. Shear stresses are also observed to cause valvular ECs to align perpendicular to the direction of flow, unlike vascular ECs, which align parallel to shear flows (12). These two cell types share many similarities, but this observation underscores the need to understand valvular cells as distinct cell types.

Hydrostatic pressure can also cause mechanotransductive effects in heart valves.

Increases in synthesis of collagen and sulfated GAGs were seen with increases in the magnitude of cyclic hydrostatic pressure applied to excised porcine aortic leaflets (33).

When the frequency of this cyclic pressure was increased above 72 beats per minute

(bpm), DNA synthesis increased, suggesting increased cell proliferation. Similar results were exhibited by porcine pulmonary valve leaflets: cyclic hydrostatic pressures of 100 mmHg induced increases in collagen and sulfated GAG content compared to static groups and leaflets subjected to only 30 mmHg. However, the cyclic pressure alone did not preserve the native valve phenotype.

In addition to mechanotransductive effects, mechanical stimulation influences tissues in other ways. Cell-seeded aortic valve tissue engineering scaffolds subjected to dynamic flexure demonstrated increased stiffness and increased cellularity through the middle of the scaffold (34). The investigators noted that this dynamic motion increased fluid perfusion through the scaffold. With increased perfusion, gases and nutrients were constantly being distributed throughout the scaffold. The non-vascular valve leaflet likely relies on its constant motion to infuse its tissue with fresh nutrients carried in the surrounding blood. Additional studies strongly suggest that multiple modes of mechanical stimulation are required to maintain the ECM integrity and structure and cellular behavior in engineered valve constructs (35, 36). Aortic valve leaflets that were cultured *ex vivo* under static mechanical conditions show reduced cell viability and tissue degradation compared to those subjected to organ culture (37). While a lack of dynamic stimulation is not the only non-physiologic aspect of this scenario, it surely makes a significant contribution to these non-native characteristics. The importance of mechanical stimulation plays a large role in the development of the paradigm of organ-level valve culture.

Methods of Studying Valve Biology

Cell culture is widely used as a powerful tool to study cellular behavior and responses to stimuli in a easily controlled and reproducible environment. By isolating cells from the ECM and plating them onto a standard substrate, cellular responses to specific stimuli can be examined, free from distortion caused by variations in the ECM. Cell culture is limited, however, because it does not accurately simulate the cells' natural environment and consequently cannot accurately recreate their natural behaviors. This is certainly the case for the study of valve cells, which quickly undergo phenotypic modulation away from their native state (38). As just discussed in the previous section on heart valve biology, a variety of external stimuli influence the behavior and responses of valve cells. The two cell types, VICs and VECs, interact with each other through molecular and mechanical signals. They also remodel the ECM composition and structure of the valve tissue through synthesis and degradation. and conversely vary their behavior with changes in this ECM environment. The macroscopic mechanical stresses and strains of diastole and systole also affect cell phenotype and proliferation, ECM composition, valvular structure and more; reciprocally, the valve's structure and composition can enhance or inhibit its intended control of blood flow. The ubiquitous presence of circulating molecular signaling agents adds to this mix of complex interactions influencing and modulating valve cell behaviors in a manner that cannot be examined through cell culture.

The use of animal models successfully overcomes these drawbacks of cell culture studies. Animal models go beyond simulating the mitral valve's natural architecture and environment by retaining the valve within its original source. Aside from clinical trials,

animals provide the only current paradigm capable of such an holistic analysis and include many distal factors which may influence valve behavior more subtly, such as circulating cells and hormones. These studies, however, provide very little opportunity to control variations between individual animals, especially for larger mammals which have not been bred into standardized lines. It is also difficult to precisely control important parameters, such as blood pressure, heart rate, blood chemistry, renal influences. Animal studies can be laborious because of the supervision and conscientious care of the animals required, as well as the expertise needed to subject an animal to any experimental treatment. Heart valve models often involve large mammals, such as pigs and cows, which entail larger costs. Studies in smaller mammals are difficult due to anatomic size and require smaller equipment. Animal studies are difficult and costly because an entire animal must be kept alive in humane conditions.

In recent years, artificial tissue scaffolds have been seeded with valve cells or similar cells to create valve constructs. These constructs have been used both as candidates for a tissue engineered heart valve (37) and also as a vehicle to study valve cells (29). These constructs combine some of the benefits of cell culture and animal models: a reproducible, pre-defined 3D environment that allows a pre-defined set of cells to interact with their surrounding architecture. However, they are not yet capable of accurately reproducing the anisotropic material properties nor the varied laminar structure of valvular tissue (39).

Organ culture brings many aspects of animal models and introduces them into a much more flexible and controllable paradigm. A mitral valve organ culture method provides for the entire valve organ to be sustained *ex vivo*, allowing for experiments that subject

the whole valve to a treatment condition instead of just the cells. It also integrates many levels of interaction (cells, tissue structure, mechanics, and biochemical influences) found in healthy native tissues. It does this in a setting where it is easier to control those interactions. The disadvantage of organ culture compared to cell culture would be the difficulty of isolating and replicating mechanisms of tissue behavior. Compared to animal models, organ culture cannot recreate the entirety of systemic influences, but this is also a benefit as these uncontrollable distal influences could serve to confound experimental results as much as contribute to them. In order to gain a more complete understanding of valvular biology and responses to environmental variation, it is essential to study valves in a holistic setting that incorporates cells, ECM, tissue structure, and mechanics. *Ex vivo* organ culture techniques provide this setting along with a higher level of control than either standard cell culture or animal models.

Prior and Current Relevant Work

Other work has been published describing systems designed to mimic the mechanical environment of a variety of cardiovascular organs. They have all created some sort of mock circulation, or flow loop, to simulate the mechanical effects of circulatory blood flow experienced by vasculature (40, 41), tri-leaflet valves (34, 35, 42), and mitral valves. They have been applied towards multiple related objectives: hemodynamic flow analyses, conditioning natural and engineered valve prostheses, and examination of tissue responses to various physiological, pathological, and treatment conditions.

The system described by Hildebrand was developed to mechanically condition engineered aortic and pulmonary valves (42). A electronically controlled pressure regulator is used to create a pneumatic physiological pressure waveform in a mock

ventricle. The pressure is transferred across a taut membrane to the nutrient medium that also acts as the system's flow medium, propelling the medium through the aortic valve port and through the flow loop. The flow loop is based on a windkessel model, placing a compliance chamber, flow resistor, and raised medium reservoir in line with a circulatory loop of tubing that returns the medium to the mock ventricle through a mechanical mitral valve. This system uses a algorithm-controlled variable flow resistor to dynamically uncouple pressure and flow rates, so that they may be varied independently, allowing raised or lowered pressures while maintaining a constant flow rate. This system has recently been used to simulate the flow conditions of the right heart for use in mechanically conditioning tissue engineered pulmonary valves (35); compared to static culture, these valves demonstrated increased DNA content as well as increased collagen content and synthesis.

A similar system has been designed for the organ culture of aortic valves and uses a piston pump to create sinusoidal cyclic pressure with amplitudes in the physiologic range (37). The author notes that insufficient oxygenation rates could create an adverse environment, including altered pH, and lead to cell death. These effects were eliminated with the introduction of a novel gas perfusion method. The system has been shown to maintain sterile conditions over a period of 96 hours and has been used to culture porcine aortic valves for 48 hours. These dynamically cultured valves had comparable levels of collagen, sulfated GAGs, and elastin as freshly excised porcine aortic valves. Statically cultured valves had significantly less sulfated GAGs and elastin and a trend towards reduced collagen, compared to both fresh and dynamically cultured valves. This study

strongly demonstrates that, after only two days, mechanical stimulation significantly aids in maintaining valve architecture during organ culture.

A more recently developed system (43) builds on this common flow loop design with the goal again of culturing engineered aortic valves. The mock ventricle in this system has been shaped to have a smooth contour that greatly reduces flow turbulence and promotes velocity uniformity through the aortic valve. The aortic valve holder has also been designed with artificial sinuses that are meant to recreate the unique flow profile around the valve leaflets. No results confirming sterility of the system have been published.

Another flow loop system has been developed to analyze the flow characteristics of and mechanical forces in mitral valves in various geometrical arrangements. These non-sterile studies have described the effects of modifying chordal placement (44), papillary muscle placement (45) and annulus shape (45). These flow loops feature positionable force-sensitive rods holding the chordae in place, able to measure the force needed in the papillary muscles, as well as clear windows for video and Doppler imaging. The valve annulus is sutured in place and the papillary muscles are bound by dacron fabric, which is then sutured to the placement rods. Because these are hemodynamic studies and not organ culture the system is filled with a simple saline solution and only a handful of cardiac cycles are performed.

These prior works formed a foundation for the work presented in this dissertation, leaving unmet the need for a mitral valve organ culture system. Organ culture of these valves requires the provision of both a mechanical and nutrient environment that induces the healthy maintenance of mitral valve tissues and cells. The next chapter will discuss the

development of an organ culture system for mitral valves, as well as its mechanical characterization.

Chapter 3 DESIGN AND MECHANICAL EVALUATION OF A PHYSIOLOGICAL MITRAL VALVE ORGAN CULTURE SYSTEM

Introduction

Chapter 2 detailed the need for continued research into heart valve biology and pathogenesis as well as the motivation to pursue an organ culture experimental model. A review of existing valve culture systems indicated the need for an organ culture system, designed for the mitral valve, that simulates the valve's native hemodynamic environment. This chapter documents the first aim in meeting this need:

Design and mechanically characterize a mitral valve organ culture system capable of reproducing the valve's physiologic mechanical environment.

Thus, the aim of this work was to design a bioreactor system that will provide physiological mechanical stimulation for sterile organ culture of a mitral valve, especially for longer term studies which would enable detection of slower remodeling changes in the valvular microstructure.

Methods

Design Criteria

Design criteria for the mitral valve organ culture system were categorized as functions, objectives, or constraints (46). The central function of this design was to maintain an organ cultured mitral valve in its native functional state by simulating its *in vivo* nutritional and mechanical environment. Valve cells *in vivo* are provided with nutrients

and mechanical stimulation to remain viable, retain their phenotypic activity, and promote stability in ECM composition. *Ex vivo*, the valve must be immersed in a nutrient medium and housed in a system that recreates the normal valve annular size and shape as well as the position of the chordae tendineae. This geometry is essential to proper coaptation of the valve leaflets, thereby preventing retrograde flow during systole, and to unrestricted forward flow during diastole (45, 47, 48) (Figure 2.1).

To develop a system that most effectively performs these desired functions, several objectives were defined. The most important objective was to maximize the time period that mitral valves remain viable. Also of significance was the objective to minimize the changes in tissue structure and composition. Another objective was to maximize the ease of operation, such as replacing the culture medium under sterile conditions, which must occur at least every two weeks (49). Reducing complexity minimizes possible contamination and allows longer culture periods. In order to mimic *in vivo* conditions, a third objective was to create physiological flow rates (~5.0 L/min) and pressures (peak of 120 mmHg). A related objective was to maximize flexibility and control of flow rates and pressure levels to match the variety of physiologic and pathophysiologic heart rates, blood pressures, and cardiac outputs and thus allow a system user to perform investigations related to alterations in cardiac mechanics. In order to effectively use the system to conduct experiments, additional objectives were to maximize consistency and repeatability of culture conditions and maximize the number of valves in culture concurrently.

The design was also dependent on several constraints. This system design was required to retain sterility throughout bioreactor assembly, valve dissection, valve insertion into the

bioreactor, organ culture system operation and medium replenishment. As a second constraint, the system must not leak to prevent contamination or altered mechanics through loss of fluid volume. Third, the system size was also constrained to fit within an incubator to maintain temperature and gas composition.

Design Overview

Based on these design criteria, a mitral valve organ culture system was designed around a mock ventricle that uses a pressure-controlled bladder pump to produce pulsatile flow (Figure 3.1). Generally, fluid systems can be controlled through flow or through pressure differentials; by controlling pressure, this system allows closer control of the pressure differentials across the mitral valve, but makes flow rates difficult to adjust or predict. The mock ventricle/pumping chamber includes inflow and outflow ports that house the tissue mitral valve and mechanical aortic valve. A slack, dome-shaped silicone rubber membrane separates a culture medium-filled compartment from an air-filled compartment. A computer-controlled pressure regulator increases the air pressure, pushing the membrane into the medium-filled side and propelling medium out of the mechanical aortic valve, until the 'ventricular' air pressure is decreased to a level lower than pressure in the inflow medium, the 'atrial' pressure. At this point, medium flows back into the ventricular chamber through the mitral valve, pushing the silicone membrane back into the air-filled side of the chamber. 'Aortic' and 'atrial' pressure heads are created by elevating a medium reservoir, open to the air through a venting filter. A compliance chamber between the ventricular chamber and medium reservoir mimics the compliant nature of the circulation.

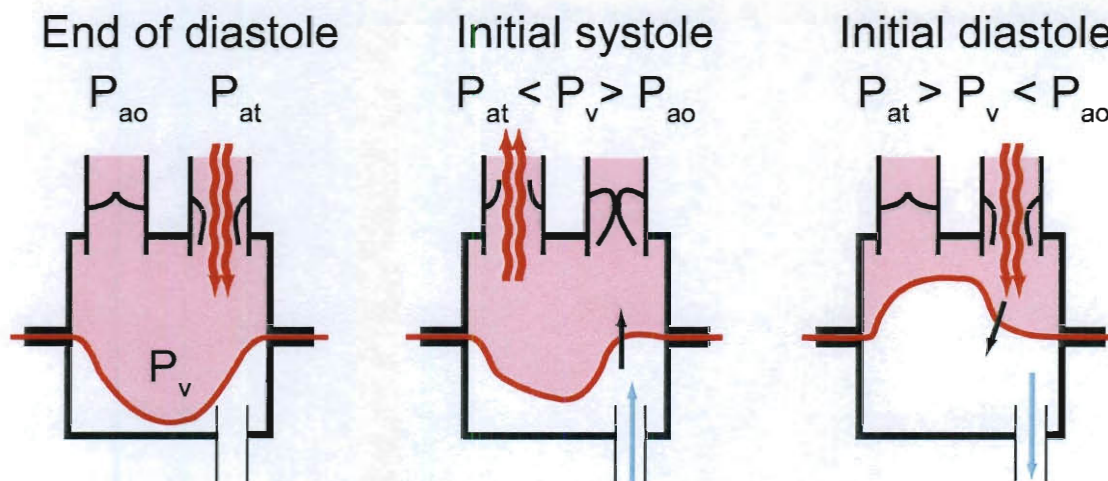


Figure 3.1. Pumping schematic. This diagram depicts flow into and out of the ventricular chamber during a simulated cardiac cycle. A raised medium reservoir provides an atrial filling pressure, P_{at} , which propels medium into the ventricular chamber through the mitral valve. The aortic valve prevents the aortic pressure, P_{ao} , from producing retrograde flow into the ventricle. As ventricular pressure, P_v , is increased pneumatically, it overcomes P_{ao} and medium flows out the aortic valve, while the mitral valve closes. As P_v is decreased, the aortic valve closes and the mitral valve opens again to allow flow into the ventricular chamber. The black arrow indicates movement of the silicone membrane separating culture medium from air. Dual wavy arrows indicate flow of medium. The single narrow arrow indicates air flow.

The main determinants for material selection were sterilization and biocompatibility. All the organ culture system parts were fabricated with materials able to withstand repeated cycles of autoclaving without deformations or other adverse effects; these materials have also never been reported to cause toxicity or affect tissue viability. The primary materials contacting culture medium include polycarbonate, silicone rubber, polypropylene, polyurethane tubing, and polyurethane coated nylon fabric. Stainless steel was used in chordal attachments and aluminum was used for an external frame.

The electronic components of the system were coordinated through a LabView (National Instruments, Austin, TX) virtual instrument (VI). This custom VI used an arbitrary signal based on an archetypical ventricular pressure pulse as the basis for the pressure pulse sent

to the proportional pressure regulator. The VI allowed real-time adjustment of the signal magnitude, displayed instantaneous pressure and flow rate signals, and computed the average flow rate. The VI communicated with a National Instruments Data Acquisition (DAQ) unit in the main electrical control box that routed the appropriate power and communication sources to the computer, flow meter, proportional pressure regulator, and pressure sensor. The containment of all electrical wiring within the box with plugs for each instrument allowed for extremely quick and easy setup of the electrical system.

Flow Control and Measurement

An Airfit Tecno Basic PRE-U proportional pressure regulator (Parker Origa USA, Glendale Heights, IL) was used to create pressure pulses for the system.

Two filter/regulator units were used on a compressed air source at 5.5 bar to produce a clean and stable air supply at 1.5 bar. Supported by this pressure source, the proportional pressure regulator translated a voltage signal into a pressure waveform ranging 0-200 mbar (0-150 mmHg). Pressure in the air-side of the ventricular chamber was recorded by a pressure transducer (Model EW-68075-40, Cole Parmer, Vernon Hills, IL). Flow into the ventricular chamber was measured using an ultrasonic flow meter (Transonic Systems, Ithaca, NY) that detects mass flow through tubing without contacting the fluid. The specific model, 14 PXL, was chosen for its range of measurable flow rates, 0.025-50 L/min, and was factory calibrated for both water at 25° C and culture medium M199 at 37° C.

Flow Loop Components

The system components were connected with clear PVC or Tygon tubing. Original versions of the system used only 5/8" ID Tygon tubing, but most sections of tubing were later replaced with 1/2" ID PVC tubing to reduce the inertial mass of fluid in the system and allow greater flow in response to pressure pulses. Although narrower tubing does also increase flow resistance, the tubing diameter was still large enough so that these contributions to flow resistance were negligible. Approximately 1.5 L of cell culture medium acted as the flow medium for the system and provided nutrients; this medium was M199 with Earle's salts and L-glutamine (Sigma, St. Louis, MO), supplemented with 10% bovine growth serum (Hyclone, South Logan, UT) and anti-microbials (200 IU/mL penicillin, 200 ug/mL streptomycin, and 500 ng/mL amphotericin B, (Mediatech, Manassas, VA)) (50). For a period of seven days, such a large volume of medium provides sufficient nutrients for a single valve and remains effective (49), so the culture medium was replaced once a week.

The ventricular chamber was 6.5" long and 4.5" in diameter (Figure 3.2). The silicone rubber membrane separating the medium-filled and air-filled compartments was positioned at the midpoint of the chamber. This membrane was molded into a dome shape with a thickness of .015", which allowed deformation during each pumping cycle without inducing significant resistance or tension within the membrane. At the ends of the chamber were caps with ports for the pressure transducer and the inflow and outflow of air and culture medium. A simple external frame was tightly clamped around the chamber with toggle latches to prevent leaking; additionally, many junctions in the flow circuit were fitted with silicone o-rings and tightened with hose clamps. A mechanical

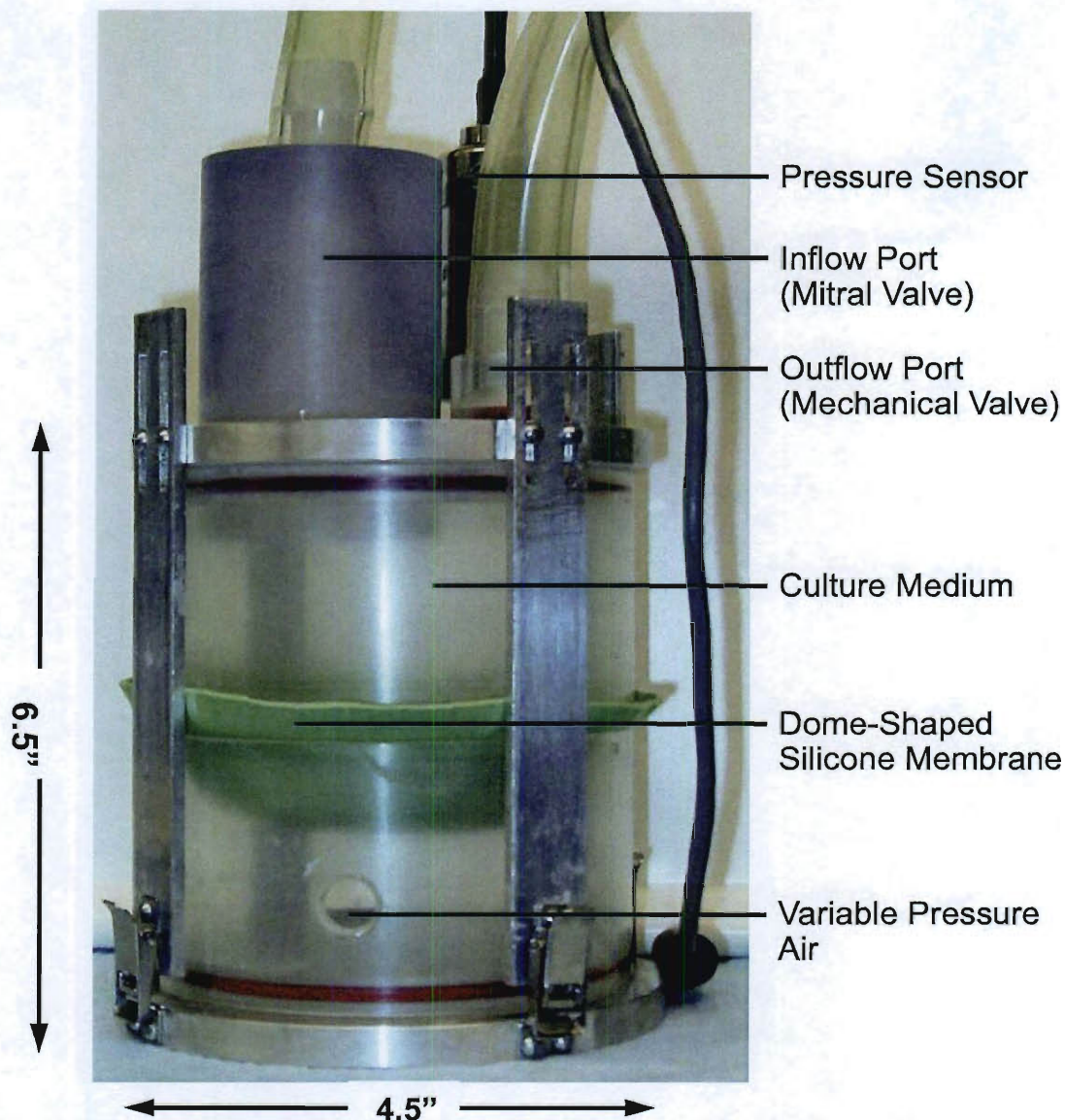


Figure 3.2. Ventricular Chamber. Pulses of pressurized air act through a dome-shaped silicone membrane diaphragm to pump culture medium through a mechanical aortic valve. The mitral valve allows medium to flow back into the ventricular chamber. Thus, the valve cells receive mechanical stimulation from both the hydrostatic pressure pulses and the shear flow across the valve surfaces.

aortic valve (Carbomedics, Austin, TX) was housed in the outflow port of the ventricular chamber. The valve was held in place by a snugly fitting ring that slides into the outflow port around the valve (Figure 3.3). The cultured mitral valve was held similarly in the inflow port of the ventricular chamber.

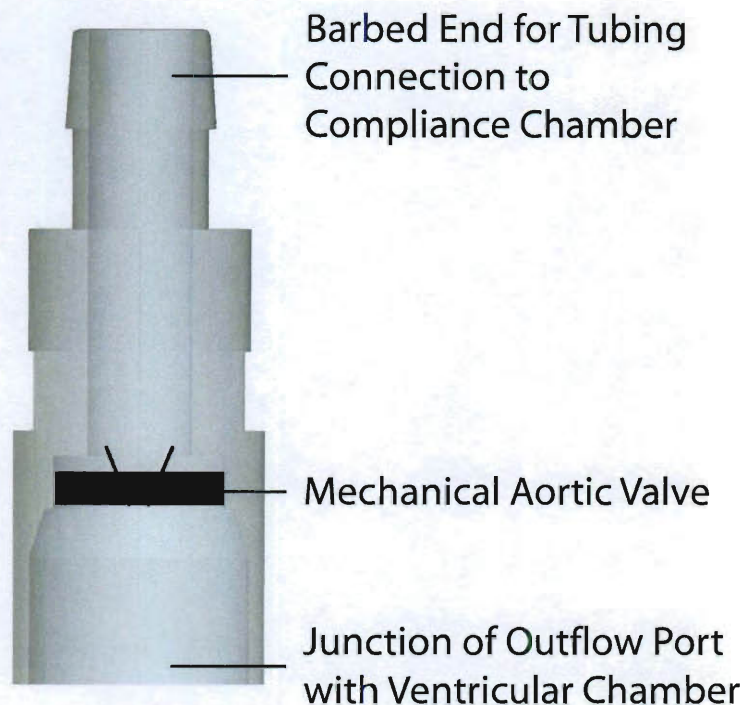


Figure 3.3. Outflow port with mechanical aortic valve. A polycarbonate ring fits snugly into the outflow port, holding the valve in place.

A primary function of this design was to hold the cultured mitral valve in a physiologic position. In the hemodynamic flow loop previously described (44, 45, 48), the mitral valve annulus was sewn to a swatch of Dacron and the papillary muscles were tied to a pair of metal posts, which was appropriate for the non-sterile mechanical studies performed. Our design adapted these concepts for an organ culture system that was intended to operate continuously for weeks instead of hours. The mitral valve was obtained from a pig heart obtained from a local abattoir within three hours of death. The valve was dissected out of the heart inside a sterile biological safety cabinet with steam sterilized tools and gently washed in a 'rinsing' M199 culture medium, as described above, fortified with increased anti-microbials (1000 IU/mL penicillin, 1000 ug/mL

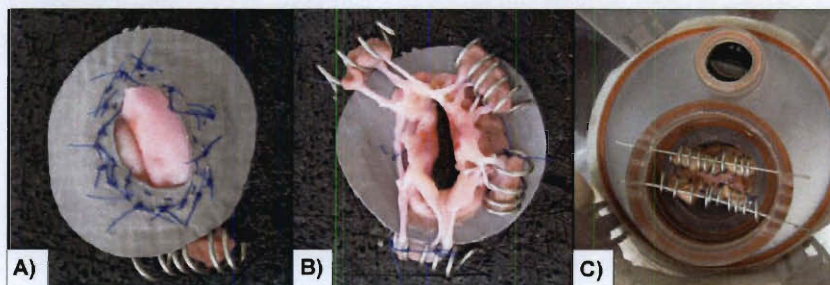


Figure 3.4. Mitral Valve Attachment. A) Excised Porcine valve sutured to a nylon-coated polyurethane swatch. B) Trimmed papillary muscles bound by steel coils. C) Valve annulus clamped into place and papillary muscles anchored by straight steel wires.

streptomycin, and 2500 ng/mL amphotericin B). Before dissection, the valve annulus was sized using an annuloplasty sizing set (Duran Ancore, Medtronic, Minneapolis, MN). The valve annulus was sewn, using non-biodegradable 3-0 Ethilon sutures (Ethicon, Somerville, NJ), to an appropriately sized orifice on a circular swatch of sterilized polyurethane-coated nylon fabric (McMaster-Carr, Robbinsville, NJ) (Figure 3.4). Care was taken during this process to ensure the valve annulus attained an anatomically proper “D” shape. The fabric swatch was then clamped within the inflow port. The chordae tendineae were also held in place relative to the inflow port to prevent valve prolapse. During dissection, the tips of the papillary muscles were detached from the left ventricular wall, retaining the connection with the chordae. The papillary tips held the chordae in place and were held in place by helical stainless steel wires wound around the papillary tips and interwoven between the chordae tendineae. These helices were in turn attached to the interior of the inflow port with additional stainless steel wires.

The remaining system components were the compliance chamber and atrial reservoir, both fabricated from polycarbonate bottles (Nalgene, Rochester, NY) modified with tubing ports. The compliance chamber had ports for medium inflow and outflow and

contained approximately 400 mL of trapped air during operation. The atrial reservoir had ports for medium inflow and outflow as well as an air vent port, which connected to a sterile 0.2 μm venting filter to allow gas exchange and to provide venting to an atmospheric reference pressure.

Results

Mechanical Evaluation

Several mechanical evaluations were performed to determine whether the organ culture system could produce pressure and flow response waveforms mimicking a range of physiological conditions. The first of these evaluations was conducted at room temperature (25° C) with water as the flow medium. The atrial reservoir and compliance chamber were raised 15 inches above the ventricular chamber and the system positioned exactly as it would be in an incubator; a mechanical heart valve was placed in the mitral position. Sinusoidal pressure control signals with a peak of 70 mmHg were used to determine the frequency response capabilities of the system (Figure 3.5 A&B). The measured pressure tracked the control signal within 10 mmHg at 1 Hz, and remained fairly accurate at a frequency of 3 Hz, reaching within 15 mmHg of the peak control signal. These indicators of the temporal response to a pressure control signal indicated that the system is capable of recreating a physiologic pressure pulse. Next, to mimic a systolic pressure pulse, the signal was modified to create 60 and 75 bpm 'physiological' signals with pressure peaks ranging 75-150 mmHg (Figure 3.5 C&D). The pressure

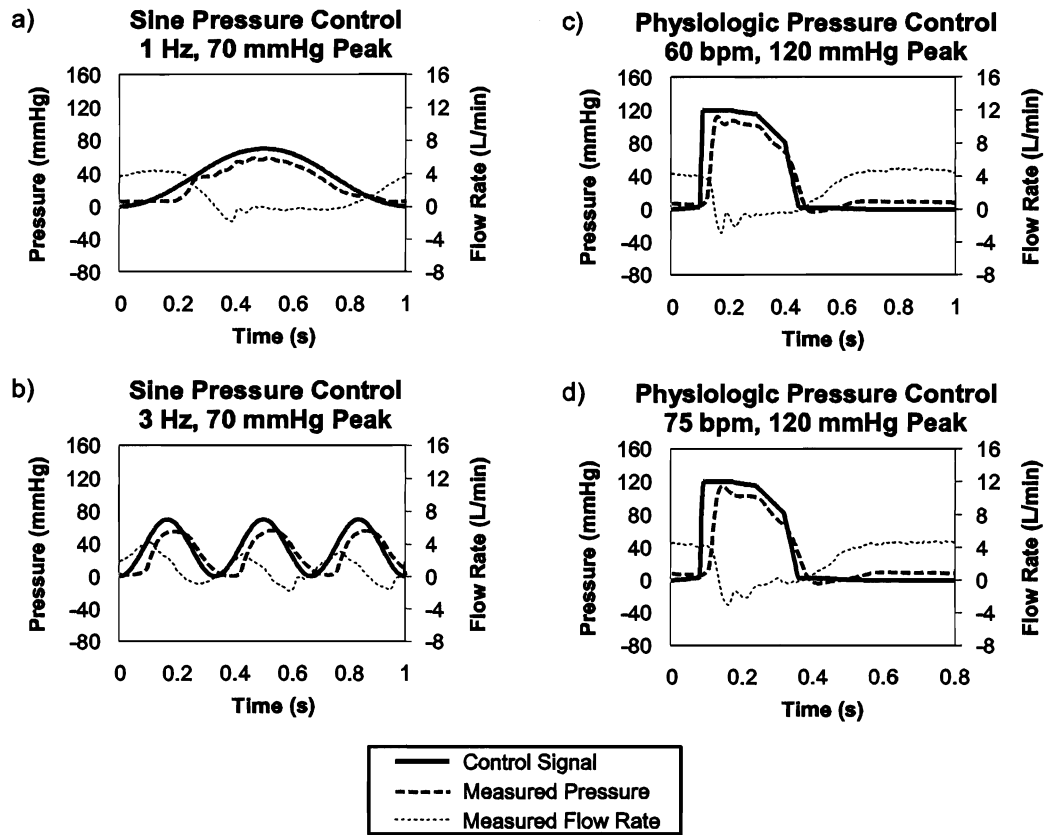


Figure 3.5. Flow Waveforms. Sinusoidal pressure control signals at a) 1 Hz and b) 3 Hz with peaks of 70 mmHg and a mechanical outflow valve. Also, physiologic pressure control signals at c) 60 and d) 75 bpm with peaks of 120 mmHg and a mechanical outflow valve. Similar waveforms were recorded for control signals with peaks ranging from 75-150 mmHg.

response tracked the control signal closely in these evaluations, over the full range of peak pressures. In each evaluation the measured pressure followed the control signal to its peak, within 5-10 mmHg, after a short lag of approximately 0.05 s. At the highest pressures, the atrial filling pressure was inadequate to fully replenish fluid in the ventricular chamber and the excess fluid breached the atrial reservoir air vent after a few minutes. The maximum peak pressure that could be sustained in the system without such a breach was 145 mmHg. These breaches were later prevented by modifying the silicone

diaphragm to have a smaller range of displacement. The range of pressures that can be achieved by the current system is 0 to 150 mmHg, the approximate

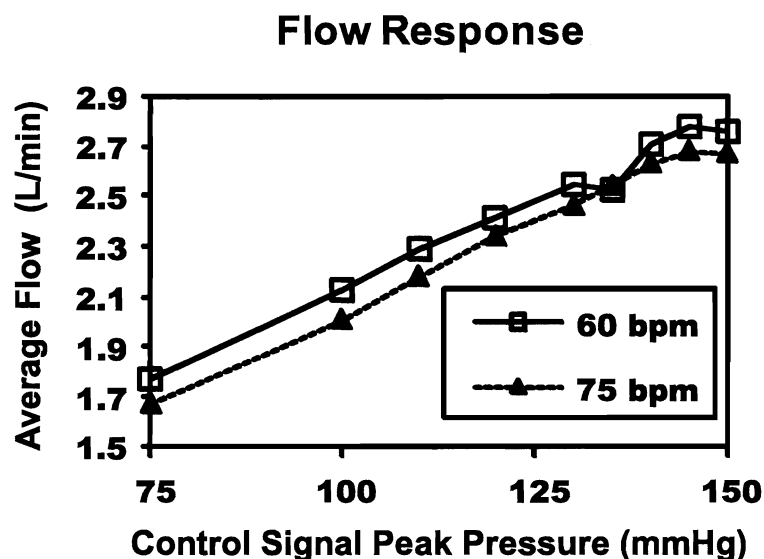


Figure 3.6. Average flow rate vs. control signal peak pressure in organ culture system with mechanical valves in mitral and aortic positions.

range of the proportional pressure regulator, and allows for the simulation of a range of heart pressures from hypotension to hypertension. This range also would allow the possibility of using this system to perform mechanical conditioning of engineered tissue constructs by applying gradually increasing pressures. Increases in peak pressure resulted in linear increases in average flow rate, while pulse frequency had little effect on flow rate (Figure 3.6). The maximum average flow rate recorded in the system is nearly 3 L/min, which is lower than a typical porcine cardiac output of 5 L/min (51).

Similar system response characteristics were found when the system was evaluated with a porcine mitral valve in place. The system was filled with culture medium and placed in an incubator at 37° C. The flow response was recorded within 3 hours of assembling the system. The response included a spike of retrograde (negative) flow during systole as the

mitral valve leaflets were pushed up and then pressed together to close the orifice (Figure 3.7). As diastole began, there was a surge of flow through the valve resulting from the pressure built up in the compliance chamber, decreasing until the next systolic period. At the highest peak pressure of 150 mmHg, the average flow rate reached 2.6 L/min. This evaluation demonstrated the ability of the organ culture system to house a properly functioning mitral valve and mimic its physiological flow environment. Although the data shown in Figure 3.7 was performed using a single typical specimen, we have observed throughout the system's development and evaluation that variations in valve size and geometry as well as inherent variation in the attachment procedure produce minor variations in flow response.

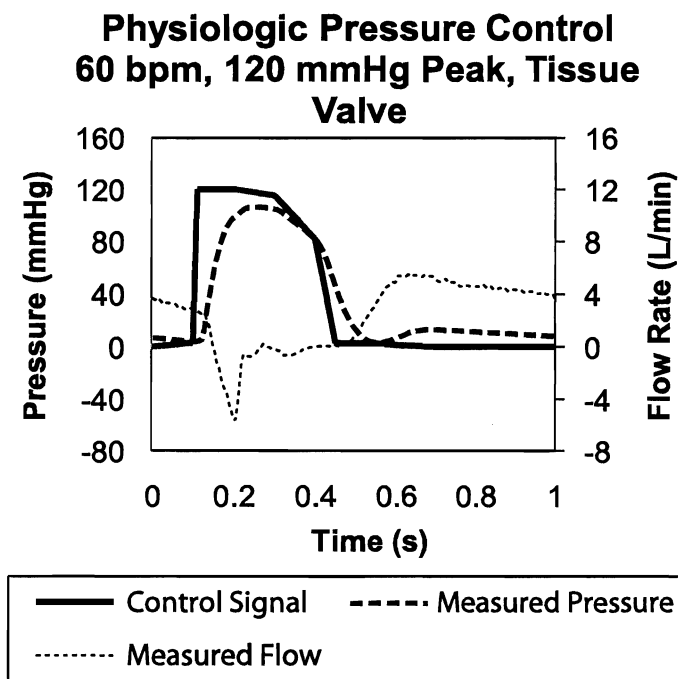


Figure 3.7. Flow waveforms produced from a physiologic pressure control signal at 60 bpm with a pressure peak of 120 mmHg and an explanted porcine mitral valve as outflow valve. Similar waveforms were recorded for control signals with peaks ranging from 75-150 mmHg.

In repeated trials with porcine mitral valves (during the sterility testing described below), prolonged retrograde flow was occasionally observed during systole when high pressures caused leaks to form along the valve annulus, and would increase in magnitude with time. Such leaks introduced non-physiological flow behavior and were reduced by reinforcing annular attachments with additional sutures.

Sterility

Sterility of this system was demonstrated through several progressively more complicated trials. First, the system was set up under zero-flow conditions with a mechanical valve in the mitral position and tested for the duration of a week. In this evaluation, each component was steam sterilized and then assembled and filled with M199, without antimicrobial additives, in a biological safety cabinet. After one week, multiple medium samples were collected from distant parts of the system. No sign of contamination was seen in the medium under microscope and after one day of culture of medium samples swabbed on agar plates, even when contamination was visible on positive control agar plates. In subsequent testing of the organ culture system, porcine mitral valves were subjected to physiological pulsatile flow with standard culture medium, as described previously. At this time, eleven valves have been tested in the system for a range of 3 days to 3 weeks. Every seven days, the system was removed from the incubator and placed in a biological safety cabinet where the culture medium was completely drained and refilled. The drained medium was found to be free of contamination, demonstrating no observable discoloration and turbidity. The pH of the drained medium was also frequently checked as a readout for oxygenation and accumulation of harmful metabolic products; in all cases the medium was found to retain the pH of the original medium.

During these culture periods, the system was also observed to have no persistent leaks, which aided in preventing contamination.

Discussion

Development of an organ culture system provides a new and powerful tool for studying mitral valve biology by recreating the approximate mechanical environment experienced by mitral valves *in vivo*. This system builds upon the existing paradigms of cell culture and animal models by making possible the *ex vivo*, controlled study of mitral valve tissue and cells experiencing physiologically relevant mechanical, cell-cell, and cell-ECM interactions. The novelty of this design lies in the applicability to mitral valves, as well as the pending demonstration of the extended culture period.

Mechanical evaluations have shown this system to successfully create a mechanical environment similar to that of the native mitral valve. The most notable discrepancy is the difference in average flow rate, although a flow rate of at least 2 L/min is expected to provide sufficient shear stress stimulation in conjunction with physiological hydrostatic pressure to maintain native valve characteristics. If desired, modifications to the shape and size of flow components and pressure control waveform may provide a more physiologic flow rate. For example, molding a silicone diaphragm shaped more like the interior of the left ventricle may encourage more physiological flow fields, displacing more medium.

Despite this room for improvement, the system described above demonstrates the possibility of long-term culture of intact heart valves in a physiological mechanical environment. In addition to culturing mitral valves, this system could be readily modified

to culture any of the other 3 cardiac valves or possibly other cardiovascular tissues. These mechanical performance characteristics are intended to contribute to the primary goal of this design, maintaining valve cellular and microstructural viability; evaluating these characteristics will be the focus of Chapter 4.

Chapter 4 ORGAN CULTURE OF MITRAL VALVES AS A NOVEL

EXPERIMENTAL PARADIGM

Introduction

The design and mechanical characterization of a dynamic, pulsatile flow loop system for the organ culture of a mitral valve was described in Chapter 3, with additional design details in Appendix A. This system provides a physiologic pressure profile to produce dynamic flow and mimic the native environment of the mitral valve. The current chapter focuses on the following aim:

Further develop the organ culture system to integrate a porcine mitral valve in a sterile environment with adequate oxygen and nutrients. Evaluate the cultured valves to determine the effect of the dynamic mechanical environment.

The effectiveness of the dynamic organ culture system can be demonstrated by showing that valves cultured in the system better retain native characteristics better when compared to valves cultured without mechanical stimulation (static culture). The purpose of the work described in this chapter was to compare the structure, composition, and material properties of porcine mitral valves dynamically cultured for 3 weeks with statically cultured and freshly harvested specimens.

Materials & Methods

Organ Culture System

The porcine mitral valve was located within the inlet port of the pumping chamber and a mechanical aortic valve was located at the outlet port. The entire system was filled with approximately 1.4 L M199 culture medium, supplemented with 10% Bovine Growth Serum (BGS, Thermo-Hyclone, Logan, UT) and 1 % anti-microbial solution (200 IU/mL penicillin, 200 ug/mL streptomycin, and 500 ng/mL amphotericin B; Mediatech, Manassas, VA). The pressure waveform was controlled by a Virtual Instrument programmed with LabView software (National Instruments, Austin, TX) and approximated a left ventricular pressure cycle.

Harvest, Preparation, and Culture of Valves

The following procedure was followed to integrate porcine mitral valves into the organ culture system. A more detailed set of instructions can be found in Appendix B: Flow Loop Operating Manual. Pig hearts were obtained from a local abattoir (Fisher's Ham and Meats, Spring, TX). Within six hours postmortem, the entire mitral valve was harvested intact, including the papillary muscles. Porcine mitral valves were assigned to three groups: freshly (F) excised mitral valves: $n_F = 7$, statically (S) cultured valves: $n_S = 7$, and dynamically (D) cultured valves: $n_D = 5$. Group F valves were harvested in a non-sterile environment and immediately prepared for mechanical, histological and biochemical analyses.

Valves intended for static or dynamic organ culture (Groups S & D) were harvested in a biological safety cabinet with sterilized surgical tools to maintain a sterile procedure. After harvest, these mitral valves were stored in sterile Phosphate Buffered Saline (PBS) augmented with a high dose (10%) anti-microbial solution for two hours, or in two cases for 14 hours under refrigeration. This step was intended to reduce any pre-existing microbial contamination resulting from the slaughter and pre-harvest handling of the heart. During harvest and preparation, handling of the valve surfaces was minimized to avoid disrupting the endothelium.

Groups S and F were then prepared for integration into the organ culture system. Group S (static culture) valves were prepared similarly to Group D (dynamic culture) valves to isolate the effects of mechanical stimulation. The valve annuli were sutured to an orifice cut into a circular swatch of nylon-coated polyurethane (McMaster-Carr, Santa Fe Springs, CA) (Figure 3.4a). Each swatch was paired by visual inspection to best match orifice and annulus dimensions. After preparation, group S valves were placed in a cell culture flask and submerged in approximately 75 mL M199 culture medium with 10% BGS (Figure 4.1). These flasks were maintained in a humidified incubator at 37° C and 5% CO₂ for a duration of 21 days; the culture medium was exchanged every 2-3 days.

As the preparation of group D valves continued, the papillary muscles were trimmed and bound by helical steel wires so that the chordae extended out perpendicular to the helical axis (Figure 3.4b). After this preparation, the valves were again stored in a fresh sterile PBS/10% anti-microbial solution for up to two hours. The valves were then fitted into the inlet port of the organ culture system and the papillary muscle helices were anchored in place with straight steel wires to hold the chordae in an extended position (Figure 3.4c).

The entire organ culture system was then assembled from steam sterilized components in a biological safety cabinet and filled with M199 culture medium. The system was placed in the incubator and connected to the electronic control system.



Figure 4.1. Static culture environment. Group S valves were prepared for dynamic culture but instead submerged in a cell culture flask filled with culture medium.

For each valve in Group D, the organ culture system was run for 21 days with a 60 bpm cycle and peak pressure of 120 mmHg. The culture medium was exchanged every 7 days. Upon draining the system, the pH of the culture medium was measured to detect whether insufficient gas exchange or cellular metabolites affected the biochemistry of the culture medium. During operation of the organ culture system, pressure within the ventricular chamber and flow through the mitral valve were measured and recorded at least three times per hour to track the system and valve function. Flow measurements of full pumping cycles were selected from five time points during each valve's culture: Days 1, 4, 7, 14, and 21. The total flow rate was calculated by integrating the instantaneous flow rate. Forward flow was calculated from the integral of all positive flow values and retrograde flow from the integral of all negative flow values.

After 21 days of culture, groups S & D were removed from the culture flasks and organ culture system and prepared for analysis. Valves from all three groups were photographed and dissected into seven sample sections (Figure 4.2). These sections were identified as: radial strip from the anterior leaflet (AR), circumferential strip from the anterior leaflet (AC), two anterior strut chordae (Ch), remaining anterior leaflet tissue (Ant), radial strip from the posterior leaflet (PR), remaining posterior leaflet tissue (Post). The Ant and Post sections were used for biochemical analyses, while the other sections were reserved for material testing and were subsequently prepared for histological analyses.

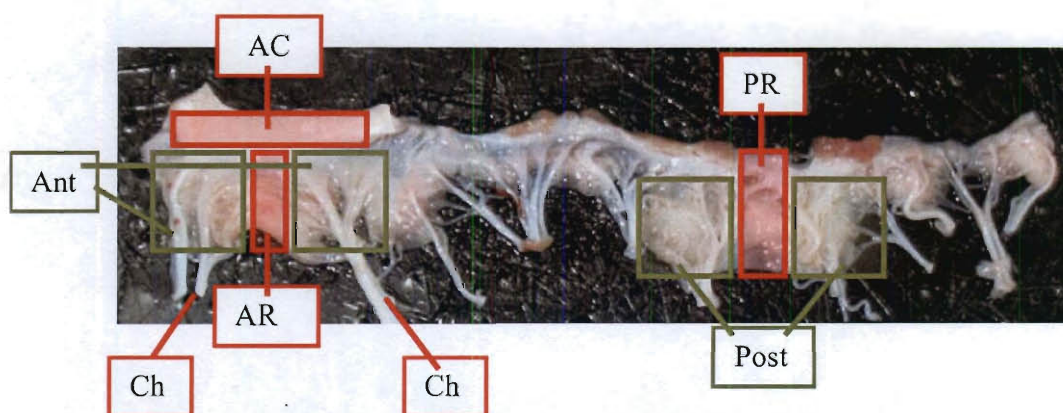


Figure 4.2. Mitral valve sections. After culture, the valves were dissected into seven sections. Five were used for materials testing and histology: AC – Anterior Circumferential, AR – Anterior Radial, PR – Posterior Radial, Ch (x2) – Chordae Tendineae. Two were used for biochemical assays: Ant – Anterior Leaflet, Post – Posterior Leaflet.

Biochemical Analyses

Each Ant and Post tissue sample was weighed before and after freeze-drying to determine water content. These samples were then rehydrated in ammonium acetate, minced, and digested with approximately 10 mg/mL Proteinase-K (Invitrogen, Carlsbad, CA) at

60°C for 16 hours or until digestion was judged complete by visual inspection, at which time the samples were heated to 70°C for 30 minutes to denature the Proteinase-K (52). Cellularity was measured with the fluorescent PicoGreen dye (Invitrogen) to quantify DNA content (53). Because DNA content is constant among porcine cells, this is a direct measurement of relative cellularity. Glycosaminoglycan (GAG) content was measured through an uronic acid colorimetric assay (54). Collagen content was measured through a colorimetric assay that detected hydroxyproline, an amino acid found nearly exclusively in collagen in a proportion of 131 µg hydroxyproline per 1000 µg of type I collagen (55).

Materials Testing

The remaining sections (AR, AC, PR, and Ch) were subjected to a uniaxial tensile testing regimen using an EnduraTEC ELF 3220 (Bose, Eden Prairie, MN). These tests were conducted in a water bath filled with PBS maintained at 37° C. Prior to testing, the thickness, width, and gauge length of each sample were measured for calculation of stress and strain. Load and displacement values were recorded as the valve sections were stretched according to a predetermined displacement regimen. The regimen included three phases of elongations of increasing magnitude in order to demonstrate a broad range of stress-strain responses for each specimen regardless of its length or other elongation limits. As shown in Table 4.1, each phase began with a preconditioning regimen of several 1 Hz triangle waves, followed immediately by a 0.5 Hz elongation segment of the same magnitude, which was used to determine a tensile modulus. Phase 1 consisted of a simple load-elongation test. During phases II and III, after the preconditioning the elongation was held for a period of 60 seconds to observe viscoelastic

stress relaxation behavior. Displacement was then returned to zero and the samples were rested for 60 seconds before the next elongation phase.

Table 4.1. Materials Testing Regimens

	Phase		
	I	II	III
Elongation magnitude (mm)	2	3	5
Pre-conditioning cycles	25	6	6
Stress relaxation duration (s)	0	60	60
Rest period (s)	60	60	N/A

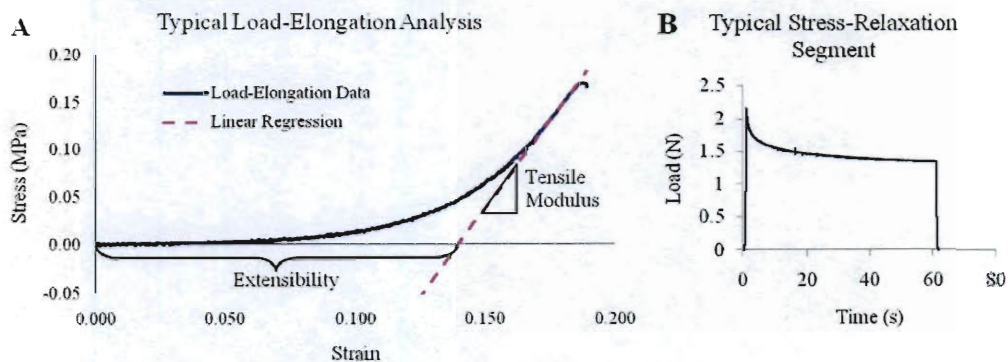


Figure 4.3. Material testing data analysis. A) A typical load-elongation curve. A linear regression was fit to the linear portion of the curve. The slope of the regression was interpreted as the tensile modulus and the x-intercept as the extensibility. B) A typical stress relaxation curve. A bi-exponential decay was fit to the entire curve.

Afterwards, the post-transition modulus, extensibility, and stress relaxation rate constants for each tested specimen were calculated from the load-displacement data (Figure 4.3).

Stress was calculated by dividing the load data by the cross-sectional area of the sample.

Strain was calculated by dividing the displacement data by the gauge length. The elastic

tensile modulus was determined for each phase by performing a linear regression on the

steepest portion of the stress-strain curve of the 0.5 Hz elongation segment using Excel software (Microsoft Corp, Redmond, WA). This "post-transition" modulus (56) often varied among phases, depending on the strain experienced. When specimens were not elongated to a sufficiently high enough strain, they demonstrated decreased tensile moduli. In addition, strains that were too large often caused tissue or grip failure during pre-conditioning and also resulted in reduced moduli. Because the three-phase testing protocol provided three strain windows, the greatest value of the modulus that was calculated from the three phases was selected as the most representative of the post-transition modulus of each tissue specimen. Extensibility, which demonstrated the tissue specimens' capacity to deform without requiring a significant load, was defined as the x-intercept of the linear regression used to calculate the modulus. The stress relaxation data were modeled as a bi-exponential decay, described by the following equation.

$$y = y_0 + A_0 e^{-k_{\text{fast}} x} + A_1 e^{-k_{\text{slow}} x}$$

The K_{fast} and K_{slow} parameters were calculated iteratively using GraphPad Prism (GraphPad Software, LaJolla, CA). The parameter y_0 was determined as the plateau stress, an asymptotic value approximated by the stress at the end of the 60 second relaxation period.

Histological Staining

After tensile testing, the sections were fixed with formalin overnight, dehydrated using a series of graded alcohols, soaked in xylene, and embedded in paraffin blocks according to standard procedures for histological processing. Tissue blocks were sliced into 5 μm thick cross-sections and affixed to glass slides. Tissue cross-sections were stained with a

Movat Pentachrome to visualize ECM and the layered leaflet structure. Samples were also stained with Picrosirius Red to observe collagen fiber alignment. As described in Table 4.2, immunohistochemical (IHC) staining was also used to localize several markers of cell and tissue phenotype. In order to control for the staining intensity of the hematoxylin counterstain and any non-specific binding, negative controls for each secondary antibody were performed with no primary antibody on every specimen. In addition, a set of hematoxylin-only slides were prepared to quantify non-specific binding and as a measure of cellularity.

Prior to analysis of the staining results, most slides were digitally scanned at 7200 dpi with a slide scanner (PathScan Enabler IV, Meyer Instruments, Houston, TX) to facilitate analysis. The Picrosirius Red slides were instead imaged with a Leica DMIL microscope (Buffalo Grove, IL) under polarized light using the 10X objective and photographed using a Leica DFC 320 imaging system and ImagePro software (Media Cybernetics, Bethesda, MD). Radial sections were imaged at the valve insertion, mid-leaflet, and at the free-edge. They were then analyzed semi-quantitatively for staining brightness and the uniformity of collagen alignment and sorted into four grades for each characteristic (Figure 4.5). Movat-stained sections were analyzed semi-quantitatively for delineation of the distinct layered structure, abundance of saffron-stained collagen, and abundance of alcian blue-stained GAGs (57). Slide images were randomized and two blinded observers assigned a grade of 1 to 4 for each characteristic.

Table 4.2. Immunohistochemistry Markers. Antibody sources: A) Abcam, Cambridge, MA. B) Lab Vision, Fremont, CA. C) A gift from Dr Larry Fisher, NIH. D) Associates of Cape Cod, East Falmouth, MA. HA is detected using HA binding protein, not an antibody. E) Millipore, Billerica, MA. F) Dako, Carpinteria, CA.

Marker	Dilution	Secondary Antibody	Antigen Retrieval	Relevance
Caspase-3 ^A	1:50	Rabbit	Citric Acid – Heat Mediated	Marker for cellular apoptosis
CD-31 ^B	1:50	Rabbit	Citric Acid – Heat Mediated	Endothelial cell marker
Decorin ^C (LF-122)	1:500	Rabbit	Chondroitinase ABC	Collagen formation and organization
Hyaluronan ^D (HA)	1:250	N/A	None	Located in areas of compressive loads
Proliferating Cell Nuclear Antigen (PCNA) ^A	1:500	Rabbit	Citric Acid – Heat Mediated	Denotes magnitude of cellular proliferation
Prolyl-4-Hydroxylase (P4H) ^E	1:200	Mouse	Citric Acid – Heat Mediated	Enzyme marker of collagen synthesis
Smooth Muscle α -Actin (SM α A) ^F	1:1000	Mouse	Citric Acid – Heat Mediated	Valve cell activation, localized in valve lesions
Versican ^D	1:500	Mouse	Chondroitinase ABC	Located in areas of compressive loads, disrupted in valve disorders

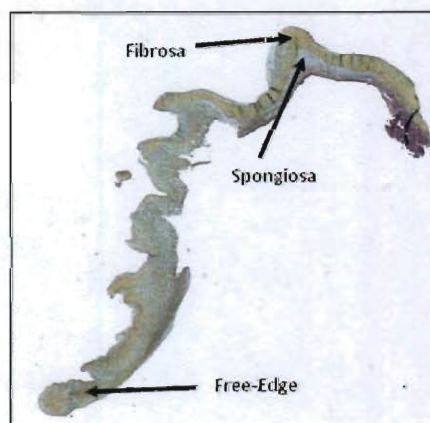


Figure 4.4. A typical radially oriented section of the mitral valve. The Fibrosa, Spongiosa, and Free-edge regions are indicated. Yellow saffron staining indicates collagen, blue staining indicates PGs, and black indicates elastin or cell nuclei.

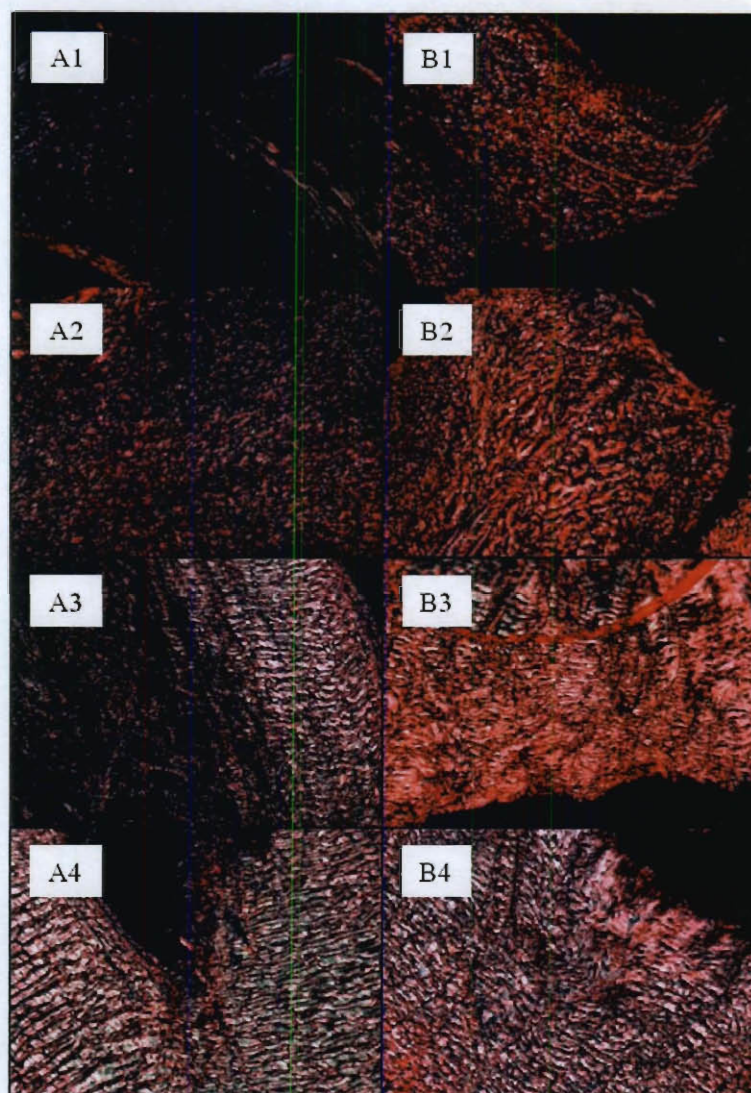


Figure 4.5. Picrosirius Red Grading. A) From 1 to 4, little to high staining brightness. B) From 1 to 4, little to high collagen organization and alignment.

Slides stained with IHC were analyzed to determine the relative staining intensity of each marker, both throughout the tissue cross-section as well as in individual valve layers (Figure 4.4) when such layers were apparent in staining. Calculation of average staining intensity was automated with a batch macro in ImageJ (NIH, Bethesda, MD) that utilized particle analysis to isolate tissue sections from the image background. The resulting value

was a measurement of the average staining intensity of each cross-section. Because CD-31 is a marker for endothelial cells, the intensity of anti-CD-31 immunostaining was not analyzed throughout the tissue sections. Instead, endothelial staining in these sections was observed under a Leica DMIL microscope using the 5X objective and photographed using a Leica DFC 320 imaging system and ImagePro software.

Statistical Analysis

Statistical calculations were performed using JMP software (SAS, Cary, NC). Average values were calculated and are expressed here as mean \pm SE. Each group of data was analyzed by a two-way ANOVA, separating specimens by experimental group (F/S/D) as well as valve section (Post/Ant or AR/AC/PR/Ch). ANOVA was also performed on staining intensity measurements isolated from specific valve regions. This data was separated by valve section and compared across experimental group and region. When results were inconsistent across valve sections, data was also analyzed by one-way ANOVA across experimental group. In certain cases, sections were separated into radially oriented (AR/PR) and AC/Ch “section types” that share similarities in typical loading and structural characteristics. Separate two-way ANOVAs were performed on each section type across section and experimental group. When ANOVA suggested statistical differences, a Tukey's test was used for post-hoc analysis between groups with the level of significance set at 0.05.

Results

Flow Through the Mitral Valve

After introduction into the organ culture system all mitral valves demonstrated roughly physiological flow patterns, clearly indicating proper opening and closing of the valve leaflets. These valves consistently showed a gradual, and statistically significant ($p < 0.001$) increase of retrograde flow, from an average of 0.4 ± 0.1 L/min to 1.7 ± 0.3 L/min, as the culture period progressed (Figure 4.6). Combined with the constant forward flow, this resulted in a significant ($p < 0.05$) drop in the total (net) flow rate from 2.2 ± 0.1 L/min on Day 1 to 1.0 ± 0.4 L/min on Day 21. The recorded pressure patterns did not change significantly during the 21 days of culture (data not shown).

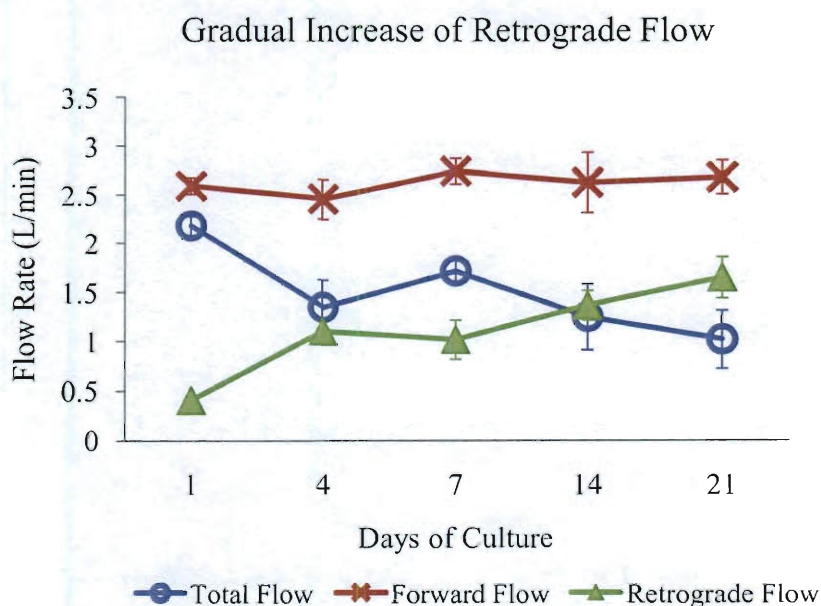


Figure 4.6. Average flow characteristics through the mitral valve. This chart represents the culture periods of five separate valves.

Macroscale Anatomy

Valves from groups F, S, and D typically exhibited slightly different appearances. Compared to the control valves, the leaflets in the static group were observed to be enlarged. The leaflets in the dynamic group were not visibly enlarged, but did appear less glossy than those in the other groups. A two-way ANOVA of thickness measurements indicated a significant thickening of valve leaflets and chordae under both dynamic ($p = 0.0262$) and static ($p = 0.0003$) culture conditions compared to fresh leaflets and chordae (Table 4.3).

Table 4.3. Thickness (mm) of Valve Sections in Different Groups.

Tissue Section	Fresh	Static	Dynamic
AC	1.00 ± 0.09	1.30 ± 0.07	1.30 ± 0.11
AR	1.19 ± 0.17	1.67 ± 0.12	1.48 ± 0.25
PR	1.10 ± 0.14	1.51 ± 0.15	1.38 ± 0.20
Ch	1.17 ± 0.08	1.46 ± 0.11	1.35 ± 0.07

Biochemical Assays

Biochemical assay measurements for all four analytes were consistent between anterior and posterior leaflet sections, so these sections were grouped and analyzed together. The valves cultured under static conditions contained significantly more water by weight ($90.6 \pm 0.3\%$) than fresh valves ($88.9 \pm 0.4\%$, $p = 0.0055$) and dynamically cultured valves ($88.4 \pm 0.7\%$, $p = 0.0257$) (Figure 4.7). The statically cultured group was also remarkably different with regards to cellularity (Figure 4.8), with only a small fraction of DNA ($1.1 \pm 0.2 \mu\text{g}/\text{mg}$ dry wt) compared to fresh valves ($10.3 \pm 0.7 \mu\text{g}/\text{mg}$, $p < 0.0001$) and dynamically cultured valves ($6.9 \pm 1.1 \mu\text{g}/\text{mg}$, $p < 0.0001$). There was also a smaller,

Tissue Hydration by Weight

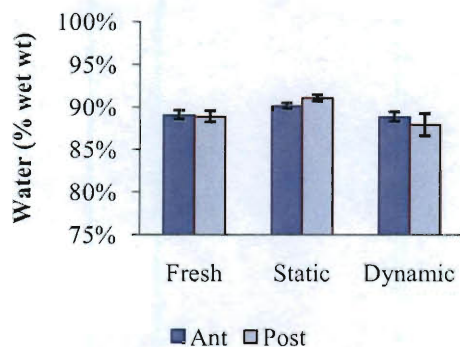


Figure 4.7. Tissue hydration by weight.

Cellularity

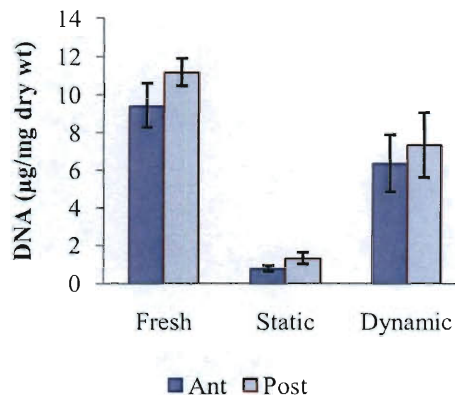


Figure 4.8. DNA measurement by tissue weight. DNA mass is proportional to cellularity.

Collagen Concentration

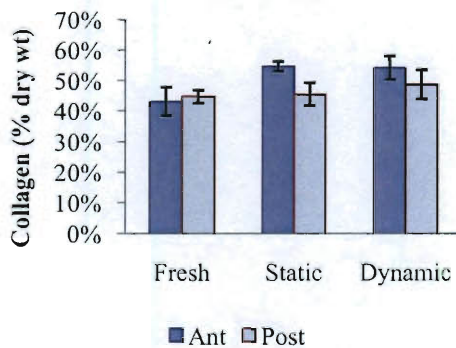


Figure 4.9. Collagen concentration by weight. Collagen is determined by measuring hydroxyproline.

GAG Concentration

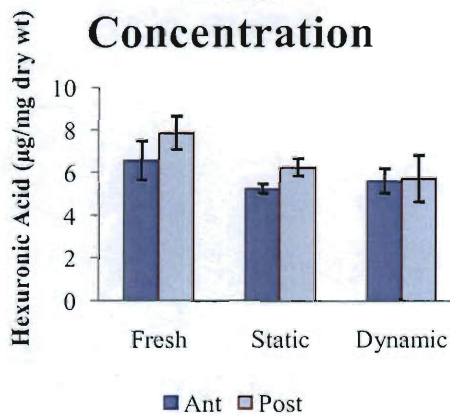


Figure 4.10. GAG concentration by weight. GAG content is determined by measuring uronic acid.

but still significant, difference between the cellularity of fresh and dynamically cultured mitral valves ($p = 0.0045$).

The analyses of ECM composition gave mixed results. There was no statistically significant difference in hydroxyproline and thus collagen concentration between groups (Figure 4.9), although there was a trend of slightly greater collagen concentration in the dynamic and static culture groups when compared to fresh valve leaflets ($p = 0.1104$).

Compared with fresh leaflets, there was a statistically insignificant loss of glycosaminoglycans during static culture, and also during dynamic culture (Figure 4.10); the GAG concentrations were similar between the two culture groups.

Materials Testing

Mechanical testing of the leaflets and chordal specimens also showed mixed results between the different groups. Due to the considerable differences in the magnitude of the tensile moduli, the only two-way ANOVA that was performed was on the radial specimens with leaflet section as one factor (AR vs. PR) and the 3 culture groups as the other factor. The two-way ANOVA analysis of tensile modulus for the radially oriented specimens did not detect a significant difference between experimental groups. The results did indicate a trend of lower tensile moduli in the static culture specimens compared to fresh specimens ($p = 0.2974$) and dynamically cultured specimens ($p = 0.0976$) (Figure 4.11a). The pattern between groups was different for the stiffer AC and CH specimens (Figure 4.11b). The fresh chordae had tensile moduli significantly greater than those from both the static ($p = 0.0191$) and dynamically ($p = 0.0373$) cultured valves. The AC specimens showed the same pattern, but without statistical significance.

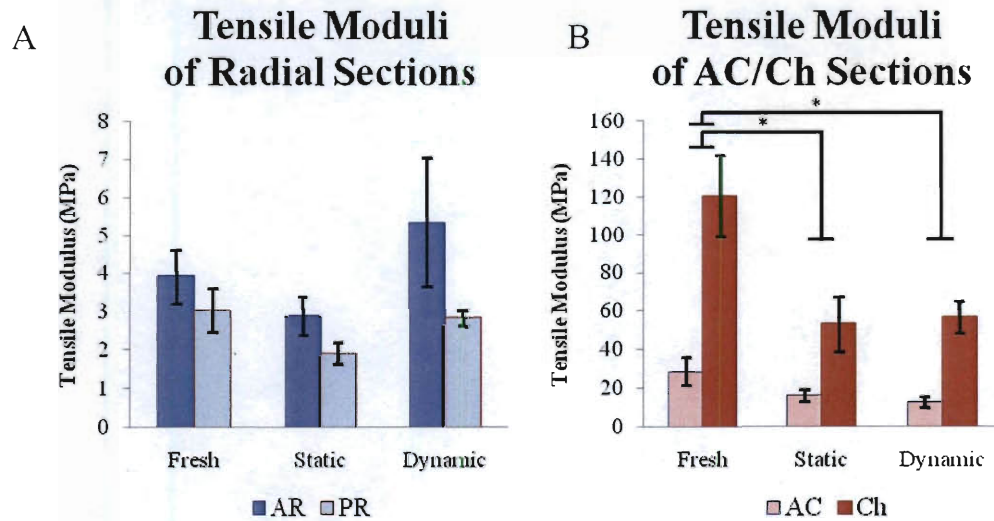


Figure 4.11. Tensile elastic moduli. A) Radially oriented sections. B) AC and Ch sections. *: indicates significance, $p < 0.05$.

Comparisons of extensibility between groups did not find any significant differences, whether analyzed as an overall pattern using a two-way ANOVA or within sections using a one-way ANOVA (Figure 4.12). Similarly, the stress relaxation time constants did not vary between treatment groups (data not shown), whether analyzed as an overall pattern using a two-way ANOVA or within sections using a one-way ANOVA.

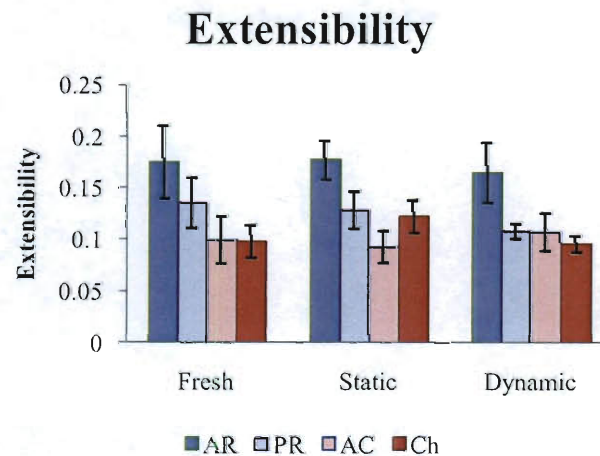


Figure 4.12. Extensibility among all sections and treatment groups.

Histology and Immunohistochemistry

A two-way ANOVA performed on laminar delineation grades of Movat-stained cross-sections with section and treatment group as factors did not suggest any significant differences, nor did separate two-way ANOVAs for each section type (Radially oriented vs AC/Ch). However, a trend in radially oriented sections suggested a decrease in average delineation grade from fresh valves to static and dynamic culture valves (Figure 4.13a). The trend in the AC and Ch sections suggested an increase for static culture valves and a decrease for dynamic culture valves (Figure 4.13b). A two-way ANOVA indicated a significant decrease in the collagen staining intensity of all sections from dynamic culture valves compared to fresh valves ($p = 0.0002$) and static culture valves ($p < 0.0001$) (Figure 4.14 and Figure 4.15). This decrease was not seen in static culture samples. Grading of GAG staining intensity of radially oriented samples from fresh valves was found to be significantly greater ($p < 0.0001$) than that of static and dynamic culture valves (Figure 4.16a). The ANOVA for AC/Ch specimens detected no effect of experimental group, but the grading results did suggest a weak trend of decreased GAG intensity in static valves compared to fresh and dynamic culture valves (Figure 4.16b).

Picrosirius Red images exhibited varying levels of staining brightness and collagen organization between sections and valve regions, but no statistically significant differences were detected between experimental groups (Figure 4.17).

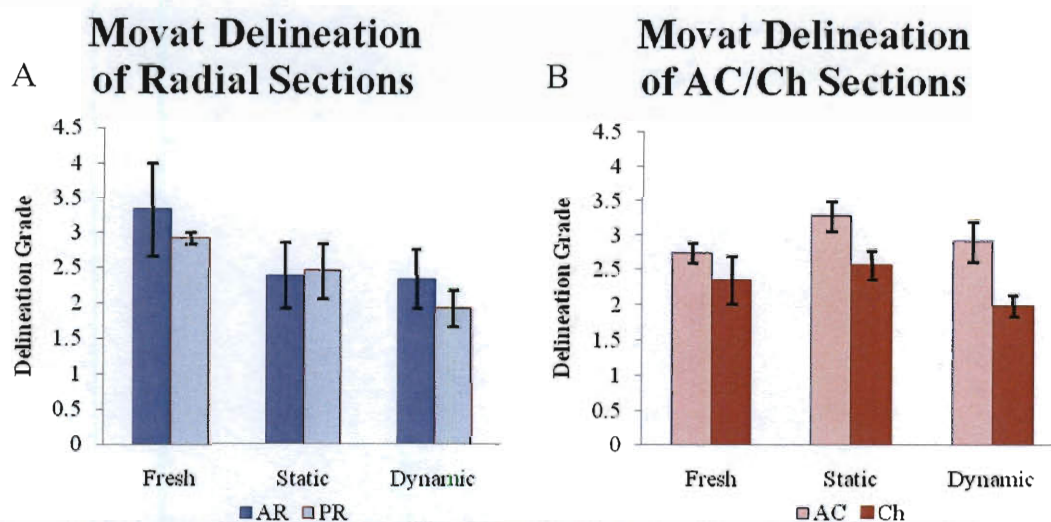


Figure 4.13. Delineation grading of Movat stained tissue sections. A) Radially oriented sections. B) AC and Ch sections.

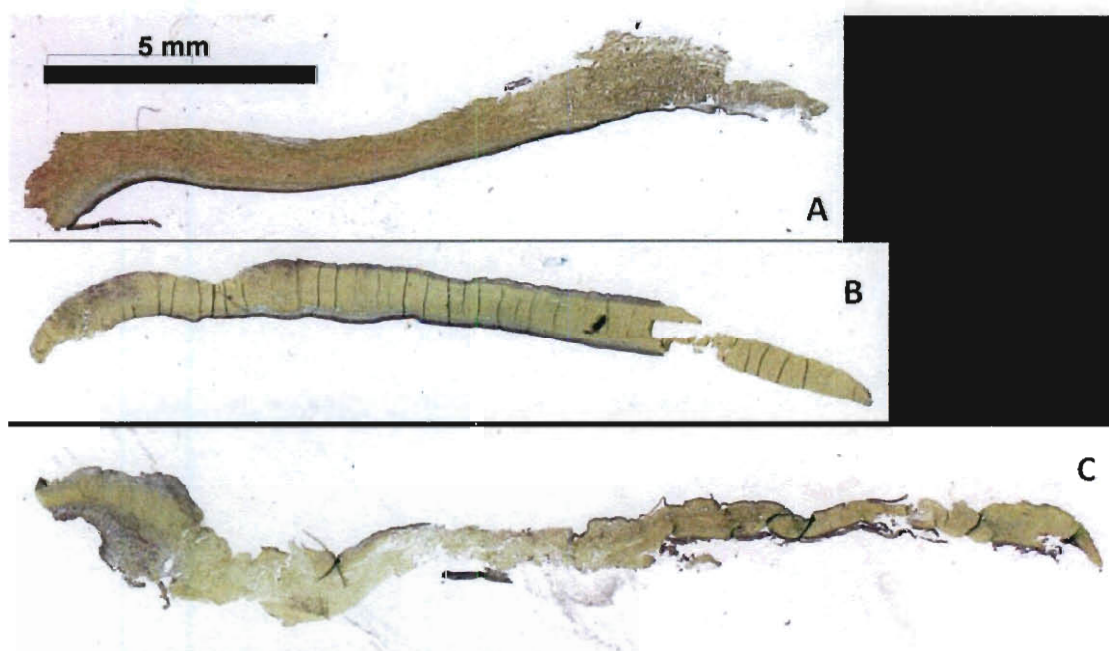


Figure 4.14. Movat stained AC tissue sections. A) Freshly harvested valve. B) Static culture valve. C) Dynamic culture valve

Movat Collagen Intensity

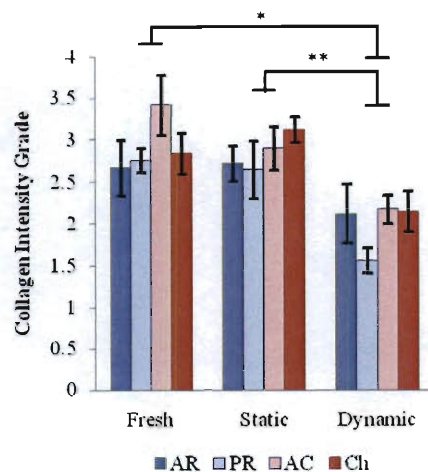


Figure 4.15. Collagen intensity grading of Movat stained tissue sections. Significant differences; *: $p = 0.0002$, **: $p < 0.0001$.

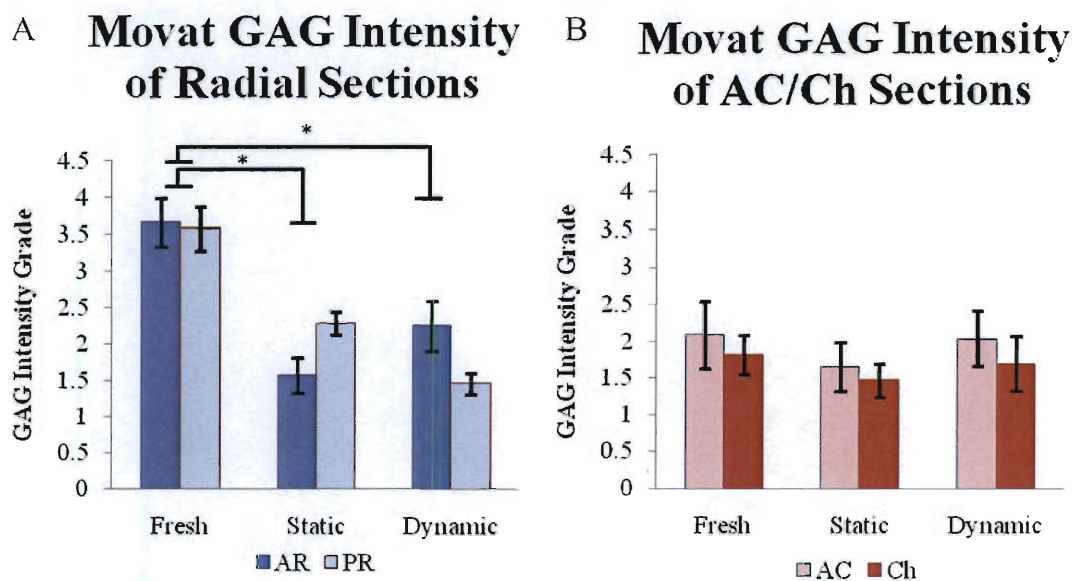
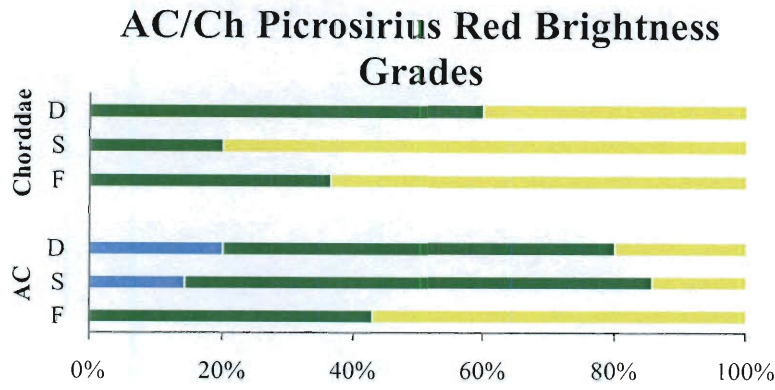
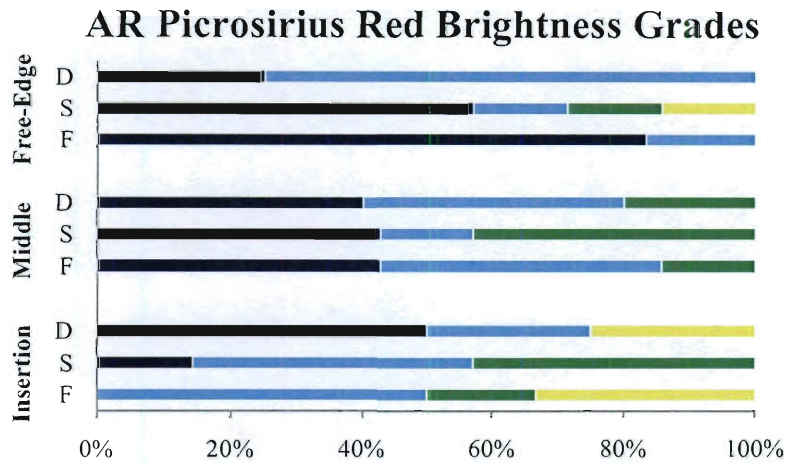


Figure 4.16. GAG intensity grading of Movat stained tissue sections. A) Radially oriented sections. B) AC and Ch sections. *: indicates significance, $p < 0.05$.

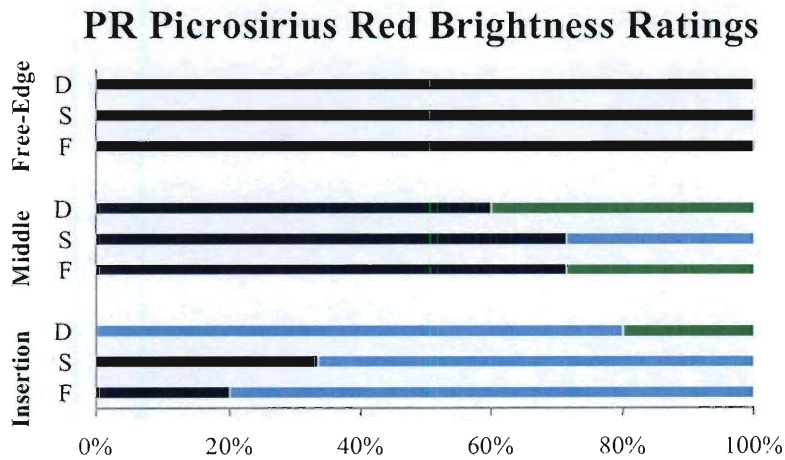
A) 1 - Little to None 2 - Low 3 - Medium 4 - High



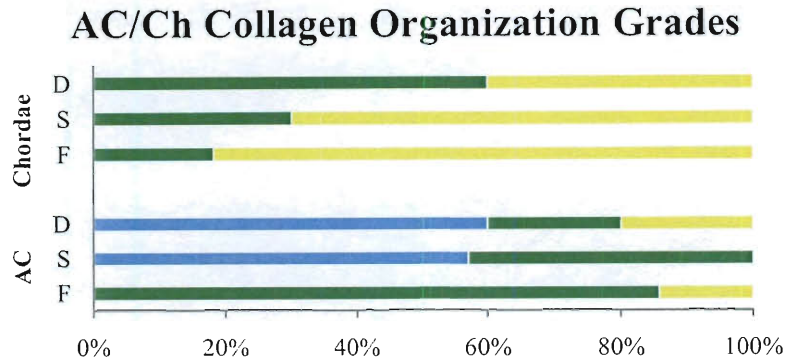
B)



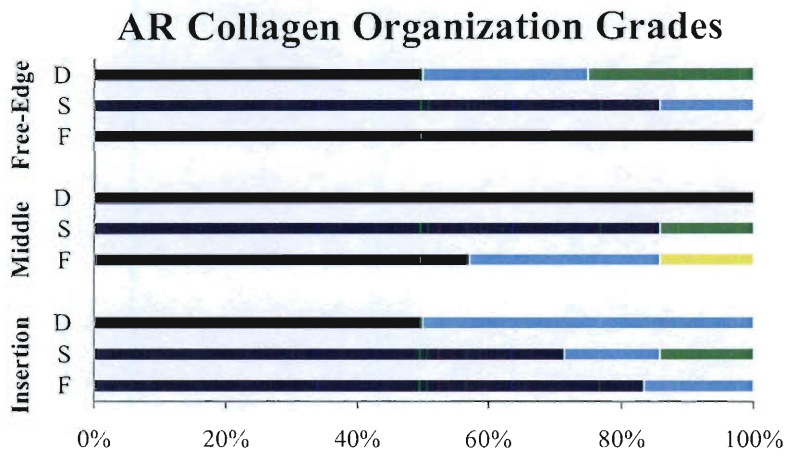
C)



D)



E)



F)

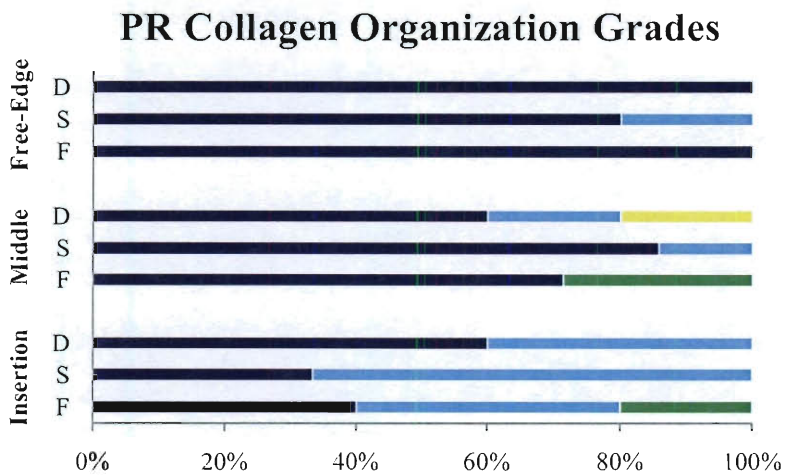
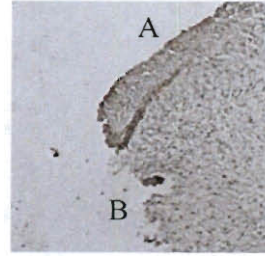


Figure 4.17 Picrosirius Red staining results. A-C) Brightness of collagen staining. D-F) Degree of collagen fiber alignment.

Figure 4.18. CD-31 staining by IHC. A) A valve surface with staining indicating an endothelial cell layer. B) An edge created by dissection without staining.



Observation of CD-31 IHC sections confirmed continuous endothelial cell layers in all samples, from all groups. Figure 4.18 shows a valve surface with staining indicating an endothelial cell layer and a surface created by dissection without staining.

Based on the separate patterns of hematoxylin staining intensity measurements (Figure 4.19), these results were separated by section type and analyzed by two-way ANOVAs. Within radially oriented sections, the three experimental groups were determined to have significantly different hematoxylin staining intensities ($F > S$, $p = 0.0289$; $S > D$, $p = 0.0229$; $F > D$, $p < 0.0001$). Within AC and Ch sections, hematoxylin staining intensity in dynamic culture specimens was significantly less than fresh ($p = 0.0368$) specimens.

PCNA staining intensity in radially oriented sections of fresh valves was significantly greater than the corresponding sections in static culture valves ($p = 0.0392$) and showed a trend of being greater than the corresponding sections in dynamic culture valves ($p = 0.0524$) (Figure 4.20a). PCNA staining in AC and Ch sections was consistent across experimental groups (Figure 4.20b). Caspase 3 staining intensity did not indicate any differences across groups (Figure 4.21). SM α A staining intensity (Figure 4.22) was analyzed by a two-way ANOVA and produced no significant results. Performing one-way ANOVAs for each section detected the SM α A staining intensity for the AC section

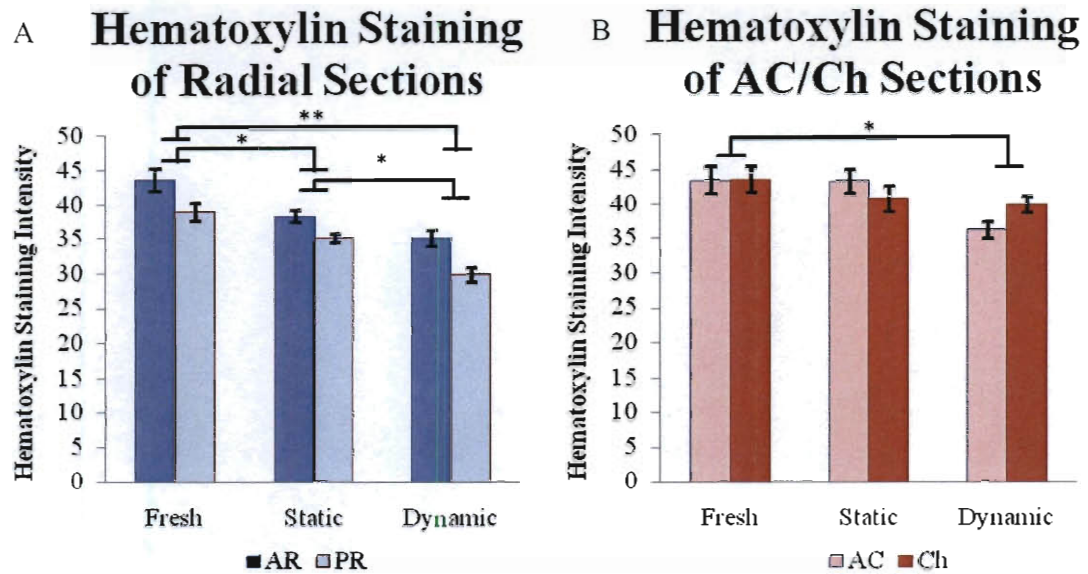


Figure 4.19. Hematoxylin staining intensity. A) Radially oriented sections. B) AC and Ch sections. Significant differences; *: $p < 0.05$, **: $p < 0.0001$.

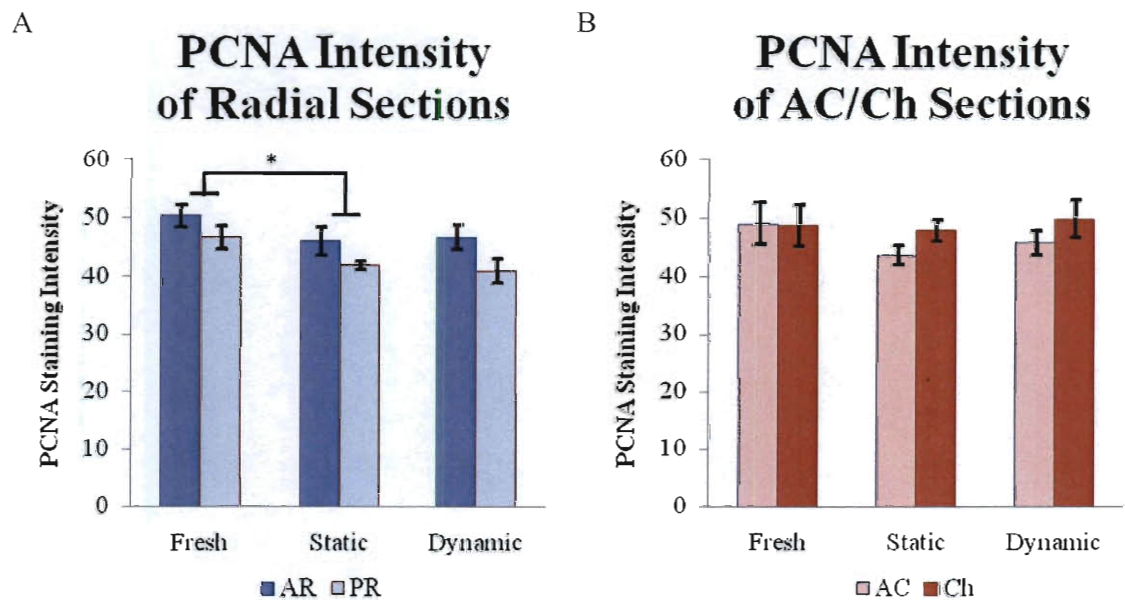


Figure 4.20. PCNA staining intensity by IHC. A) Radially oriented sections. B) AC and Ch sections. *: indicates significance, $p = 0.0392$.

A Caspase 3 Intensity

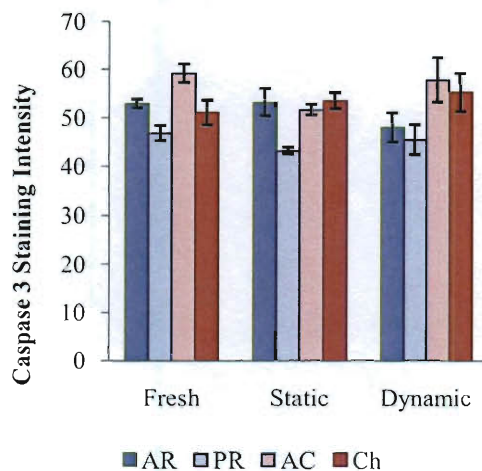


Figure 4.21. Caspase 3 staining intensity by IHC.

B SM α A Intensity

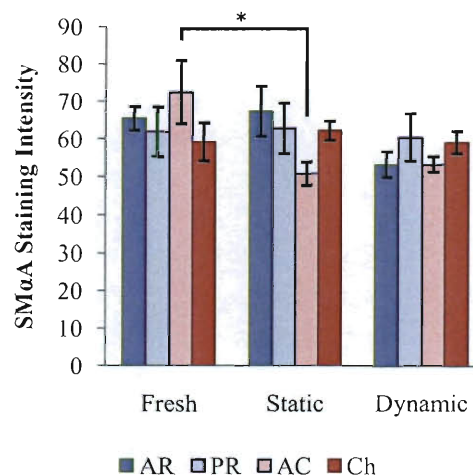


Figure 4.22. Smooth Muscle α -Actin staining intensity by IHC. *: indicates significance, $p = 0.0365$.

of static culture valves was significantly less than ($p = 0.0365$) for fresh valves. Notably, the SM α A staining intensity of the AC section of dynamic culture valves was nearly equal to that of static culture valves.

P4H staining intensity was analyzed throughout the tissue cross-sections as well as in valve regions (Figure 4.23). A one-way ANOVA performed across groups found that P4H staining intensity throughout the thickness of PR sections of static culture valves was significantly less than the staining intensity in fresh valves ($p = 0.0475$). Each valve region was analyzed by a two-way ANOVA with tissue section and experimental group as the factors and no effects were detected so one-way ANOVAs were performed within each tissue section. Analysis of the free edge of AR sections found more intense staining in static culture valves than fresh valves ($p = 0.0314$). In the same regions, the average dynamic valve staining intensity was very similar to that of fresh valves. In addition to

these analyses, another two-way ANOVA, with experimental group and valve region as the factors, was performed within each valve section. This analysis found an effect of experimental group within AR sections, but post-hoc tests found no significant differences. In the AR sections the staining intensity in static culture valves suggested an increase compared to dynamic culture valves ($p = .0626$) or fresh valves ($p = 0.0823$).

Decorin stained specimens were also analyzed through their full cross-section and within specific regions (Figure 4.24). None of the analyses found a significant effect of experimental group, but the average measured decorin staining intensity was greatest in the tissues from the dynamic control group in all measured valve regions.

The results of versican staining intensity analysis are shown in Figure 4.25. Two-way ANOVAs of versican staining intensity separated by section type found an effect of experimental group within the AC/Ch sections. Post-hoc analysis found that staining intensity in fresh valves was significantly greater than dynamic culture valves ($p = 0.0171$). No effects were found in an analysis of the staining intensity in the isolated valve regions.

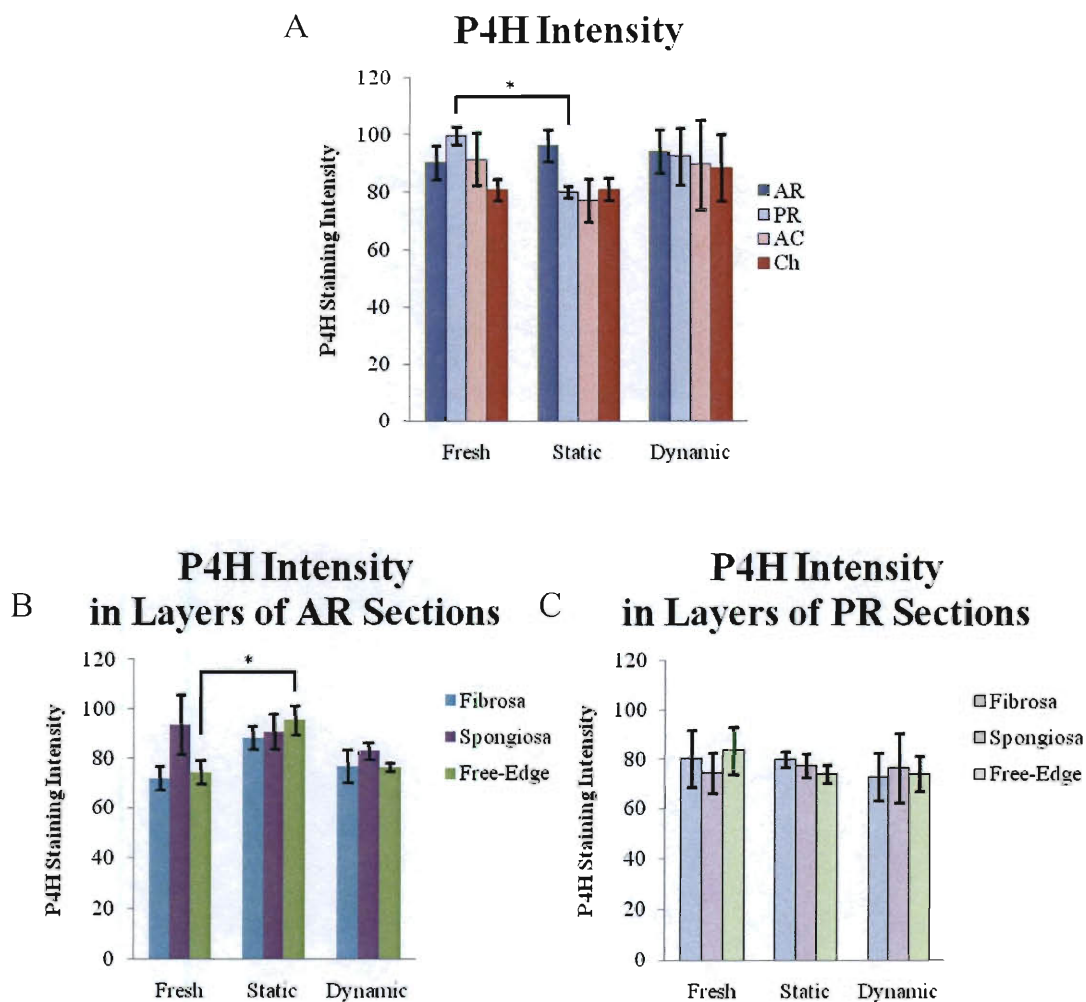


Figure 4.23. Prolyl-4-Hydroxylase staining intensity by IHC. A) Average staining intensity throughout valve sections. B) Regional staining intensity in AR sections. C) Regional staining intensity in PR sections. *: indicates significance, $p < 0.05$.

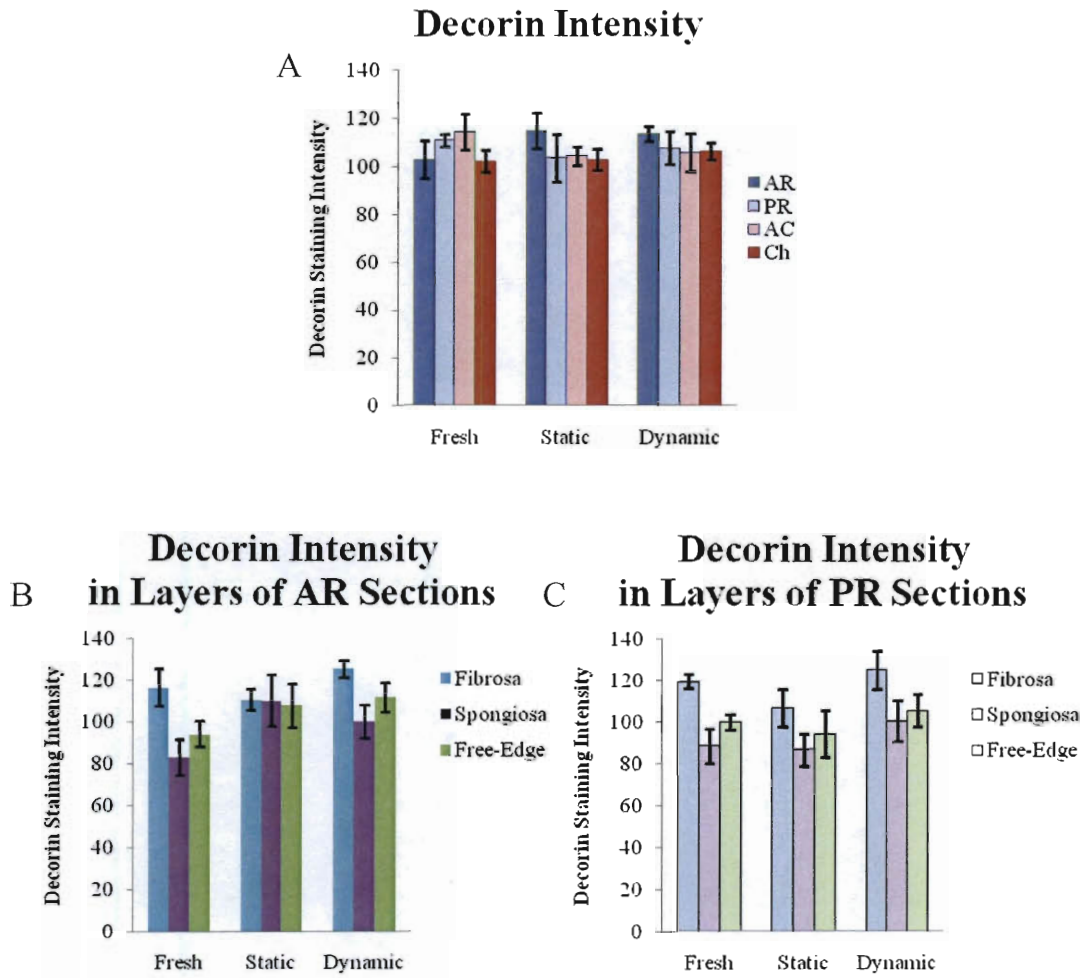


Figure 4.24. Decorin staining intensity by IHC. A) Average staining intensity throughout valve sections. B) Regional staining intensity in AR sections. C) Regional staining intensity in PR sections.

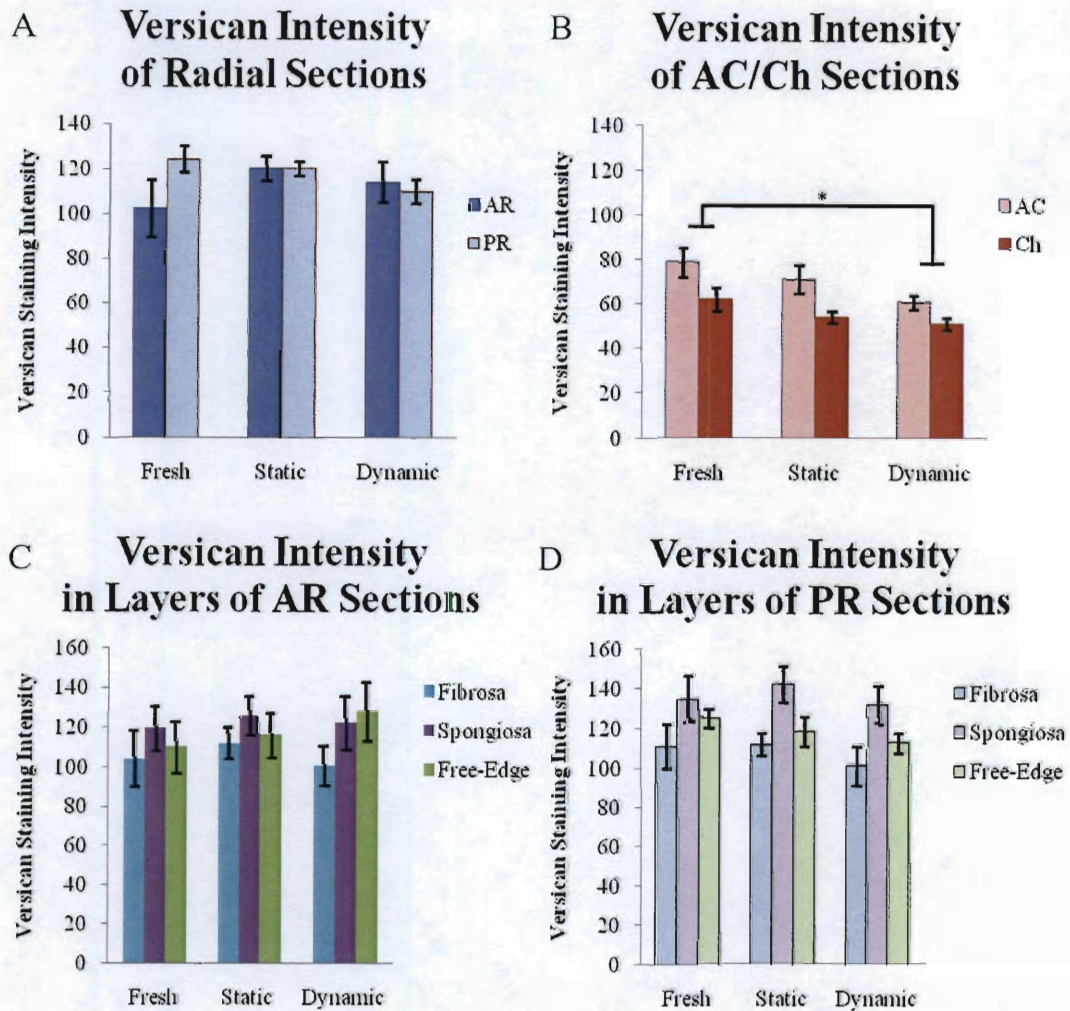


Figure 4.25. Versican staining intensity by IHC. A) Average staining intensity through radially oriented valve sections. B) Average staining intensity through AC and Ch sections. C) Regional staining intensity in AR sections. D) Regional staining intensity in PR sections. *: indicates significance, $p = 0.0171$.

A two-way ANOVA across sections and experimental groups indicated significant decreases in hyaluronan staining intensity in both the static ($p = 0.0418$) and dynamic ($p = 0.0035$) culture groups when compared to freshly harvested valves (Figure 4.26).

Analysis of staining intensity in specific valve regions did not indicate significant differences.

Analysis of the negative control and hematoxylin-only slide images indicated differences in staining intensity. The average intensities (Mean \pm SD) for Mouse secondary (54.6 ± 12.8), Rabbit secondary (47.7 ± 12.8), and hematoxylin counterstain (39.8 ± 6.0) were compared by paired t-tests and found to have significantly different staining intensities ($p < 0.0001$). This confirmed the occurrence of consistent, low-level, non-specific binding of the secondary antibodies or other components of the staining procedure.

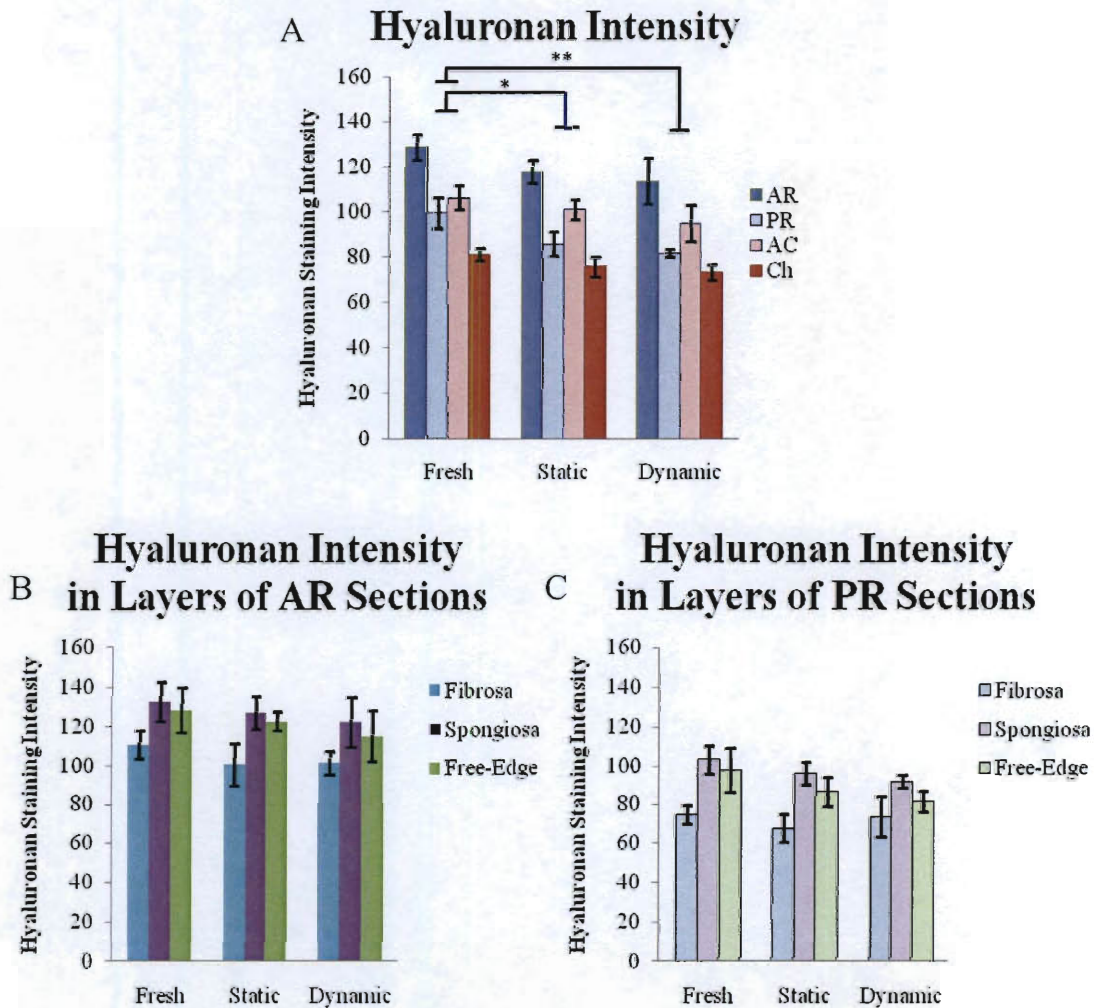


Figure 4.26. Hyaluronan staining intensity by histochemistry. A) Average staining intensity through valve sections. B) Regional staining intensity in AR sections. C) Regional staining intensity in PR sections. Significant differences; *: $p = 0.0418$, **: $p < 0.0035$

Discussion

The analyses performed in this research study, taken together with the previous studies cited earlier, have demonstrated how the absence of mechanical stimulation (static conditions) are detrimental for the organ-level culture of mitral valves. After a culture period of three weeks, the most striking physical disparities between statically cultured valves and normal valves are the overwhelming loss of cellularity, increase in water content, decrease in GAG content, and thickening of the statically cultured valve tissues. These alterations demonstrate a major degradation of the tissue and likely influenced the measured mechanical properties. The dynamic mechanical environment provided by the mitral valve organ culture system prevented some of these changes over the same three week culture period, particularly maintaining cell content and hydration. As noted earlier, similar results have been reported from comparisons of static and dynamic culture environments, for example the greater degree of cell incorporation into the middle of polymeric tissue engineering scaffolds that were exposed to dynamic flexure vs. no flexure conditions (58). The opening and closing of the mitral valve in the organ culture bioreactor in this present study also induced flexure and stretch of the valve tissue, which likely allowed for the perfusion of culture medium into the valve tissue.

The reduction in GAGs in both static and dynamically cultured valves suggested biochemically was confirmed by histology and immunohistochemistry, with both groups demonstrating loss of alcian-blue-staining hydrated GAGs and loss of hyaluronan and versican during the culture period. In contrast, the abundance of the small PG decorin (whose GAGs do not commonly stain blue using Movat) was preserved in both culture groups. It has been previously demonstrated in engineered tissue constructs that cyclic

mechanical stimulation modulates the production of various types of GAGs and proteoglycans by mitral valve cells (30), and over time leads to a greater production of sulfated GAGs and lower production of unsulfated GAGs by leaflet cells (29). Similar increases in the synthesis of sulfated GAGs were found in aortic valve leaflets subjected to cyclic hydrostatic pressure (33). The measured results did not meet the expectation that the dynamic culture environment would create this type of cyclic strain and pressure within the valve tissue and mitigate the GAG loss found in static culture. The retention of decorin and decrease in other GAGs is likely due to their specialization for tensile and compressive load-bearing functions, respectively (59). Increases in retrograde flow through dynamically cultured valves may have been associated with poor coaptation of the valve leaflets and a resulting reduction of compressive stresses in much of the valve.

The calculated tensile moduli support the role of dynamic organ culture in maintaining native valve properties. The radially oriented sections showed a significant increase in the tensile moduli of dynamic culture valves compared to static culture valves, retaining similar properties as the radial sections of fresh valves. Biochemical measurement of collagen, the principle tensile-load bearing component, showed no difference between the dynamic and static culture leaflets, with both suggesting higher collagen concentration than leaflets from fresh valves. Conversely, the AC or Ch sections showed no difference in tensile moduli between dynamic and static culture valves; both showed decreases compared to fresh valves. In these tissues, collagen was not measured biochemically, but IHC staining for decorin and P4H, markers associated with collagen and collagen synthesis, did not indicate any differences between fresh valves and either group of cultured valves. It is surprising that consistent levels of collagen concentration would be

found in tissues with such different tensile properties. However, these measurements of collagen concentration and synthesis do not indicate collagen types or fiber orientation. The decreases in tensile moduli may be accompanied by a shift towards more collagen III, which is common in heart valves but is less stiff than collagen I. In their native state, most collagen fibers in the AC and Ch sections are highly aligned along the axis of tensile loading used in this study (7, 60). A distorted strain distribution through the valve could lead to non-alignment or misalignment of collagen fibers within these sections. This adverse remodeling could result in the demonstrated decreases in tensile moduli in static and dynamic culture. While the dynamic culture does maintain collagen concentration and tensile properties in radial leaflet sections, it does not maintain the mechanical properties of the AC and Ch sections.

Comparisons of the dynamically cultured valves with freshly harvested mitral valves indicated many similarities but also some distinctive differences, such as in collagen content and associated mechanical behavior. We are currently evaluating these differences to guide our next generation of the organ culture system. For example, the differing effects of the dynamic culture environment on the tensile mechanical behavior of the valve sections may be explained by the way the chordae tendineae were mounted into the system, which could have subjected the various chordae to non-native stretch magnitudes. *In vivo*, the native chordae attach along the papillary muscles in the ventricle wall; we observed that this region of papillary chordal insertions may be as long as 2 cm, resulting in some chordae being anchored much closer to the valve leaflet than others. The current *ex vivo* system assembly, in contrast, holds all chordae at the same distance from the leaflets, which we believe improperly distributed stress through these chordae

and to the leaflets. Indeed, others have used *ex vivo* flow loops to demonstrate that different papillary muscle positions will affect leaflet strains and strain rates (61). This result could explain the trend of decreased tensile moduli in the chordal and circumferentially oriented leaflet tissues observed in the current study.

In the future development of the organ culture bioreactor, a more natural configuration of the chordae tendineae and papillary head, together with associated motion during the systolic phase, should provide a more physiological distribution of stress through the chordae and leaflets, encouraging ECM regulation that more closely maintains native properties. This could be achieved by preserving the existing helical coils that wrap around the papillary muscles, but adapting their anchoring wires to angle away from the valve orifice.

Another factor leading to less than optimal stress distribution and remodeling may have been the absence of both normal left ventricular suction and active atrial systolic pumping during the ventricular diastolic phase (62, 63). Modification of the fluid pumping system to provide this suction and pumping to fill the ventricular chamber, instead of the passive diastolic filling from the atrial reservoir, should also contribute to a more physiologically faithful organ culture system for the mitral valve.

We attempted to validate the data from this study through comparisons with other published measurements, but as this is the first long-term organ culture study of the mitral valve, we were limited to comparing the data from group F (fresh controls) to other published measurements of heart valves. In terms of biochemical measurements, the concentrations of water and GAGs (hexuronic acid) were consistent with previously

reported values (6). The concentration of DNA in these porcine valves was greater than previously found in healthy human mitral valves (64), but that may have been expected as the human valves were from older adults and valve cellularity has been shown to decrease with age (56). The DNA content also compares well with amounts measured in porcine aortic valve tissue after only 48h of culture under various levels of hydrostatic pressure (22). With respect to physical and material properties, the thickness and elastic moduli of the leaflet samples closely matched previously reported values (56). The extensibilities for fresh control leaflets were slightly lower than previously reported in that work, but demonstrated a similar pattern of greater extensibility along the radial direction (0.16 ± 0.02 mm/mm) than along the circumferential direction (0.10 ± 0.03 mm/mm) or in the chordae (0.10 ± 0.02 mm/mm). The stress relaxation parameters were also similar to (although slightly greater than) values for similar sections in the same prior study. The finding that our control data were consistent with previously reported magnitudes and patterns gave us confidence in the authenticity of the data patterns from the dynamic and static organ cultured groups.

In conclusion, despite some room for improvement, the mitral valve organ culture system described was able to maintain the cellularity of cultured valves through the use of a dynamic mechanical environment. This system provides an environment for studying valve biology that is more physiologically relevant than static organ culture and that integrates the structural organ-level interactions that are necessarily removed in cell culture studies. Such a tool can be of significant utility in investigating the causes of mitral valve disease. Chapter 5 demonstrates this capability.

Chapter 5 SIMVASTATIN INHIBITS ANGIOTENSIN-II INDUCED MITRAL VALVE REMODELING IN AN *EX VIVO* ORGAN CULTURE MODEL

Introduction

This chapter shifts focus from the development and testing of the organ culture system to its implementation as an experimental model. The aim, as introduced in Chapter 1, is to:

Employ the organ culture system to study the ex vivo effects of Angiotensin II, alone and in combination with Simvastatin, on mitral valve tissue.

Background

The AHA estimates that in 2010, a 40-yr old man or woman has a 1 in 5 risk of developing heart failure (HF) within their lifetime (1). This widespread disease, in which the heart's ability to pump blood is reduced and thus it cannot meet the body's needs, generally occurs in the left heart. It begins with an initial ailment, commonly hypertension or myocardial infarction, decreasing the ventricular ejection fraction. The resulting ventricular dilation further decreases the myocardium's force of contraction. The disease can also develop towards hypertrophy as the heart remodels to impede the dilation. In either case, the heart is weakened, contributing to progression of the disease state.

During HF, a host of vasoactive agents are found in the bloodstream in elevated levels, including angiotensin II (AII), part of the renin-angiotensin System that is meant to regulate total blood volume and pressure (65). In addition to being a potent vasoconstrictor, AII has also been found to affect the turnover of extracellular matrix

(ECM) molecules in cardiovascular cells. An *in vitro* study of human cardiac fibroblasts demonstrated an increase in collagen synthesis caused by AII (66). AII acted to stimulate incorporation of proline, a major component of collagen, with effects maximized with a AII concentration of 10 nM to 10 μ M. Blocking the angiotensin type-1 receptor (AT-1), but not type-2 receptor (AT-2), inhibited these effects.

The valves of the heart show signs of dysfunction in the development and progression of HF. A study of dilated cardiomyopathy found mild to severe mitral regurgitation (MR) in a majority of cases (67). The effects of MR often further contribute to the decline in cardiac output. MR can occur either as a result of defects within the valve (known as organic MR), or as functional MR, in which the valve is anatomically healthy but dysfunctional because of external factors such as changes to cardiac anatomy.

Determining the cause of MR is important because the most effective treatment differs based on the underlying cause (67). In cases of dilated cardiomyopathy, cardiac remodeling displaces papillary muscles and dilates the valve annulus. These geometric alterations pull apart the valve leaflets, preventing ideal leaflet coaptation (68).

Additionally, elevated levels of AII and other hormones associated with HF may cause pathological remodeling in the mitral valve leading to MR, although the effects of such altered blood chemistry on valves have received little attention. Mitral valves from HF patients demonstrated increased cell, glycosaminoglycan (GAG), and collagen content as well as decreased tissue hydration seemingly resulting from altered cardiac geometry (64). Based on this altered anatomy, the MR found in HF does not appear to be functional, but it is unclear as to the relative effects of mechanical- and biochemical-based remodeling.

Statins, also known as HydroxyMethylGlutaryl Coenzyme A Reductase Inhibitors, are effective in reducing high cholesterol (69, 70) and are attributed with additional benefits in treating a variety of cardiovascular diseases (71), including heart failure (72, 73) and for selected patients with valve disease(74). Statins have also been shown to decrease vascular fibrosis caused by AII (75) and would be a good candidate to prevent adverse AII-induced valve remodeling.

With the pathogenesis of MR only now being adequately investigated, prevention is not yet feasible and treatments have, until recently, been limited to surgical interventions (76). The current study investigates the possible role of AII in pathological remodeling of the mitral valve. Further, simvastatin is evaluated for any ability to inhibit any effects of AII, as a representative of the class of statin drugs. In order to provide a culture environment more physiologically appropriate than a cell culture study, we utilized the *ex vivo* organ culture system described and characterized in Chapter 3 and Chapter 4. This system provides a physiological level of mechanical stimulation and helps to maintain cultured mitral valves in a more native state, most notably retaining high levels of cell viability.

Materials and Methods

Organ Culture System

Details of the assembly and function of the mitral valve organ culture system have already been described. In brief, the system is a mock circulation consisting of three major components: a “ventricular” pumping chamber that housed the porcine explant valves, a compliance chamber that conditioned the flow response, and a raised and vented

reservoir that supplied an “atrial” filling pressure. An electronic pressure regulator created a pneumatic pumping action through a silicone diaphragm. The pulsatile pressure waveform was controlled by a Virtual Instrument created with LabView software (National Instruments, Austin, TX) and configured with a peak of 120 mmHg and frequency of 60 beats per minute.

Harvest, Preparation, and Culture of Valves

The harvest and preparation of the mitral valves and the culture system assembly were performed with the procedures described in Chapter 4.

Each treatment group used approximately 1.4 L M199 culture medium, supplemented with 10% Bovine Growth Serum (BGS, Thermo-Hyclone, Logan, UT) and 1% anti-microbial solution. The Control group (CTRL, n=5) had no extra supplement. The AII Low group (AL, n=4) was supplemented to include 10 nM AII (EMD Chemicals, Gibbstown, NJ). The AII High group (AH, n=4) was supplemented with 10 μ M AII. The Simvastatin group (Sim, n=4) was supplemented with a 10 μ M dose of AII and 10 μ M of Simvastatin (EMD Chemicals). These concentrations were chosen based on concentrations previously shown effective *in vitro* (66, 75, 77-79). The entire system was maintained in a humidified incubator at 37° C and 5% CO₂ for 21 days; the culture medium was drained and replaced every 7 days. Previous studies of both AII (80) and simvastatin (81) have confirmed their stability in the heated environment for this duration. Pressure within the ventricular chamber and flow rates just upstream from the mitral valve were recorded throughout the culture period. Flow measurements of full pumping cycles were selected from five time points during each valve’s culture: Days 1,

4, 7, 14, and 21. The total flow rate was calculated by integrating the instantaneous flow rate. Forward flow was calculated from the integral of all positive flow values and retrograde flow from the integral of all negative flow values.

After the 21 day culture period, the valves were removed from the organ culture system and prepared for analysis. The valves were each photographed and then dissected into seven sample sections. These sections were identified as: anterior leaflet radial strip (AR), anterior leaflet circumferential strip (AC), two anterior strut chordae (Ch), the remaining anterior leaflet tissue (Ant), posterior leaflet radial strip (PR), and the remaining posterior leaflet tissue (Post). While the Ant and Post sections were used for biochemical analyses, the other sections were reserved for material testing and were subsequently prepared for histological analyses. Note that the remaining chordae were dissected from the leaflet samples.

Biochemical Analyses

Biochemical assays were performed on each Ant and Post specimen according to the procedures described in Chapter 4. These assays measured water, DNA, GAG, and collagen content.

Materials Testing

Uniaxial tensile load-elongation tests were performed on each AC, AR, PR, and Ch specimen according to the procedures described in Chapter 4. Equipment faults rendered stress relaxation data unusable due to sample size.

Histological and Immunohistochemical Staining

After tensile testing, the sections were immersed in formalin overnight, dehydrated using a series of graded alcohols, soaked in xylene, and embedded in paraffin blocks according to standard procedures for histological processing. The tissue blocks were then sliced into 5 μm thick cross-sections and set onto positively-charged glass slides. Tissue cross-sections were stained with a Movat Pentachrome to visualize ECM and the leaflet structure. Samples were also stained with Picrosirius Red to observe collagen fiber alignment as described in Chapter 4. An Alizarin Red stain was applied to indicate the extent of any calcification, which would be marked by dark red staining over the pink background.

Immunohistochemical (IHC) staining was also used to localize several markers of cell and tissue phenotype. IHC was performed according to standard procedures involving primary antibodies that demonstrate valve cell phenotype or tissue ECM composition (Table 5.1), biotinylated secondary antibodies (Jackson ImmunoResearch, West Grove, PA), visualization via a chromogen reaction, and a nuclear hematoxylin counterstain. In order to control for non-specific binding, negative controls for each secondary antibody were performed with no primary antibody on every specimen. In addition, a set of hematoxylin-only slides were prepared to quantify nuclear staining.

Three markers were stained to investigate the modulation of valve cell phenotype. The AII type-1 receptor (AT-1) was selected because it has been found to mediate increased synthesis of collagen in human cardiac fibroblasts (66). It has also been found by immunohistochemistry in greatly elevated levels in sclerotic aortic valves, co-localized

Table 5.1. Immunohistochemistry Markers. Sources: A) Abcam, Cambridge, MA. B) Lab Vision, Fremont, CA. C) A gift from Dr Larry Fisher, NIH. D) Associates of Cape Cod, East Falmouth, MA. HA is detected using biotinylated HA Binding Protein in place of a primary and secondary antibody. E) Millipore, Billerica, MA. F) Dako, Carpinteria, CA. G) BioVision, Mountain View, CA.

Marker	Dilution	Secondary Antibody	Antigen Retrieval	Relevance
Angiotensin II Receptor 1 (AT-1) ^A	1:200	Mouse	Citric Acid – Heat Mediated	Mechanism for AII effects, elevated in sclerotic valves
CD-31 ^B	1:50	Rabbit	Citric Acid – Heat Mediated	Endothelial cell marker
Collagen III ^C	1:500	Rabbit	None	Collagen sub-type
Decorin ^C	1:500	Rabbit	Chondroitinase ABC	Collagen formation and organization
Hyaluronan ^D	1:250	N/A	None	Located in areas of compressive loads
Prolyl-4-Hydroxylase (P4H) ^E	1:200	Mouse	Citric Acid – Heat Mediated	Enzyme marker of collagen synthesis
Smooth Muscle α -Actin (SM α A) ^F	1:1000	Mouse	Citric Acid – Heat Mediated	Valve cell activation, localized in valve lesions
Transforming Growth Factor- β (TGF- β) ^G	1:20	Rabbit	Citric Acid – Heat Mediated	Downstream AII product, increases collagen, biglycan synthesis
Versican ^D	1:500	Mouse	Chondroitinase ABC	Located in areas of compressive loads, disrupted in valve disorders

with Smooth Muscle α -Actin (SM α A) (82). SM α A was also selected for IHC staining and is a marker for 'activated' valve interstitial cells found in developing, diseased, and otherwise remodeling mitral valves (18, 83). Increased SM α A expression has been shown to occur *in vitro* after the addition of Transforming Growth Factor- β (TGF- β), an effect that is inhibited by simvastatin (78). TGF- β was also selected for IHC staining because it is a downstream product of AII, mediated by AT-1 (84). TGF- β has been implicated in the formation of valvular lesions in part because it induces increased production of sulfated GAGs and hyaluronan from aortic valve cells (85). These three markers were examined together to detect phenotypic modulation of valve cells under the prescribed culture conditions and to attempt to explain mechanisms for any resulting ECM modulation.

Collagen was the focus of another three IHC markers. Prolyl-4-Hydroxylase (P4H) is an enzyme involved in the early stages of collagen synthesis (86). More intense P4H staining is suggestive of increased collagen synthesis. Collagen I and III are the two major collagen subtypes found in valve tissues (87). Collagen III content can vary independently of collagen I and IHC staining can indicate regional distributions of collagen III within the valve. Decorin is a Small leucine-rich proteoglycan (SLRP) that mediates the formation and organization of collagen fibrils (88) and its core protein has a binding site for TGF- β (89).

Hyaluronan is a large GAG molecule and versican is a large PG. Both molecules can bind substantial volumes of water and they are found in valve regions that typically experience compressive stresses (6). These markers were evaluated using IHC to detect major changes in ECM composition and because their regional distribution can be indicative of

valve disorders (90). It should be noted that the procedure for staining hyaluronan does not involve primary and secondary antibodies but rather the biotinylated Hyaluronan Binding Protein (HABP).

After completing staining procedures, most slides were digitally scanned at 7200 dpi with a PathScan Enabler IV slide scanner (Meyer Instruments, Houston, TX) to facilitate digital and observational image analyses. The Picrosirius Red slides were instead imaged with a microscope system (Leica DMIL, Buffalo Grove, IL) under polarized light. Radial sections were imaged at the valve insertion, mid-leaflet, and at the free-edge. They were then analyzed semi-quantitatively for staining brightness and the uniformity of collagen alignment and sorted into four grades for each characteristic. Movat-stained sections were randomized and analyzed using a semi-quantitative scale for distinct delineation of the layered structure, abundance of saffron-stained collagen, and abundance of alcian blue-stained GAGs (57). Every specimen was graded on a scale of 1 to 4 for each attribute. Slide images from IHC were analyzed to measure the relative staining intensity of each marker throughout the tissue cross-section. Calculation of average staining intensity was automated with a batch macro in ImageJ (NIH, Bethesda, MD) that utilized particle analysis to isolate tissue sections from the image background. The resulting value was a measurement, ranging 0-255, of the average staining intensity of the region analyzed within each cross-section.

Statistical Analysis

Statistical calculations were performed using JMP software (SAS, Cary, NC). Average values were calculated and are expressed here as mean \pm SE. Each data set was analyzed

by two-way ANOVA, separating specimens by both treatment group and valve section. Data sets were also analyzed by one-way ANOVA across treatment groups when results were inconsistent across valve sections. In certain cases, sections were separated into radially oriented (AR/PR) and AC/Ch “section types” that share similarities in typical loading and structural characteristics. Separate two-way ANOVAs were performed on each section type across section and experimental group. A Tukey’s test was used for post-hoc analysis with a level of significance set at 0.05.

Results

Flow Measurements

Average flow measurements varied among the experimental groups but demonstrated the same trends (Figure 5.1). A two-way ANOVA comparing time points and experimental groups found that average forward flow generally increased a very small amount after 21 days, from 2.62 ± 0.10 L/min to 2.86 ± 0.06 L/min. Over the same period, retrograde flow immediately increased significantly, from 0.66 ± 0.09 L/min on day 1 to 1.06 ± 0.09 L/min on day 4 ($p = 0.0140$) and to 1.37 ± 0.10 L/min on day 21 ($p < 0.0001$). Due to the greater increase in retrograde flow than forward flow, total flow decreased, also significantly, from 1.96 ± 0.13 L/min to 1.49 ± 0.12 L/min ($p = 0.0194$). Between groups, the two-way ANOVA detected a significantly lower retrograde flow for AL samples than Sim ($p = 0.032$) or AH ($p = 0.02$) and significantly greater total flow for AL samples than Sim ($p = 0.02$), AH ($p = 0.0054$), and CTRL ($p = 0.0014$). The same analytical techniques suggested no differences between the peak ventricular pressures of

the selected pumping cycles. The overall average peak pressure was 108.7 ± 0.8 mmHg, lower than the target peak of 120 mmHg.

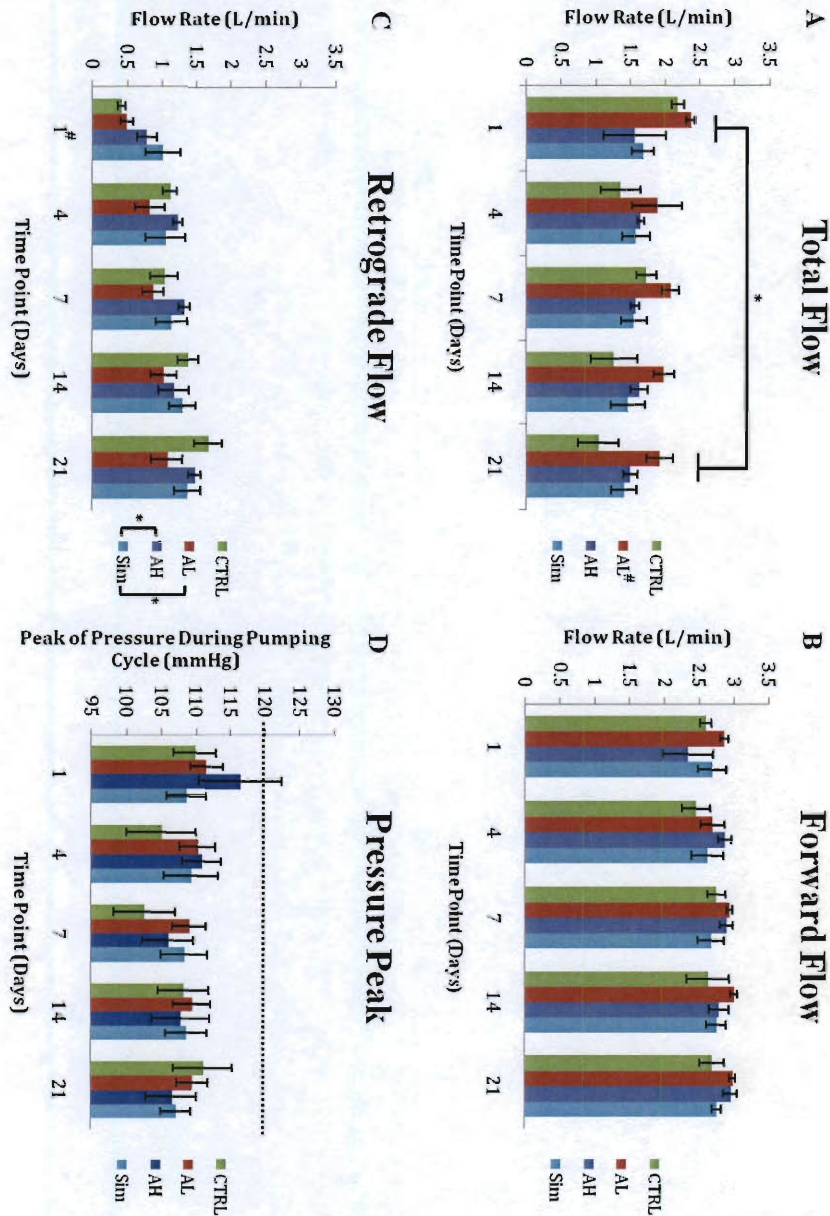


Figure 5.1. Flow Characteristics. A) Total (net) flow rate through the mitral valve. B) Forward flow rate through the mitral valve into the ventricular chamber. C) Retrograde flow rate from the ventricular chamber back through the mitral valve. D) The peak pressure reached in the ventricular chamber during the pumping cycle. #: Significantly different than all other comparison sets, $p < 0.014$. *: Indicates significant difference, $p < 0.0313$.

Table 5.2. Thickness (mm) of Valve Sections in Different Groups.

Tissue Section	Control	10 nM AII	10 μ M AII	10 μ M AII + 10 μ M Simvastatin
PR	1.2 \pm 0.1	1.3 \pm 0.1	1.4 \pm 0.1	1.4 \pm 0.1
AR	1.4 \pm 0.1	1.3 \pm 0.1	1.2 \pm 0.1	1.4 \pm 0.2
AC	1.3 \pm 0.1	1.3 \pm 0.1	1.4 \pm 0.1	1.3 \pm 0.1
Ch	1.4 \pm 0.1	1.4 \pm 0.1	1.3 \pm 0.1	1.2 \pm 0.1

Macroscale Anatomy

The photographs of valves taken immediately upon removal from the organ culture system did not suggest any macroscale differences in the valve groups. The same is true for thickness measurements taken prior to materials testing (Table 5.2). No significant differences in thickness were detected across experimental groups by 1-way ANOVA.

Biochemical Analyses

A two-way ANOVA performed on the results of the biochemical assays measuring DNA content and tissue composition did not reveal any statistically significant differences between groups (Figure 5.2). These collective analyses suggested increases in collagen content ($p = 0.0931$) and DNA content ($p=0.1645$) and decreases in GAG content ($p = 0.1553$) as a result of dose-dependent responses to AngII and the corresponding inhibitive effects of Simvastatin on collagen content ($p = 0.1215$) and GAG content ($p = 0.1673$). There were no significant differences in tissue hydration. This same data is detailed in Table 5.3Error! Reference source not found..

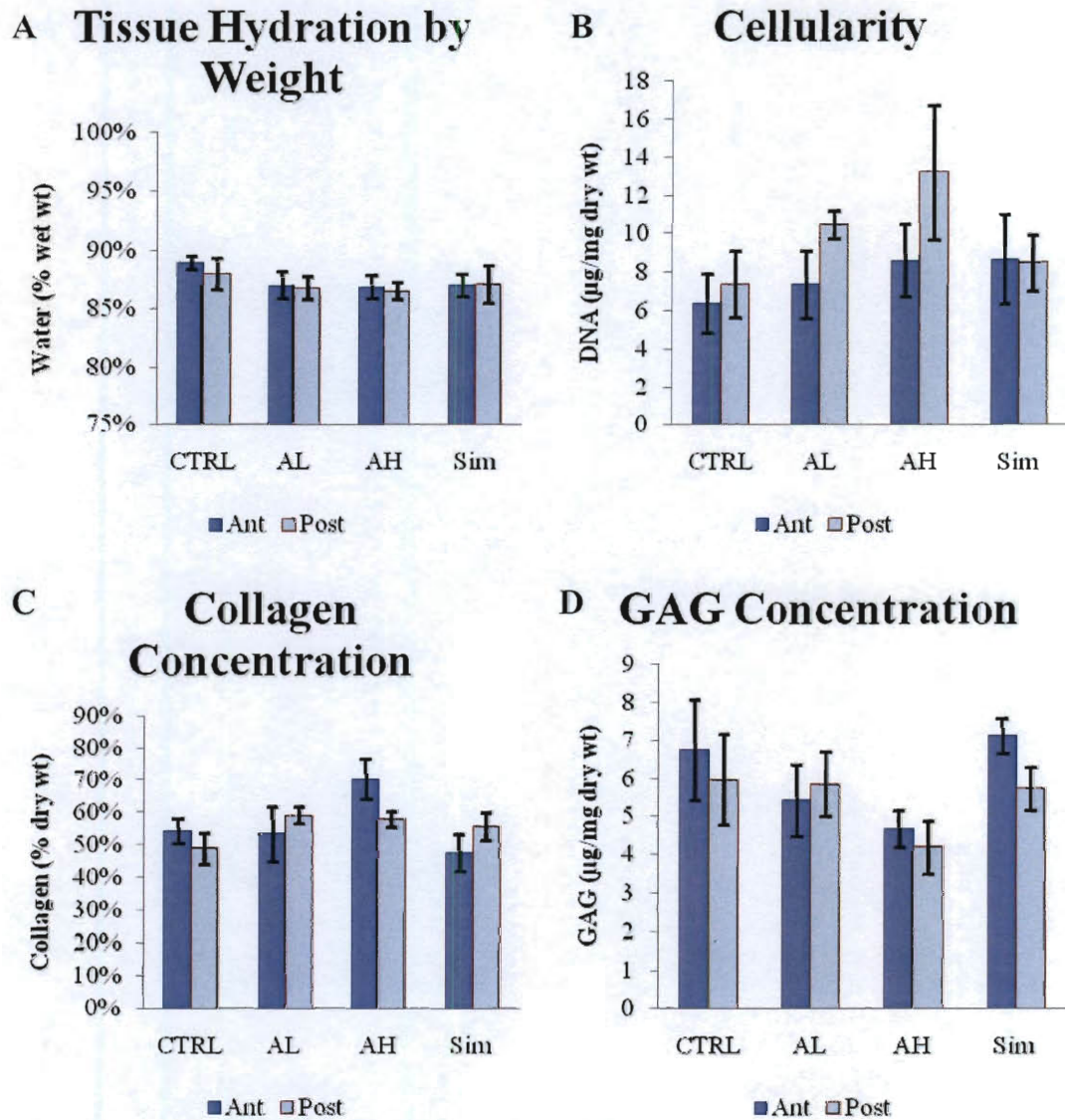


Figure 5.2. – Biochemical Assay Results. The values for the Ant and Post sections were not statistically different and were grouped together for analysis. A) Average hydration. B) Average collagen content, based on measurement of hydroxyproline. C) Average glycosaminoglycan (GAG) content, based on measurement of uronic acid. D) Cellularity, based on measurement of DNA.

Table 5.3. ECM Composition and DNA Content by Treatment Group. Anterior and Posterior sections are grouped together.

	Control	10 nM AII	10 μ M AII	10 μ M AII + 10 μ M Simvastatin
Hydration (% wet wt)	88.4 \pm 0.7	86.9 \pm 0.7	86.7 \pm 0.6	87.0 \pm 0.9
Collagen (% dry wt)	51.6 \pm 3.1	56.3 \pm 4.2	64.2 \pm 3.9	51.7 \pm 3.7
GAG content (μ g/mg dry wt)	6.36 \pm 0.85	5.63 \pm 0.60	4.43 \pm 0.40	6.42 \pm 0.43
DNA content (μ g/mg dry wt)	6.87 \pm 1.10	8.93 \pm 1.05	10.92 \pm 2.05	8.59 \pm 1.27

Materials Testing

Because of the evident differences in both the scale and patterns of tensile modulus results, the data from radially oriented sections was analyzed separately from the AC/Ch sections (Figure 5.3). When the radial sections were considered together in a two-way ANOVA across group and section the tensile modulus of the Sim group radial sections (5.9 \pm 2.1 MPa) was found to be greater, though not significantly, than that of the AL group radial sections (2.6 \pm 0.3 MPa, $p = 0.1423$). A two-way ANOVA performed on data from AC and Ch sections suggested as trends that the tensile moduli of Sim specimens (85.9 \pm 19.1) was greater than CTRL specimens (41.6 \pm 8.0, $p = 0.0630$) and AH specimens (48.2 \pm 10.6, $p = .1891$).

Extensibility measurements demonstrated a much stronger pattern of results (Figure 5.4). A two-way ANOVA across section and group was performed on this data. The AII low dose (AL) samples did not demonstrate any difference from CTRL samples. The high dose (AH) samples, however, did demonstrate a significantly greater average extensibility (0.168 \pm 0.013) than the CTRL (0.114 \pm 0.009, $p = 0.0005$) and AL (0.112 \pm 0.011, $p = 0.0012$) samples. The extensibility of Sim samples (0.133 \pm 0.010) did not

demonstrate a significant difference with any other treatment group, but data suggested that the Sim treatment reversed the increased extensibility of AH samples ($p = 0.1743$).

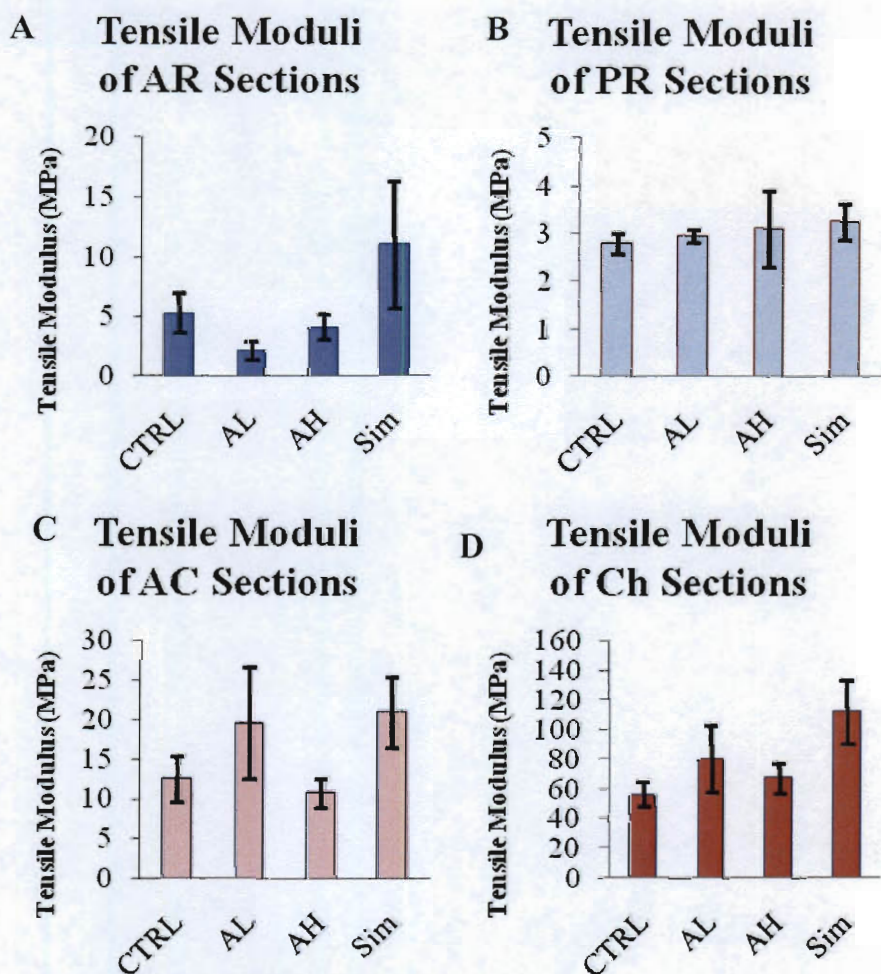
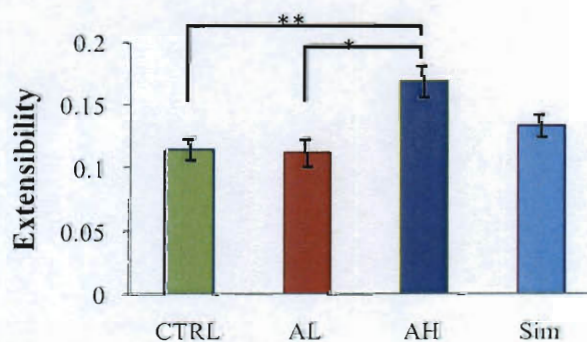


Figure 5.3. Tensile modulus mea: statistical analysis. A) AR Section

Figure 5.4. Extensibility across experimental groups. Values from separate sections were analyzed together. Stars indicate significance: *, $p = 0.0112$; **, $p = 0.0005$.

Average Extensibility by Group



Histology and Immunohistochemistry

Because of the disparate patterns in different tissue sections, the Movat results were analyzed separately by one-way ANOVA. Grading of layer delineation in Movat-stained group (data not shown). The grading of saffron collagen staining demonstrated significantly increased collagen intensity in the chordae when treated with increasing concentrations of angiotensin II ($p = 0.0245$). A strong trend suggested inhibition of this increase associated with the addition of simvastatin ($p = 0.0514$) (Figure 5.5a). The grading of Alcian Blue GAG staining suggested two contrasting effects (Figure 5.5b). Among the radial sections, GAG staining in the Sim specimens was less intense than CTRL specimens ($p = 0.1082$). A one-way ANOVA found that this relation was significant when limited to only PR samples ($p = 0.0457$). Among AC and Ch specimens, GAG staining was increased in the Sim group, compared to AH (trend, $p = 0.1296$). Alizarin Red staining did not indicate any calcific nodes in any samples.

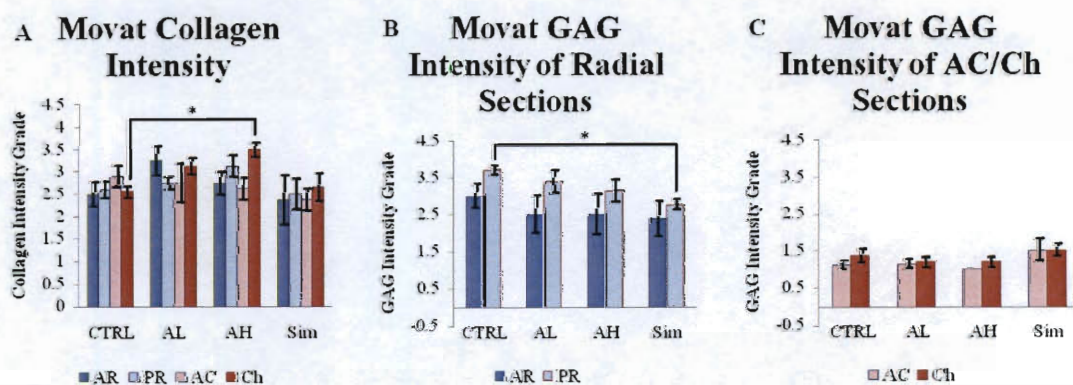
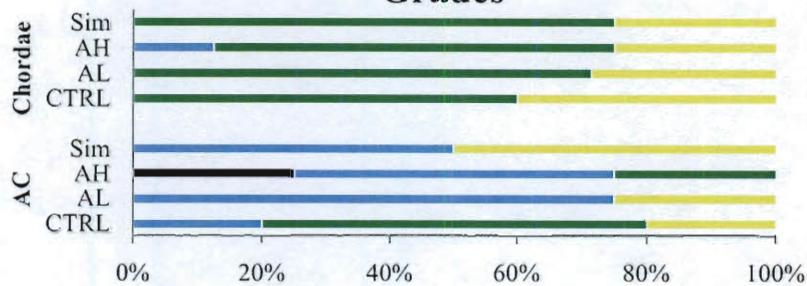


Figure 5.5. Movat Grading Results. A) Saffron staining for collagen. B) Alcian Blue staining for GAGs. Movat-stained sections were graded on a 1-4 scale for each property by a blinded observer. *: Indicates significance, $p < 0.0457$.

■ 1 - Little to None ■ 2 - Low ■ 3 - Medium ■ 4 - High

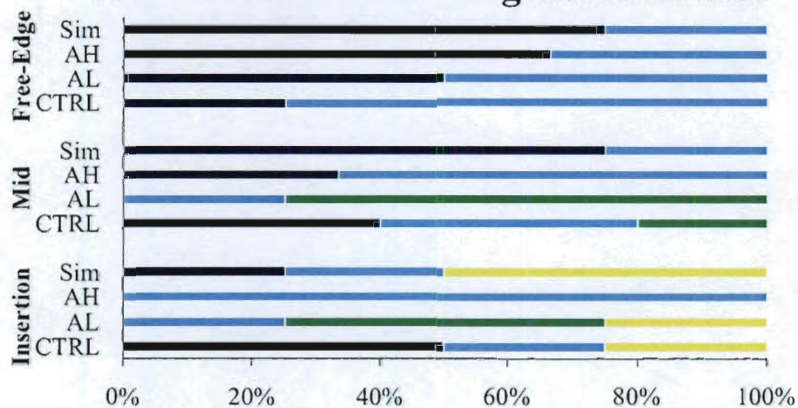
A)

AC/Ch Picrosirius Red Brightness Grades



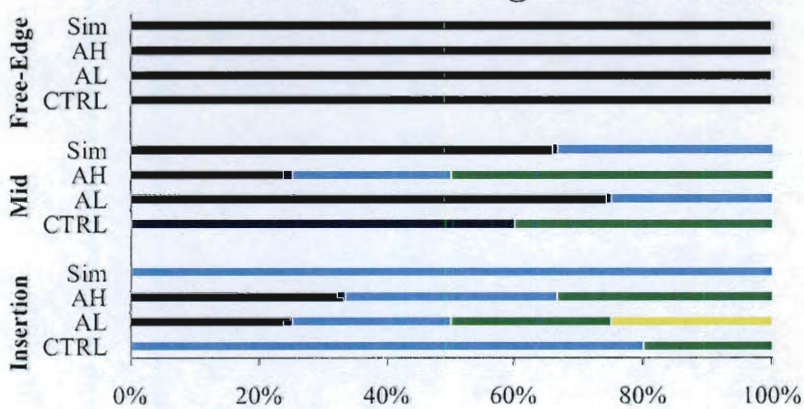
B)

AR Picrosirius Red Brightness Grades



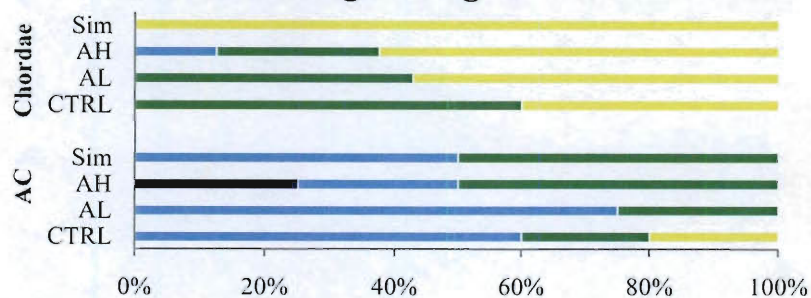
C)

AR Picrosirius Red Brightness Grades



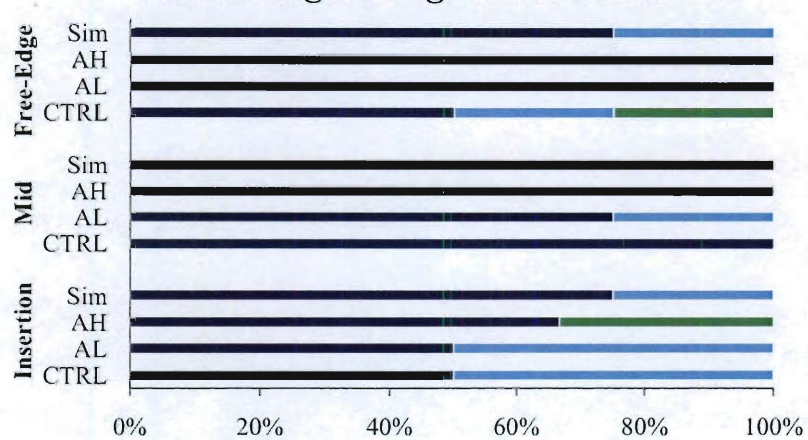
D)

AC/Ch Collagen Organization Grades



E)

AR Collagen Organization Grades



F)

PR Collagen Organization Grades

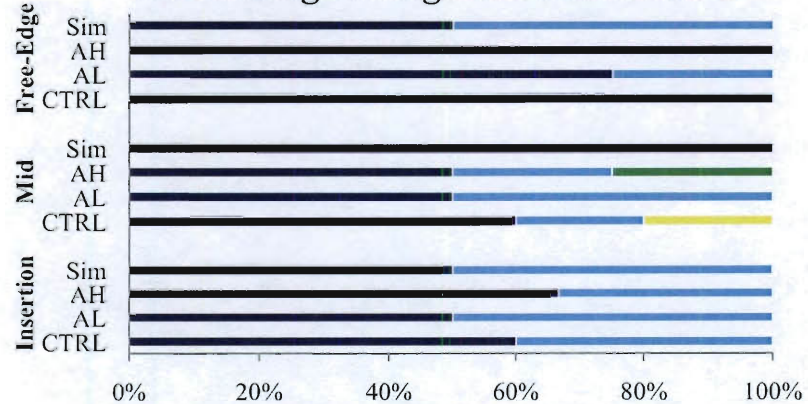


Figure 5.6 Picrosirius Red staining results. A-C) Brightness of collagen staining. D-F) Degree of collagen fiber alignment.

Picrosirius Red images exhibited varying levels of staining brightness and collagen organization between sections and valve regions, but no statistically significant differences were detected between experimental groups (Figure 5.6).

A one-way ANOVA of collagen III IHC in PR sections suggested that the staining intensity of AH samples was less than CTRL samples, although this was only a trend ($p = 0.0849$). A two-way ANOVA within the AC/Ch section type demonstrated that collagen III staining was significantly less intense in Sim samples than CTRL samples ($p = 0.0026$). Trends in the same analysis suggested Sim staining was also less than AL ($p = 0.1075$) and AH ($p = 0.1109$). The collagen III intensity results are shown in Figure 5.7. IHC staining for decorin, P4H and SM α A produced no significant or notable results (data not shown).

IHC staining for neither AT-1 nor TGF- β produced significant results or patterns consistent between tissue groups (data not shown). However, these markers were co-localized and the intensity results of the two markers appeared to match each other well (Figure 5.8a). Performing a linear regression on the two data sets confirmed the moderate correlation ($R^2 = 0.47$, Figure 5.8b).

Statistical analysis of staining for hyaluronan indicated no significant differences in intensity between the AII-treated groups and the control group. HA staining in the Sim group was significantly less intense than all other groups ($p < 0.001$). Again, this comparison is most clear with all tissue sections grouped together (Figure 5.9a).

Hyaluronan staining intensity was also measured in specific regions of the radially oriented sections: the fibrosa, spongiosa, and free-edge (Figure 5.9b&c). These region-

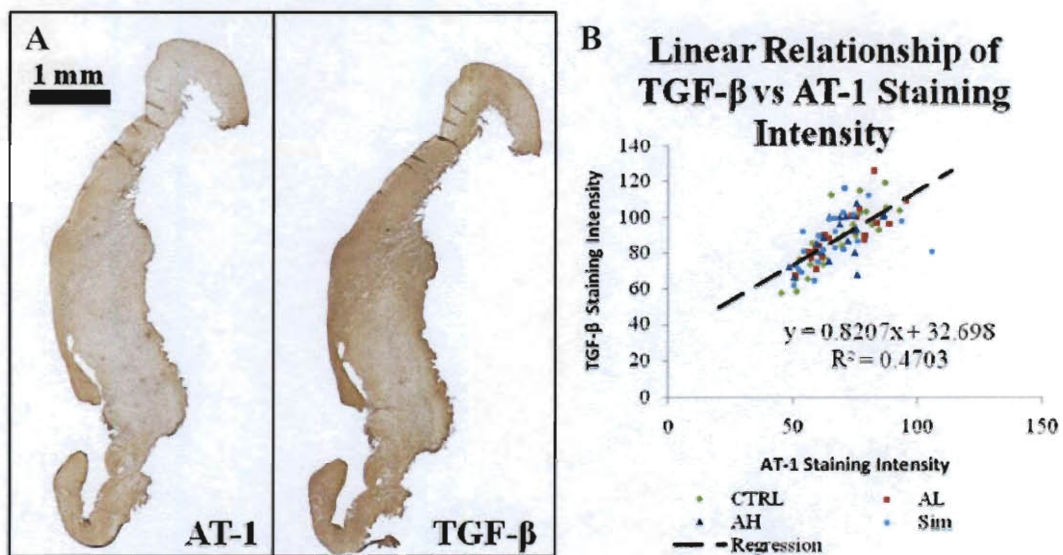
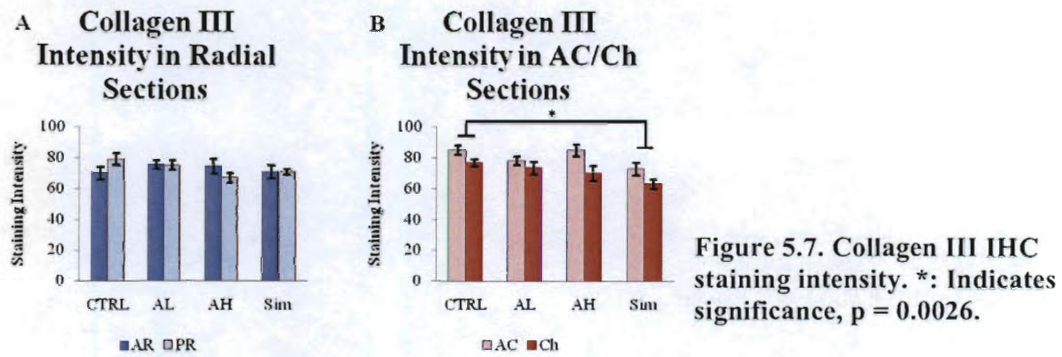


Figure 5.8. A) IHC staining of Angiotensin II Receptor I (left) and TGF- β (right). The staining patterns indicate co-localization of these markers. B) Linear regression correlation AT-1 and TGF- β staining intensity ($R^2 = 0.47$).

specific measurements confirmed the results of the more general intensity measurements.

A two-way ANOVA across sections and groups demonstrated that, in the fibrosa, hyaluronan staining intensity of CTRL was significantly greater than Sim ($p = 0.0098$). Further, the free-edge region of PR sections showed significantly increased staining intensity in AL ($p = 0.0128$) and AH ($p = 0.0083$) specimens, compared to Sim. In addition, a three-way ANOVA was performed on the region-specific data, comparing

results across section, group, and region. This analysis found that the Sim regional staining intensity of hyaluronan was significantly less than all other experimental groups ($p < 0.003$). Versican staining intensity results indicated divergent patterns between sections, so the tissue sections were analyzed separately. In the radial sections, AR and PR (Figure 5.10a), the staining intensity in the CTRL group was significantly greater than for AL ($p = 0.0409$) and Sim ($p < 0.0001$). In addition, radial section staining in AH was significantly greater ($p = 0.0211$) than Sim. Among AC and Ch sections (Figure 5.10b), the most intense versican staining was in the AL group, which stained more strongly than for the Sim group ($p = 0.0291$) or the CTRL group (0.0365).

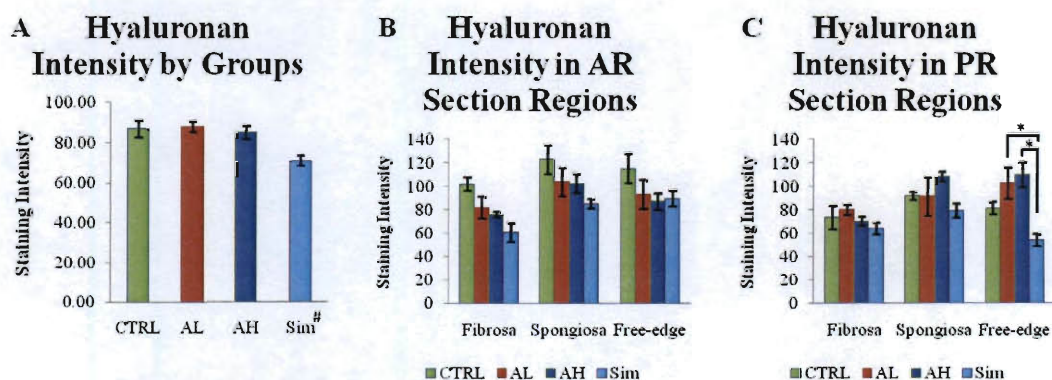


Figure 5.9. Hyaluronan Staining Intensity. A) Intensity measured as an integral of the entire tissue cross-section. B) Intensity measured in specific valve regions of AR sections. C) Intensity measured in specific valve regions of PR sections. Significance: *, $p < 0.0128$; #, Indicates a significant difference in Hyaluronan staining intensity between Sim specimens and all other groups, $p < 0.001$. Other significant comparisons not shown.

A two-way ANOVA, across group and valve section, determined an effect of experimental group on hematoxylin staining intensity as an indicator of cell density (Figure 5.11). Post-hoc analysis found significantly more intense staining for both the low ($p = 0.0298$) and high ($p = 0.0012$) concentrations of AII, compared to CTRL.

Further, the Sim group had an average staining that was comparable to CTRL and significantly less intense than the AH samples ($p = 0.0037$).

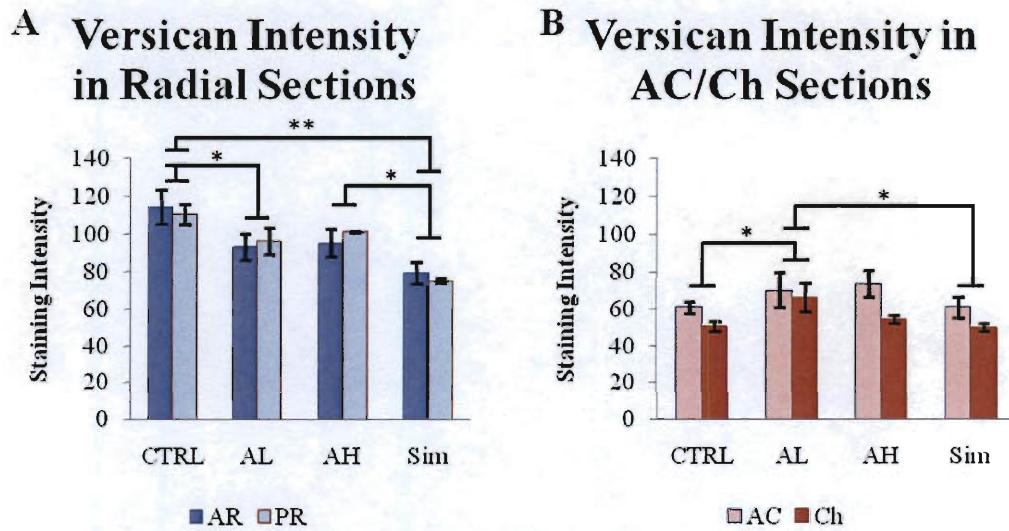


Figure 5.10. IHC Versican Staining Intensity. A) Radial sections, AR and PR. B) AC and CH sections. Significance: *, $p < 0.0409$; **, $p < 0.0001$.

Hematoxylin Intensity by Groups

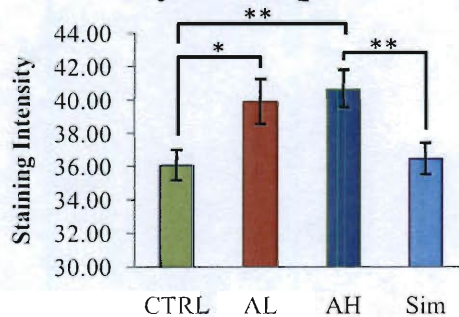


Figure 5.11. Hematoxylin staining intensity across experimental groups. Significance: *, $p = 0.0298$; **, $p < 0.0037$.

Discussion

This study investigated the role of AII, a chemical overly abundant in the blood of heart failure patients, on mitral valve remodeling *in vitro*; the results suggest an increase in cellularity, a decrease in GAG content, a minor increase in collagen content, and decreased hydration. A previous study examining the effects of HF on human mitral valves without apparent MR found increases in all three components and a decrease in hydration (64). The prior study had concluded that the ECM remodeling was indirectly caused by cardiac remodeling and dilation. Dilation can change the stress distribution within the valve, even without precipitating MR, and leading to adverse valve remodeling. By controlling for any altered mechanical environment, the current study shows that at least some of the valvular tissue remodeling is the result of tissue responses to the biochemical changes accompanying HF. Given the number of other hormones elevated in HF, including Endothelin-1, Transforming Growth Factor- β , Vasopressin, Tumor Necrosis Factor- α , Norepinephrine, and others, there is good reason to believe in a strong role of altered blood chemistry in mediating valve remodeling.

The biochemical PicoGreen assay suggested that valvular DNA content increased with increasing AII concentration. Hematoxylin staining for cell nuclei also increased with increasing AII concentration. Both of these effects were inhibited by the addition of Simvastatin to the culture medium. These results show that AII induces valvular cell proliferation and that Simvastatin inhibits this effect. Previous studies have demonstrated that AII induces cell proliferation *in vitro* in sheep cardiomyocytes (91) and rat cardiac fibroblasts (92, 93) through an Endothelin-1 mediated pathway. Our results show a

similar effect in cultured porcine valvular tissue, an effect which may also act through endothelin-1.

Measurement of uronic acid content suggested a decrease in GAG content induced by AII and inhibited by simvastatin. In the case of versican, the AII-induced decrease was confirmed through IHC in radial sections, but the addition of simvastatin further decreased staining intensity. Staining intensity of hyaluronan also showed somewhat contrary results with the addition of simvastatin. Staining of decorin did not indicate any changes in staining intensity with any treatment. To clarify these results, more sensitive techniques are needed that encompass a larger span of PGs, such as biglycan, the production of which has been found to be induced by AII *in vitro* (94).

The hydroxyproline assay showed an increase in collagen content associated with incubation with AII. This increase was inhibited by the addition of simvastatin. This pattern was reflected by grading of collagen staining in Movat stains of radial and chordal specimens and suggests that AII induces collagen synthesis in porcine valve cells, as has been shown for rat cardiac fibroblasts (95) and human cardiac fibroblasts (66). The inhibitive effect of simvastatin was also expected. Collagen III staining was found to decrease with the addition of simvastatin. This suggests that, while simvastatin inhibits an increase in total collagen content, it may also cause a shift in the proportion of collagen types present in the valve.

Remodeling of the major ECM components of valve tissue should be indicative of the tissue's material properties. In this case, the increases in tensile modulus in the AL and AH treatment groups compared to controls may be a function of increased collagen

content, though the Sim group also showed a larger increase in tensile modulus without an increase in total collagen. Since Sim also tended to have lower collagen III staining intensity, it is possible that the increase in tensile modulus was due to a shift from collagen III to collagen I, which results in stiffer tissue along the fiber orientation. Extensibility is dependent on the ability of collagen fibers to straighten out their natural crimp before bearing larger loads. The increase in extensibility of AH and AL specimens compared to controls may relate to changes in collagen organization or orientation.

The addition of AII to the culture medium resulted in increased cellularity. A SM α A-positive phenotype is associated with the adverse valve remodeling of myxomatous valve disease and the development of valvular lesions. While the current data was inconclusive, it is likely that an increase of SM α A-positive cells is a mechanism for the demonstrated effects of AII on cultured valves and a mechanism through which elevated blood levels of AII during HF contribute to the development of valve disorders. In a previous study, TGF- β induced SM α A expression in aortic valve cells was inhibited by the addition of simvastatin through a Rho-mediated pathway (78). A similar effect was not demonstrated in this study.

Several factors served as limitations regarding the results of this study. Analysis of the negative control and hematoxylin-only slide images indicated small differences in staining intensity. The average staining intensities were appreciable for mouse secondary (47.3 ± 1.2), rabbit secondary (41.5 ± 0.8), and hematoxylin counterstain (38.1 ± 0.6). This confirmed the occurrence of minimal, but consistent, non-specific binding of the secondary antibodies or other components of the staining procedure. In addition, the significant differences between the flow characteristics of experimental groups may have

influenced the mechanical stimulation experienced by cultured valves. However, few of the significant results follow patterns similar to the magnitudes of total flow or retrograde flow, suggesting that these effects are overwhelmed by the biochemical effects of AII and simvastatin. Also, the current study found only diffuse AT-1 and TGF- β staining, perhaps because the lack of circulating lipoproteins and macrophages precluded the development of inflammation or because the 3 week culture period was not a long enough time to develop the conditions for localization. Additionally, localization of AT-1 may be prompted by AII synthesis by localized angiotensin converting enzyme (ACE).

In conclusion, the results of this study show that angiotensin II modulates ECM synthesis and turnover and increases cellular proliferation in mitral valve tissue. Also, simvastatin inhibits some of the effects of angiotensin II on mitral valve tissue and produces further effects on mitral valve tissue, both exaggerating some of the effects of angiotensin II and affecting properties unaltered by angiotensin II. These findings demonstrate that the pathologic ECM remodeling of mitral valves during heart failure is at least partially due to biochemical responses that do not rely on an altered mechanical or geometric environment. Additionally, this study has also demonstrated the utility of the mitral valve organ culture system in conducting relevant, novel, and unique *ex vivo* experiments.

Chapter 6 CONCLUSIONS, DISCUSSION, AND FUTURE DIRECTIONS

In the overview (Chapter 1), we hypothesized that a physiological mechanical environment would help maintain the native characteristics of mitral valves in organ culture and serve as a novel experimental paradigm. In order to test this hypothesis, a mitral valve organ culture system was developed, characterized, validated, and implemented in a novel experiment according to the specific aims:

Design and mechanically characterize a mitral valve organ culture system capable of reproducing the valve's physiologic mechanical environment.

Further develop the organ culture system to integrate a porcine mitral valve in a sterile environment with adequate oxygen and nutrients. Evaluate the cultured valves to determine the effect of the dynamic mechanical environment.

Employ the organ culture system to study the ex vivo effects of Angiotensin II, alone and in combination with Simvastatin, on mitral valve tissue.

The previous chapters described in detail the process of completing these aims as well as the results and outcomes.

Aim 1 Conclusions

While the design process is documented in Appendix A, Chapter 3 describes the resulting design of a computer controlled flow loop system powered by a pneumatic bladder pump. Characterization of the system determined that it could create a ventricular pressure pulse with a physiologically relevant pressure range and a pulsatile flow rate nearing a physiological average. Sterility tests confirmed the system's resistance to contamination

when filled with culture medium. This characterization was a crucial step in testing the hypothesis: We needed to produce a physiological mechanical environment in order to determine the effect of that environment. Satisfactory completion of this aim allowed further development and testing of the organ culture system.

Aim 2 Conclusions

The second aim addressed biological design issues and tested the biological effectiveness of the system in conducting the organ culture of a mitral valve. A valve attachment technique was able to satisfactorily integrate a porcine valve into the organ culture system and allow it to open and close with each cycle. At the beginning of each experiment, the valve opened and closed properly, as was demonstrated by the recorded pressures and flow rates. Compared to a static culture environment, this dynamic environment greatly increased cell viability and maintained tissue hydration in the leaflets. However, the resulting leaflet ECM composition resembled that of statically cultured valves. Retrograde flow increased during the culture period, likely indicative of incomplete leaflet coaptation. Material properties of some tissue sections were maintained at native levels, but others were not. This discrepancy is possibly the effect of unnatural stress distributions. These separate properties that failed to retain native physiological values during dynamic culture are likely related, though the root cause is unclear. Despite these drawbacks, the organ culture system succeeded in helping to culture viable mitral valve tissue, fulfilling the first condition of the global hypothesis.

Aim 3 Conclusions

The final aim used the organ culture system developed in the first two aims to study the *ex vivo* response of mitral valves to Angiotensin II, both alone and in combination with Simvastatin. Effects of Angiotensin II were generally dose-dependent and suggested the development of a more fibrous tissue. Cell content was also increased. Simvastatin treatment did inhibit many of these effects, returning the valve to a more natural composition. However, Simvastatin altered some other tissue characteristics that Angiotensin II did not, and some Angiotensin-II induced effects were exaggerated by the addition of Simvastatin. This study showed that Angiotensin-II has the potential to induce pathologic valve remodeling and that the preventative or reactive use of statins would also have potential for adverse effects. By producing these results, the organ culture system has demonstrated its validity as a novel experimental paradigm and fulfilled the second condition of the universal hypothesis.

Impact/Importance of Work as a Whole

Ex vivo organ culture will provide many benefits and opportunities in the study of valve biology. This is partially because mechanical stimulation elicits cellular responses and also can modulate the responses of cells to other stimuli (88). In addition, valve cells modulate their behavior based on their environment – the presence of multiple cell types (25) and the composition of the surrounding matrix (96). This is the first published organ culture system for mitral valves and provides the paradigm to investigate the natural behavior of valve cells and their impact on mitral valve tissue in a way that is only matched or surpassed by animal models, but without the limitations or costs associated

with animal research. The work in this thesis has shown that the system can maintain biologically relevant tissues and produce valuable insights into heart valve biology.

Limitations

The completion of the three aims has revealed limitations in the studies described as well as in the organ culture system design.

While Aims 2 and 3 allowed continuous flow and pressure measurements, the more meaningful results were the product of destructive assays and were limited to a single time point per valve. In order to boost statistical power and allow time for valve remodeling to progress, all dynamic culture periods lasted 21 days. While this did allow for meaningful results, the chronological effects of dynamic culture and biochemical additives remain unknown. Some additional information may be gleaned by frequently collecting and analyzing medium samples for molecules secreted by cultured valves. But, the large volume of medium may over-dilute any quantitative assay.

In Aims 2 and 3, IHC was intended to give a more detailed analysis of ECM remodeling than the aggregate quantification provided by the biochemical assays. However, due to the limitations of tissue availability, cost, and time, it was not possible to stain for all relevant markers. As a result, the distributions of biglycan, matrix metalloproteinases (MMPs), tissue inhibitor of MMPs (TIMPs), collagen I, collagen III (Aim 2 only), and other molecules that may have provided answers to the remaining questions, were not investigated. An alternative would be to create less uncertainty by focusing on a narrower set of effects, such as collagen remodeling, and choosing markers to investigate the synthesis, sub-types, degradation, and associated molecules (such as decorin).

Dosage optimization was not performed to determine the Angiotensin II and Simvastatin concentrations for Aim 3. Instead, concentrations were based on previously published work. It is possible that these concentrations were too low, too high, or in the wrong proportion to stimulate relevant responses. It would be difficult to study a higher number of concentrations because of the difficulties of obtaining large sample sizes in this organ culture system. *In vitro* dosage optimizations may mitigate this limitation, but *in vitro* behavior may not accurately predict *ex vivo* behavior.

The organ culture system developed in this research is limited by its capacity to generate large sample sizes. The current implementation allows only two valves to be cultured at a time, while occupying nearly an entire humidified incubator. With a culture period of 21 days, increasing the sample size, culture period, or number of experimental groups adds a significant amount of time to the length of any study. Multiplexing each system to allow for four valves was initially proposed, but eventually decided against to prevent cross-influences of valves in the same culture medium. The production of a more compact system design that can share electronic components, such as the proportional pressure regulators, would be a promising direction for future development. Another option would be to remove the incubator size constraint by building or using an existing environmental chamber capable of maintaining its interior at 37° C and supplying humidified, 5% CO₂ air to the organ culture system's venting filter.

A larger environmental chamber would also allow for a greater vertical distance between the atrial reservoir and ventricular chamber. The increased filling pressure may allow the system to achieve higher, more physiological, flow rates. As proposed in Chapter 4, other options to increase the filling pressure include simulating ventricular diastolic suction and

using an additional pneumatic pumping mechanism to simulate atrial systole, priming the ventricular chamber before its systolic phase. Another potential method to increase the flow rate would be to optimize the shapes and sizes of all the flow loop components. Similar flow loop bioreactors have been designed to minimize turbulence (97). Such a modification would likely enhance flow response. Recreating a more physiologic flow rate may improve retention of native valve characteristics, increasing the relevance of this organ culture model.

The premise of this organ culture system relies on the accurate reproduction of the stress and strain distributions experienced by a mitral valve *in vivo*. In Chapter 4, modifications to the attachment of the chordae tendineae were proposed that are intended to better simulate their anatomic position. Because significant loads are applied through the chordae, their accurate positioning is important in modulating applied stresses and likely acts through mechanotransduction to influence valvular function and characteristics (48).

It must also be considered that dynamic stimulation may not be the only factor required for an ideal mitral valve organ culture model. As demonstrated in Chapter 5, circulating molecules can significantly affect valvular characteristics. The addition of growth factors or other signaling agents has been beneficial to the development of tissue engineered heart valve constructs in combination with mechanical conditioning (35) and is likely to have similar effects in organ culture. Effects may even be seen with the substitution of bovine growth serum for fetal bovine serum, which is richer in a variety of proteins.

Wide Scope of Possible Future Research

In addition to addressing these noted limitations, further use and development of the organ culture system offers a wide scope of possible investigation. The most straightforward and obvious options would be the addition of other common circulating molecules. Determining the effects of Vasopressin, Endothelin-1, Norepinephrine, and other agents related to heart failure could expand on the results from Aim 3 to better understand mitral valve remodeling and dysfunction in heart failure.

Without requiring any modifications, the flexibility of the system to produce a wide range of pressure signals allows simulation of hypertension and hypotension. Sub-physiologic pressure waveforms could be used towards a mitral valve tissue engineering model. It may also be desirable to explore the valvular response to non-physiological pulsatile pressure waveforms, such as those created by pulsatile ventricular assist devices. These variations could also extend the research of heart valves in heart failure by simulating common modes of altered cardiac hemodynamics.

The modular assembly of this system also increases its flexibility. For example, organ culture of tri-leaflet valves is achievable by simply modifying only the inlet port to accommodate these valves and reversing the direction of the mechanical valve. Such a system would not be novel, several similar configurations already exist (37, 42, 97, 98). Culture of a tricuspid valve (from the right side of the heart) should also be possible with minor modifications to the valve attachment scheme.

Conclusion

An understanding of the factors that lead to valve disease, as well as those that maintain healthy valves, are both necessary components in the development of reliable and effective valve disease treatments and prevention. This thesis described the design and development of a mitral valve organ culture system and proceeded to document its capability as a resource for scientific exploration. Given the results and insights provided by all three chapters, I am pleased that the organ culture system will continue to develop and serve as a novel experimental tool in the field of heart valve biology.

Appendix A DESIGN PROCESS

The design criteria and resulting design have already been described in Chapter 3; this appendix is intended to document the design process connecting the two.

Functions, Objectives, Constraints

In Chapter 3 the design criteria for the mitral valve organ culture system were categorized into the following functions, objectives, and constraints:

Functions

- Recreate the *in vivo* heart valve mechanical environment
- Recreate the physiological valve geometry
- Provide necessary nutrition and gas exchange for cellular metabolism
- Maintain a sterile culture environment at 37° C and 5% CO₂

Objectives

- Maximize the viability of cells in cultured valves
- Minimize the changes in tissue structure and composition
- Minimize differences in flow characteristics
- Minimize complexity of operation
- Maximize flexibility of culture conditions
- Maximize accurate control of culture conditions
- Maximize consistency and repeatability of culture conditions
- Maximize the number of valves in culture concurrently

Constraints

- Avoid microbial contamination
- Avoid leaks
- Fit within an environmental incubator

These design criteria provided bases for decisions on various design elements.

Major Design Elements

Pumping mechanism

The following options were considered to produce pulsatile pressure and flow through the system: peristaltic pumping, bladder pumping, and piston pumping.

Peristaltic pumping involves wrapping tubing around a rotor that compresses the tubing and presses fluid forward as it turns. There are many pump units commercially available that are intended for biomedical applications. Also, because no external or moving parts contact the flow medium, sterility is not compromised. However, due to the pumping mechanism, the flow and pressure achieved cannot accurately recreate physiological waveforms and it is difficult to uncouple flow rate and pulse frequency. It would also be difficult to simulate both diastolic and systolic conditions. In addition, these pumps can be large and would be difficult to implement within an incubator.

Bladder pumping uses an inflatable bladder or diaphragm to propel fluid out of the pumping chamber, then allows the bladder to deflate as fluid refills the chamber. This pumping action is similar to the cyclic contractions of the heart. Bladder pumps can be created to accurately recreate a wide variety of pressure pulses. The bladder also acts as a

barrier between the flow medium and any non-sterile pumping mechanisms A disadvantage is that the pumping system would have to be custom built.

Piston pumping is nearly identical to bladder pumping, replacing the inflating bladder with a piston that displaces fluid at a variable rate as it moves. A piston can be accurately controlled, leading to accurate control of flow rates. A moving piston, however, would involve increased risk of leaks and contamination at the interface of the piston and its casing. The size of a piston system would also be of concern.

Based on these options, a custom-built bladder pump was chosen as the pumping mechanism. The deciding factors were the flexibility of this mechanism, it's similarity to ventricular pumping, and the lack of sterility concerns. Bladder pumping also allowed for a pressure-controlled system, instead of one controlled through a direct volume displacement. Control through direct application of pressure was favored because pressure impulses were expected to better simulate the conditions of both diastole and systole. Several other cardiovascular bioreactor systems have used this approach (42, 44, 98, 99).

Variable Pressure Supply

In order to accurately control the pressure of the inflating bladder (diaphragm), a proportional pressure regulator (PPR) supplied compressed air at electrically controlled variable pressures. The initial PPR selected was a QB3 (ProportionAir, McCordsville, IN). This model had a large pressure range (0-7700 mmHg) and large air flow rate capacity. However, preliminary tests indicated the instrument was not well suited for the lower end of the pressure range, as the produced pressure waveforms were not smooth

and had a significant time lag from their control signal. The QB3 was substituted with an Airfit Tecno (Parker-Origa, Richland, MI), which had a more limited pressure range (0-150 mmHg) and maximum flow rate capability, but also a much quicker and more precise pressure response.

Ventricular Chamber

First Iteration

The first iteration of the ventricular chamber assembly is shown in Figure 6.1. The ventricular chamber was made of custom machined acrylic parts. Acrylic was chosen for its clarity, to enable monitoring of the interior, and heat tolerance, to allow steam sterilization in an autoclave. Each half of the chamber was made of three parts held together with cyanoacrylate. A square 0.05” silicone membrane was clamped between the two chamber halves, which were pressed against each other with 12 tightened bolts. Silicone was chosen because of its heat tolerance and appropriate elasticity and toughness. In order to allow the membrane to remain slack while moving back and forth to displace fluid, the membrane was deformed into a cup shape and folded over itself in the clamping area. Two openings were bored into the fluid-filled chamber half’s face to accommodate the valve holders. A threaded hole was also included to accommodate an electronic pressure sensor.

The first mitral valve holder was (Figure 6.1c) also made with acrylic and had two halves clamped together with bolts with a silicone membrane in between. The silicone membrane was a swatch with a mechanical or porcine heart valve sutured to an orifice at its center. The mitral valve holder narrowed down and was fitted with a barbed tubing

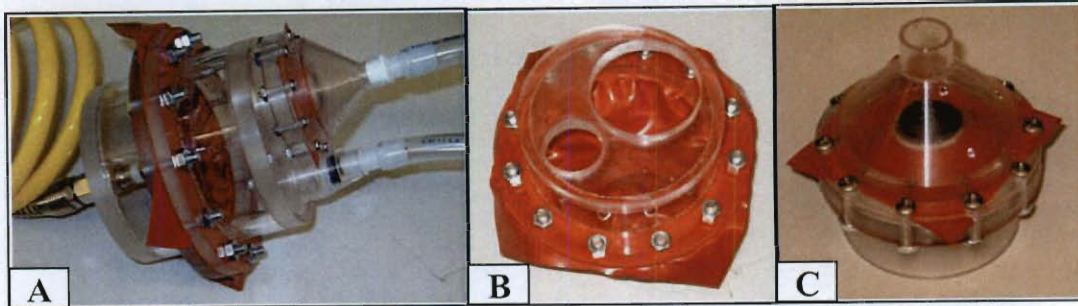


Figure 6.1. First iteration of A) Complete ventricular chamber assembly, B) Ventricular chamber only, and C) Mitral valve holder.

port on the inflow end. The outflow end was friction-fit into the corresponding opening in the ventricular chamber, using a teflon-tape wrap to secure the fit. The aortic valve holder (not shown) was a small acrylic shunt with a mechanical heart valve held in place by an acrylic ring stuck to the valve holder interior with silicone adhesive. It also was friction-fit into the corresponding ventricular chamber opening.

Initial testing showed this design to contain several major flaws. Leaks were evident at nearly all types of interfaces between components: acrylic held together with cyanoacrylate, friction-fits between parts, the valve holder tubing port, and bolt-tightened acrylic clamped around silicone. The folded silicone membrane failed to move freely when pressure was applied to the air-filled side of the chamber. Also, tightening all of the bolts was difficult and time-consuming, and risked cracking the underlying acrylic parts.

Revisions

Through several iterations, the ventricular chamber assembly was revised to correct for all of the stated flaws (Figure 3.2). All uses of adhesives and bolts were discontinued and largely replaced with the use of o-rings. The inflexible flat silicone membrane was replaced with a thinner, dome-shaped, silicone diaphragm. It was still clamped between

two halves of the ventricular chamber, but the clamping force was provided by an external frame held together with toggle clamps. The pressure sensor was moved from the fluid side of the chamber to the air side; tests with sensors simultaneously on both sides of the chamber confirmed the equivalence of the two measurement locations.

The mitral valve holder was modified towards a design more similar to the aortic valve holder. The current design consists of a single primary piece instead of two that are held together. The valve is sutured to a fabric swatch, which resists tearing much better than silicone and is also autoclaveable. The swatch is clamped in place with an interior “clamp ring” that is held into place by friction between the components, acting through a silicone o-ring.

Chordal Anchoring

The first attempt at chordal anchoring involved the simple insertion of curved steel wires through the excised papillary muscles. The wire ends were then passed through holes in the mitral valve holder wall to hold them in place (Figure 6.2).

This scheme did not work at all. The wires would easily deflect towards the valve annulus immediately. In addition, the wires would tear through the papillary muscles during tests that lasted on the order of an hour.

In order to avoid tearing, wire helices were formed that could wrap around the papillary muscles, and between chordae tendineae, without piercing any tissue. Stiffer straight wires were inserted through these helices into the valve holder wall. Additionally, multiple holes were bored in the mitral valve holder wall to allow chordae of varying lengths to be accommodated.



Figure 6.2. Early implementation of chordal anchoring. The steel wires were inserted through the papillary muscles and into the wall of the mitral valve holder.

The rest of the system has undergone further, but minor development. The following appendix contains a detailed operating guide with some further details.

Appendix B **FLOW LOOP OPERATING MANUAL**

(January, 2011)

Preparatory Steps

Two days prior to harvest and start of culture:

Prepare solutions:

- Medium (M199 w/ Hank's Salts, L-glut, etc.) w/ 10% BGS and 2% anti-microbial solution (>1.5L per valve is recommended)
- Sterile PBS w/ 10% anti-microbial solution (50mL per valve)

All parts autoclaved in autoclave bags:

Large bag (1 per valve):

- VC rings and caps
- Silicone diaphragm
- aortic port (with valve and clamp ring)

Large bag (1 per valve):

- all tubing
- hose clamps
- port plugs

Large bag (1 per valve):

- 1x1L bottle and 1x0.5L bottle (with bulkhead ports)
- 1 normal bottle closure and 1 septum closure
- Venting filter

Large bag:

- 1+ aluminum foil sheet (~13"x17") per valve to be dissected

Medium bag (1 per valve):

- Mitral valve holder, including clamp ring
- 4 straight steel wires

Small bag (1 per valve):

- several annulus attachment rings of various sizes/shapes
- 4 steel wire chordal helices per valve

Ensure that up-to-date control software (Flow Loop Controller) is installed on the control computer, along with the necessary LabView DAQmx and LabView Runtime Engine software.

One day prior to harvest and start of culture:

Pre-assembly of flow loop, partial assembly of ventricular chamber

In a hood, assemble the bottles/tubing of the flow loop. Use care when handling the tubing ends, as these surfaces will eventually contact culture medium. Tighten hose clamps around all the tubing ports, especially the port from the atrial reservoir that connects to the mitral port (this tubing is larger and does not fit unless well-tightened). Make sure the septum closure is used for the compliance chamber. Plug the tubing ends with silicone port plugs (tiny translucent top-hats). The tubing ends can be protected by stuffing them into a sterilization pouch.

In addition, assemble the air-side and medium-side of the ventricular chamber, including the frame. The entire assembly can be clamped together to keep interior surfaces protected and to ease handling. Place into a sterilization pouch for safety. Keep both items as well as funnels, and mitral ports in the hood so that they may be protected from contamination by the UV light.

Autoclaving surgical tools, dissection tray

Autoclave these and place them into a separate hood. If it is not in an autoclave bag, move the dissection tray straight from the autoclave to the hood to limit time for contamination. If it is in a bag, remove the bag carefully as it may get contaminated or have charred particles clinging to it. Also place scalpel blades and sutures in the hood. All such items, including the sterilization pouches, can be sprayed with EtOH to reduce the risk of bringing a contaminated surface into the hood. Leaving the items in the sterile biosafety cabinet where they will be exposed to the UV light overnight will further reduce this risk.

Pre-Dissection

Wear normal lab gloves for these steps (spray with 70% EtOH).

Place sterile PBS/anti in water bath until it comes to room temp (37°C is not necessary since it will cool down anyways), then wipe down with 70% EtOH and place in the dissection hood.

Place 2 50mL tubes per valve to be dissected into the dissection hood, label them 1, 1, 2, 2 ...

Make sure all dissection tools are available in the dissection hood.

Prepare a sterile 250mL beaker mostly filled with 70% EtOH for cleaning dissection tools. Tools should be placed in this beaker when not used for extended periods; allow them to dry completely before contacting the mitral valve.

Prepare a clean 1-5L beaker/tub for the bio-waste, spray/wipe it with 70% EtOH and place it in the dissection hood.

Heart Dissection

Spread one sterile sheet of aluminum foil on the dissection tray surface. A double layer may help keep the tray surface clean.

Grab a fresh heart and place it on the foil sheet in the dissection hood. To prevent blood dripping, you can saturate a paper towel with 70% EtOH, hold the heart with the paper as you carry it, and then dispose of the paper into the bio-waste container. Also dispose of your (now bloody) gloves into the bio-waste.

Open and wear a new pair of sterile gloves – these should already be in the hood. Also open up two sets of forceps and two scalpel holders; place blades on the scalpel holders.

Identify and remove the main portion of the left atrium, as well as any other tissue obscuring the mitral valve. Use one set of forceps and one scalpel to work on exterior parts of the heart. Reserve the other forceps and scalpel for contact with the mitral valve. You can also remove coagulated blood from the vicinity of the mitral valve. Dispose of removed tissue and blood into the bio-waste container.

Select an annulus attachment ring that best matches the dimensions of the valve annulus. You may want to use the valve sizing kit for this – try not to contaminate the attachment ring with anything that has touched the heart.

Next, use the reserved scalpel to cut the valve annulus away from the atrioventricular wall. Leave a margin of myocardial tissue attached and be very careful not to cut through the valve itself.

When the annulus is detached, use the exterior scalpel to slice open the left ventricle down to the apex. To avoid damaging the chordae or papillary muscles, this slice should be on the opposite side of the ventricle from the aorta. You should also visually inspect the heart interior as you cut to make sure you are not causing any damage to these valve parts.

Remove any chordae or similar structures that connect the valve to a non-papillary muscle area of the ventricle. Then cut the papillary muscles away from the ventricular wall. Leave plenty of excess tissue, as this can be trimmed later. Use the interior scalpel and the reserved forceps to manipulate the mitral valve and papillary muscles.

When the valve is completely detached, place it into one of the tubes marked '1' and submerge it with sterile PBS/anti solution. Agitate lightly to remove air pockets and to loosen coagulated blood.

Remove the foil sheet and place it in the bio-waste and replace it with a clean one.

Repeat the dissection for each heart. If sufficient quantities are available, you may want to use a new set of forceps and a new scalpel blade for each heart's interior to reduce possible cross-contamination.

Suturing

Before suturing your last valve, place your medium into a water bath to warm it up.

Put on a new pair of sterile gloves. A fresh pair of gloves may not be necessary for suturing each valve.

Take the valve out of the tube marked '1' and place it on the dissection tray. With a clean scalpel blade and unused forceps remove excessive tissue from the valve annulus, preserving a margin of connective and myocardial tissue.

Find the selected annulus attachment ring and open up a sterile suture pack; place both on the dissection tray.

Find the midpoint of the anterior leaflet segment on the attachment ring (Point A). Insert the suture needle just to the right of this point (about 1mm), and 2-3 mm from the edge. Continue the needle into the anterior leaflet annulus, again about 1mm to the right of the midpoint. The suture should cross through the 'stretchy/glossy' looking layer of the valve to ensure it does not pull through the tissue. The surfaces with rougher texture are generally created from cutting and do not support sutures as well. The suturing process is much easier if you directly hold the valve in your fingers, so be especially careful to keep your gloves sterile, generally by not touching anything outside the hood. Pull the suture through the valve and attachment ring on the other side of the midpoint. As you pull the suture through, it should bring the valve up to the attachment ring. Tie a 2x1 instrument tie to knot the suture and trim the ends of the knot with the scalpel or dissection scissors. The knot should always be next to the attachment ring, not the tissue. Continue suturing at points B, C, etc... The valve annulus at the posterior leaflet and commissures will seem too long to fit directly against the attachment ring. To attach these portions correctly they will have to form ridges/folds. Lining up the annulus with the ring

can be tricky to keep a consistent folding density. Use the geometry of the valve for cues (ie where the commissures are), and also estimate $\frac{1}{2}$ or $\frac{1}{3}$ the distance between existing suture points. You can then fill in the remaining points in an iterative process. The anterior leaflet can be secured with two to four 'long' suture knots. By the end of this process, the valve annulus should be held tightly to the attachment ring at all points – forceps should not be able to open a gap. This may take a long time – valves often need 24 knots, so you may occasionally submerge the valve into its first rinsing tube to keep it hydrated.

Next trim away excess papillary muscle tissue so that the helical coils are able to fit around them. Each papillary muscle may also be split to separate the anterior leaflet chordae from the posterior leaflet chordae. This often leaves each portion of the papillary muscle with a single line of chordal attachments. Some papillary muscles will need to be sutured together if damaged in dissection or if they are not in one contiguous piece.

Twist the helical coils around the papillary muscles, interspersing the chordae through the helical gaps. If the number or spacing of the chordae leaves the papillary muscle able to slip, tie sutures through the muscle and around the coil wire.

When finished place the valve, with ring and coils, into the unused tube labeled '1'.

Again, submerge with PBS/anti- solution and agitate lightly.

Repeat for each valve

Assembly

Take your prepared valves into the assembly hood (if this is different from the dissection hood).

Open up the mitral valve holder sterilization pouch. With sterile forceps place the valve into its appropriate position in the valve holder. Put the 'clamp ring' over the valve and press it down over the attachment ring. During this process, you will have to manipulate the coils to move them out of the way. Just before pressing the ring all the way against the opposing surface, make sure that the valve annulus is aligned correctly with the holder so that the placement wires will be able to slide through the coils in the proper orientation.

Use the placement wires to hold the coils extended from the annulus. Use the 2-3 rows of Isots in the mitral valve holder to keep the chordae elongated, but not taut or twisted.

Next, fit the mitral valve holder into the ventricular chamber assembly. Because of the wires, the mitral valve holder will have to be inserted from the inside-out. Try not to bend the wires while inserting the holder – this may make them harder to remove.

Line up the two sides of the ventricular chamber, with the membrane in between the two. Make sure that they are well aligned to prevent leaks. Flip the four buckles to hold the assembly in place. To test the tightness of the membrane, pull on its exposed edges, they should stretch and return to place. If they slip, either the two chamber sides are misaligned or the external frame must be adjusted. The ventricular chamber should now be completely assembled.

Complete the assembly by connecting the pre-assembled loop tubing. Try to twist the tubing onto the mitral and aortic ports so that, in the system's final configuration in the incubator, the tubing does not exert a twisting force on the ventricular chamber. This will take some practice.

Filling

Unscrew the closure of the atrial reservoir and place it on a clean surface in the hood, such as the inner surface of an autoclave pouch. Put a sterile funnel into the top of the atrial reservoir.

Pour medium into the system. Once the medium is at the level of the venting filter, lift the atrial reservoir above either the ventricular chamber or compliance chamber to distribute the medium. The ventricular chamber should be arranged with the aortic port high and the mitral port low. This ensures that medium can flow in through the mitral port and that air can be pushed up and out through the aortic port. Get the compliance chamber to fill quickly initially by loosening its cap – close the cap when the medium reached the cap level. Continue to fill the system through the atrial reservoir progressively.

When filled fully the compliance chamber will be about half full and all the tubing should be filled with medium. Lift the two bottles above the ventricular chamber; the ventricular chamber should be full of medium – shake out large air pockets; the atrial reservoir should have medium just above the level of the two ports. The smaller systems will take roughly 1.3L of medium to fill. The biggest system (the original one) takes around 1.7L. Once filled, make sure all caps are tightened and that there are no signs of medium leaking from the tubing ports.

Repeat for each valve/system.

Pipette ~6mL of the unused medium into a 10mL c-tube for pH testing. Label it "(sample name) 0d medium (initial-date)." This needs to be done only once per medium formulation used (not once per valve).

This is also a good opportunity to label the system(s) with lab tape so that they don't get mixed up on their way to, or while in, the incubator.

Putting the System in the Incubator, Connecting Cables, and Starting it up

Move the system into the incubator. The top rack will have to be pulled out most of the way. Move the whole system into the incubator between the top and bottom rack, with the bottles going in first. Pass them behind and onto the top rack, making sure not to invert them such that medium flows into the venting filter. Straighten out the bottles on the top rack and move the top rack back into position. Remove any twists or extraneous bends in the tubing and arrange the ventricular chamber so that the medium-filled side faces the incubator interior and the aortic port is above the mitral port.

Noting which set of connections are for Flow System A, screw the pressure transducer and the tube from the pressure regulator into the base of the ventricular chamber. When appropriate, clamp the flow meter onto tubing just upstream of the mitral port - make sure the 'Flow' arrow points towards the ventricular chamber. Also check that the flow meter is plugged into the correct plug on the control box (System A or B). The system is now ready to be started.

If it is not yet running, start the Flow Loop Controller software. Adjust the pressure to the desired peak (normally 120 mmHg) and make sure that the waveform selected is correct

(normally “Physiological Signal”). Check all the other settings. Click 'Start' and name the recording file. After a few seconds the system should begin pumping. Click 'Record Single Sample' to get a baseline recording. The flow profile should show a short spike of regurgitant flow at the onset of systole, followed by near-zero flow and then forward flow through the mitral valve during diastole. Bubbles in the tubing near the flow probe may cause a lot of noise, but they will dissipate within an hour or so. Move the flow probe (and the flow meter cable to the control box) to the other system and record a baseline cycle.

Check the pH of the saved medium in the c-tube and record it.

Operation

Every day move the flow probe from one system to the other. First unplug the connection at the control box, then switch the probe, and lastly plug the connection into the other socket on the control box. Low flow levels or abnormal waveforms can indicate problems within the system. Also monitor the fluid levels in all components of the flow loop and check for signs of contamination. Medium samples can be obtained while maintaining sterile conditions by inserting a sterile syringe (w/ needle!) in through the septum closure of the compliance chamber.

Medium Exchange

After 7 days, each system's culture medium must be replaced. Prepare by autoclaving a funnel and warming new medium in the water bath. If you'd like you can also warm some PBS/anti-microbial solution to rinse the system. Put a clean 4-5L griffin beaker in the hood to collect used medium. It is also useful to have some sterile forceps available.

Pause the first system to be processed (the corresponding waveforms should flatten out) and disconnect the pressure transducer and pressure regulator and switch the flow probe if necessary.

Draining the System

Move the entire flow loop into a sterile hood. Prepare a 10mL c-tube and a T75 flask, label them as "(sample name) 7d (or 14d) medium (initials & date)." Remove the closure from the atrial reservoir. Pipette about 6 mL of used medium into the c-tube and 6 mL into the flask. The c-tube medium's pH will be checked, recorded and compared with the 0d sample. The flask will be placed in the incubator and checked under a microscope after 1-2 days for bacterial contamination.

Put the atrial reservoir closure back and remove the compliance chamber closure (but don't spill!). Now just lift the whole system and pour the medium out into the griffin beaker. You'll probably have to shake the ventricular chamber a bit to get the medium out, and there will still be a small amount remaining. At this point you may add ~20mL of the PBS/anti-microbial solution and slosh it through the system. Drain it out (or don't, it doesn't make a big difference).

While the system is empty, visually inspect the aortic and mitral ports to see if everything is still in place. You can also replace the venting filter with a sterile one if medium has leaked into the filter.

Refilling and Restarting

Pour new medium into the system, as described earlier, and place it into the incubator.

Re-attach the pressure transducer and regulator. Resume the system's operation and move the flow probe back to check the flow/pressure waveforms.

Repeat for each system.

Stopping and Disassembly

Prepare a c-tube and T75 flask for medium collection for each system, as described above for medium exchange - label them as 21d (or whatever time point it is). Also prepare a 50mL c-tube and label with the sample names.

Stopping the system:

Just press 'Stop' on the program. Easy!

Disassembly

Next, disconnect the pressure regulator, pressure transducer, and flow meter from the systems.

Do the draining part of the medium exchange procedure. Now you should have an empty system in the hood. Remove the tubing from and unlatch the ventricular chamber. Push the mitral port out of place through the interior of the ventricular chamber. This is necessary since there are still wires holding the chordae in place. Also, try not to twist the port too much; the wires will scratch the ventricular chamber interior. During these steps some medium will spill out and that's okay, just make sure to clean it up.

Next, remove the straight wires to release the papillary muscle helices. Now you can remove the mitral valve: Push on the fabric attachment ring with your gloved finger to get it out from its position. You can also use fingers/forceps/hemastats/pliers to pull the clamp ring a little out of position to loosen the attachment ring. Twist off the wire helices and place the valve into the appropriately labeled 50mL c-tube.

Submerge the valves with PBS (non-sterile is fine).

Move the system, including all parts, out of the hood. Disassemble all parts and rinse with DI water. The compliance chamber often has a bit of medium residue in a few places. There's still no good procedure for minimizing and cleaning off the residue, so replace the chamber when you think there's too much.

Valve Dissection

You will dissect the valve and retain seven portions for various assays (Or you may decide on a different scheme better suited to your study):

- Anterior Circumferential strip (**AC**) - for tensile testing and histology
- Anterior Radial strip (**AR**) - for tensile testing and histology
- Anterior Strut Chordae (**Ch1 & Ch2**) - for tensile testing and histology
- Anterior leaflet (**A**) - for biochemical assays
- Posterior Radial strip (**PR**) - for tensile testing and histology
- Posterior leaflet (**P**) - for biochemical assays

Prepare seven labeled micro-c-tubes for each valve (labeled: "sample" "portion", eg AL3 PR).

Start by removing the sutures - cut them at the knot with a scalpel or razor blade and pull them out with forceps. Once done, make a radial cut through the middle of the lateral commissure. Lay the valve on the dissection tray, ventricular side up; this may also require splitting a papillary muscle. Take a photo of the valve, including the cap of the c-tube or something else labeled with the sample name. You may also want to record any observations, such as those on the appearance of the valve.

Start dissection by using a razor blade to cut out a ~3-5 mm wide rectangular circumferential strip from the 'anterior center' - the bottom of the strip should be just above the first set of chordae and the top should be as close to the annulus as you can get without getting the thicker connective tissue beyond the ends of the section. Take as long a strip as possible while not including any commissure tissue. Place this strip in the AC micro-c-tube along with a squirt of PBS. Use a razor blade again to cut the AR portion from between the two central rows of chordae extending from the leaflet - this strip should be as wide as possible without touching the chordae. Again, place it in the AR micro-c-tube with a squirt of PBS. Detach the rest of the anterior leaflet from the commissures and remove any annular tissue (anything above the bottom cut of the AC strip). Use pins to hold the remaining leaflet tissue down while removing the chordae with forceps and a scalpel blade. The two largest strut chordae should be at the top and must be removed completely intact and placed in micro-c-tubes (with minimal papillary muscle). Place the remaining, chordae-less, anterior leaflet tissue into the "A" micro-c-tube.

Now move to the posterior leaflet. Detach the leaflet from the adjoining commissures.

Obtain the PR section by cutting just as the AR section was cut, but all the way to the annulus. Remove all the chordae, do not worry about saving any for testing, and place the chordae-less leaflet sections into the "P" micro-c-tube. Discard any remaining tissue.

Freeze the A and P sections for biochemical assays.

Perform tensile testing on each of the remaining portions (see procedure) and then place them into labelled histology cassettes. Store them in 10% formalin overnight and begin flex/xylene dehydration the next day.

Clean-Up

Just make sure all the stuff you used is washed and, once dry, put back. Also wipe down the hood(s) and incubator.

REFERENCES

1. Lloyd-Jones D, Adams R, Brown T, Carnethon M, Dai S, De Simone G, et al. Heart disease and stroke statistics--2010 update: a report from the American Heart Association. *Circulation*. 2010 Feb;121(7):e46-e215.
2. Otto C, Lind B, Kitzman D, Gersh B, Siscovick D. Association of aortic-valve sclerosis with cardiovascular mortality and morbidity in the elderly. *N Engl J Med*. 1999 Jul;341(3):142-7.
3. Freed L, Levy D, Levine R, Larson M, Evans J, Fuller D, et al. Prevalence and clinical outcome of mitral-valve prolapse. *N Engl J Med*. 1999 Jul;341(1):1-7.
4. Kunzelman K, Einstein D, Cochran R. Fluid-structure interaction models of the mitral valve: function in normal and pathological states. *Philos Trans R Soc Lond B Biol Sci*. 2007 Aug;362(1484):1393-406.
5. Sacks M, He Z, Baijens L, Wanant S, Shah P, Sugimoto H, et al. Surface strains in the anterior leaflet of the functioning mitral valve. *Ann Biomed Eng*. 2002 Nov-Dec;30(10):1281-90.
6. Grande-Allen KJ, Calabro A, Gupta V, Wight TN, Hascall VC, Vesely I. Glycosaminoglycans and proteoglycans in normal mitral valve leaflets and chordae: association with regions of tensile and compressive loading. *Glycobiology*. 2004 Jul;14(7):621-33.
7. Cochran R, Kunzelman K, Chuong C, Sacks M, Eberhart R. Nondestructive analysis of mitral valve collagen fiber orientation. *ASAIO Trans*. 1991 Jul-Sep;37(3):M447-8.
8. Kunzelman K, Cochran R, Verrier E, Eberhart R. Anatomic basis for mitral valve modelling. *J Heart Valve Dis*. 1994 Sep;3(5):491-6.
9. Kunzelman K, Cochran R, Murphree S, Ring W, Verrier E, Eberhart R. Differential collagen distribution in the mitral valve and its influence on biomechanical behaviour. *J Heart Valve Dis*. 1993 Mar;2(2):236-44.
10. Leask R, Jain N, Butany J. Endothelium and valvular diseases of the heart. *Microsc Res Tech*. 2003 Feb;60(2):129-37.

11. Flanagan T, Pandit A. Living artificial heart valve alternatives: a review. *Eur Cell Mater.* 2003 Nov;6:28-45; discussion
12. Butcher J, Penrod A, García A, Nerem R. Unique morphology and focal adhesion development of valvular endothelial cells in static and fluid flow environments. *Arterioscler Thromb Vasc Biol.* 2004 Aug;24(8):1429-34.
13. Butcher J, Tressel S, Johnson T, Turner D, Sorescu G, Jo H, et al. Transcriptional profiles of valvular and vascular endothelial cells reveal phenotypic differences: influence of shear stress. *Arterioscler Thromb Vasc Biol.* 2006 Jan;26(1):69-77.
14. Mulholland D, Gotlieb A. Cell biology of valvular interstitial cells. *Can J Cardiol.* 1996 Mar;12(3):231-6.
15. Taylor P, Batten P, Brand N, Thomas P, Yacoub M. The cardiac valve interstitial cell. *Int J Biochem Cell Biol.* 2003 Feb;35(2):113-8.
16. Messier RJ, Bass B, Aly H, Jones J, Domkowski P, Wallace R, et al. Dual structural and functional phenotypes of the porcine aortic valve interstitial population: characteristics of the leaflet myofibroblast. *J Surg Res.* 1994 Jul;57(1):1-21.
17. Liu A, Joag V, Gotlieb A. The emerging role of valve interstitial cell phenotypes in regulating heart valve pathobiology. *Am J Pathol.* 2007 Nov;171(5):1407-18.
18. Rabkin-Aikawa E, Farber M, Aikawa M, Schoen F. Dynamic and reversible changes of interstitial cell phenotype during remodeling of cardiac valves. *J Heart Valve Dis.* 2004 Sep;13(5):841-7.
19. Barth W, Deten A, Bauer M, Reinohs M, Leicht M, Zimmer H. Differential remodeling of the left and right heart after norepinephrine treatment in rats: studies on cytokines and collagen. *J Mol Cell Cardiol.* 2000 Feb;32(2):273-84.
20. Butcher J, Barrett B, Nerem R. Equibiaxial strain stimulates fibroblastic phenotype shift in smooth muscle cells in an engineered tissue model of the aortic wall. *Biomaterials.* 2006 Oct;27(30):5252-8.
21. Heeneman S, Cleutjens J, Faber B, Creemers E, van Suylen R, Lutgens E, et al. The dynamic extracellular matrix: intervention strategies during heart failure and atherosclerosis. *J Pathol.* 2003 Jul;200(4):516-25.

22. Ikhumetse JD, Konduri S, Warnock JN, Xing Y, Yoganathand AP. Cyclic aortic pressure affects the biological properties of porcine pulmonary valve leaflets. *J Heart Valve Dis.* 2006 Mar;15(2):295-302.
23. Ku C, Johnson P, Batten P, Sarathchandra P, Chambers R, Taylor P, et al. Collagen synthesis by mesenchymal stem cells and aortic valve interstitial cells in response to mechanical stretch. *Cardiovasc Res.* 2006 Aug;71(3):548-56.
24. Weber K. Extracellular matrix remodeling in heart failure: a role for de novo angiotensin II generation. *Circulation.* 1997 Dec;96(11):4065-82.
25. Butcher J, Nerem R. Valvular endothelial cells regulate the phenotype of interstitial cells in co-culture: effects of steady shear stress. *Tissue Eng.* 2006 Apr;12(4):905-15.
26. Katsumi A, Orr A, Tzima E, Schwartz M. Integrins in mechanotransduction. *J Biol Chem.* 2004 Mar;279(13):12001-4.
27. Weston M, Yoganathan A. Biosynthetic activity in heart valve leaflets in response to in vitro flow environments. *Ann Biomed Eng.* 2001 Sep;29(9):752-63.
28. Balachandran K, Konduri S, Sucusky P, Jo H, Yoganathan A. An ex vivo study of the biological properties of porcine aortic valves in response to circumferential cyclic stretch. *Ann Biomed Eng.* 2006 Nov;34(11):1655-65.
29. Gupta V, Werdenberg J, Lawrence B, Mendez J, Stephens E, Grande-Allen K. Reversible secretion of glycosaminoglycans and proteoglycans by cyclically stretched valvular cells in 3D culture. *Ann Biomed Eng.* 2008 Jul;36(7):1092-103.
30. Gupta V, Tseng H, Lawrence B, Grande-Allen K. Effect of cyclic mechanical strain on glycosaminoglycan and proteoglycan synthesis by heart valve cells. *Acta Biomater.* 2009 Feb;5(2):531-40.
31. Merryman W, Lukoff H, Long R, Engelmayr GJ, Hopkins R, Sacks M. Synergistic effects of cyclic tension and transforming growth factor-beta1 on the aortic valve myofibroblast. *Cardiovasc Pathol.* 2007 2007 Sep-Oct;16(5):268-76.

32. Weinberg E, Mack P, Schoen F, García-Cardena G, Kaazempur Mofrad M. Hemodynamic environments from opposing sides of human aortic valve leaflets evoke distinct endothelial phenotypes in vitro. *Cardiovasc Eng*. 2010 Mar;10(1):5-11.
33. Xing Y, Warnock J, He Z, Hilbert S, Yoganathan A. Cyclic pressure affects the biological properties of porcine aortic valve leaflets in a magnitude and frequency dependent manner. *Ann Biomed Eng*. 2004 Nov;32(11):1461-70.
34. Engelmayer GJ, Rabkin E, Sutherland F, Schoen F, Mayer JJ, Sacks M. The independent role of cyclic flexure in the early in vitro development of an engineered heart valve tissue. *Biomaterials*. 2005 Jan;26(2):175-87.
35. Ramaswamy S, Gottlieb D, Engelmayer GJ, Aikawa E, Schmidt D, Gaitan-Leon D, et al. The role of organ level conditioning on the promotion of engineered heart valve tissue development in-vitro using mesenchymal stem cells. *Biomaterials*. 2010 Feb;31(6):1114-25.
36. Engelmayer GC, Soletti L, Vigmostad SC, Budilarto SG, Federspiel WJ, Chandran KB, et al. A novel flex-stretch-flow bioreactor for the study of engineered heart valve tissue mechanobiology. *Ann Biomed Eng*. 2008 May;36(5):700-12.
37. Konduri S, Xing Y, Warnock J, He Z, Yoganathan A. Normal physiological conditions maintain the biological characteristics of porcine aortic heart valves: an ex vivo organ culture study. *Ann Biomed Eng*. 2005 Sep;33(9):1158-66.
38. Yperman J, De Visscher G, Holvoet P, Flameng W. Molecular and functional characterization of ovine cardiac valve-derived interstitial cells in primary isolates and cultures. *Tissue Eng*. 2004 Sep-Oct;10(9-10):1368-75.
39. Balguid A, Mol A, van Vlimmeren M, Baaijens F, Bouten C. Hypoxia induces near-native mechanical properties in engineered heart valve tissue. *Circulation*. 2009 Jan;119(2):290-7.
40. Hahn MS, McHale MK, Wang E, Schmedlen RH, West JL. Physiologic pulsatile flow bioreactor conditioning of poly(ethylene glycol)-based tissue engineered vascular grafts. *Ann Biomed Eng*. 2007 Feb;35(2):190-200.
41. Hoerstrup SP, Zünd G, Sodian R, Schnell AM, Grünenfelder J, Turina MI. Tissue engineering of small caliber vascular grafts. *Eur J Cardiothorac Surg*. 2001 Jul;20(1):164-9.

42. Hildebrand D, Wu Z, Mayer JJ, Sacks M. Design and hydrodynamic evaluation of a novel pulsatile bioreactor for biologically active heart valves. *Ann Biomed Eng.* 2004 Aug;32(8):1039-49.
43. Ruel J, Lachance G. A New Bioreactor for the Development of Tissue-Engineered Heart Valves. *Ann Biomed Eng.* 2009 Jan;37(4):8.
44. Lefebvre XP, He S, Levine RA, Yoganathan AP. Systolic anterior motion of the mitral valve in hypertrophic cardiomyopathy: an in vitro pulsatile flow study. *J Heart Valve Dis.* 1995 Jul;4(4):422-38.
45. Jimenez JH, Soerensen DD, He Z, Ritchie J, Yoganathan AP. Mitral valve function and chordal force distribution using a flexible annulus model: an in vitro study. *Ann Biomed Eng.* 2005 May;33(5):557-66.
46. Dym CL, Little P. *Engineering design : a project-based introduction.* New York: John Wiley; 2000.
47. Jimenez JH, Soerensen DD, He Z, He S, Yoganathan AP. Effects of a saddle shaped annulus on mitral valve function and chordal force distribution: an in vitro study. *Ann Biomed Eng.* 2003 Nov;31(10):1171-81.
48. Jimenez JH, Soerensen DD, He Z, Ritchie J, Yoganathan AP. Effects of papillary muscle position on chordal force distribution: an in-vitro study. *J Heart Valve Dis.* 2005 May;14(3):295-302.
49. Clerin V, Gusic RJ, O'Brien J, Kirshbom PM, Myung RJ, Gaynor JW, et al. Mechanical environment, donor age, and presence of endothelium interact to modulate porcine artery viability ex vivo. *Ann Biomed Eng.* 2002;30(9):1117-27.
50. Lester W, Rosenthal A, Granton B, Gotlieb AI. Porcine mitral valve interstitial cells in culture. *Lab Invest.* 1988 Nov;59(5):710-9.
51. Lucke JN. Determination of the cardiac output of anaesthetised pigs using a dye dilution method. *Res Vet Sci.* 1976 Nov;21(3):364-5.
52. Grande-Allen K, Griffin B, Calabro A, Ratliff N, Cosgrove Dr, Vesely I. Myxomatous mitral valve chordae. II: Selective elevation of glycosaminoglycan content. *J Heart Valve Dis.* 2001 May;10(3):325-32; discussion 32-3.

53. Ikeda Y, Iwakiri S, Yoshimori T. Development and characterization of a novel host cell DNA assay using ultra-sensitive fluorescent nucleic acid stain "PicoGreen". *J Pharm Biomed Anal.* 2009 May;49(4):997-1002.
54. Blumenkrantz N, Asboe-Hansen G. New method for quantitative determination of uronic acids. *Anal Biochem.* 1973 Aug;54(2):484-9.
55. Stegemann H, Stalder K. Determination of hydroxyproline. *Clin Chim Acta.* 1967 Nov;18(2):267-73.
56. Stephens E, de Jonge N, McNeill M, Durst C, Grande-Allen K. Age-related changes in material behavior of porcine mitral and aortic valves and correlation to matrix composition. *Tissue Eng Part A.* 2010 Mar;16(3):867-78.
57. Stephens EH, Nguyen TC, Itoh A, Ingels NB, Miller DC, Grande-Allen KJ. The effects of mitral regurgitation alone are sufficient for leaflet remodeling. *Circulation.* 2008 Sep;118(14 Suppl):S243-9.
58. Engelmayer GC, Hildebrand DK, Sutherland FW, Mayer JE, Sacks MS. A novel bioreactor for the dynamic flexural stimulation of tissue engineered heart valve biomaterials. *Biomaterials.* 2003 Jun;24(14):2523-32.
59. Stephens EH, Chu CK, Grande-Allen KJ. Valve proteoglycan content and glycosaminoglycan fine structure are unique to microstructure, mechanical load and age: Relevance to an age-specific tissue-engineered heart valve. *Acta Biomater.* 2008 Sep;4(5):1148-60.
60. Kunzelman KS, Cochran RP. Stress/strain characteristics of porcine mitral valve tissue: parallel versus perpendicular collagen orientation. *J Card Surg.* 1992 Mar;7(1):71-8.
61. He Z, Sacks M, Bajens L, Wanant S, Shah P, Yoganathan A. Effects of papillary muscle position on in-vitro dynamic strain on the porcine mitral valve. *J Heart Valve Dis.* 2003 Jul;12(4):488-94.
62. SAMET P, BERNSTEIN W, LEVINE S. SIGNIFICANCE OF THE ATRIAL CONTRIBUTION TO VENTRICULAR FILLING. *Am J Cardiol.* 1965 Feb;15:195-202.

63. Udelson JE, Bacharach SL, Cannon RO, Bonow RO. Minimum left ventricular pressure during beta-adrenergic stimulation in human subjects. Evidence for elastic recoil and diastolic "suction" in the normal heart. *Circulation*. 1990 Oct;82(4):1174-82.
64. Grande-Allen K, Borowski A, Troughton R, Houghtaling P, Dipaola N, Moravec C, et al. Apparently normal mitral valves in patients with heart failure demonstrate biochemical and structural derangements: an extracellular matrix and echocardiographic study. *J Am Coll Cardiol*. 2005 Jan;45(1):54-61.
65. Mann DL, Bristow MR. Mechanisms and models in heart failure: the biomechanical model and beyond. *Circulation*. 2005 May;111(21):2837-49.
66. Hafizi S, Wharton J, Morgan K, Allen SP, Chester AH, Catravas JD, et al. Expression of functional angiotensin-converting enzyme and AT1 receptors in cultured human cardiac fibroblasts. *Circulation*. 1998 Dec;98(23):2553-9.
67. Blondheim DS, Jacobs LE, Kotler MN, Costacurta GA, Parry WR. Dilated cardiomyopathy with mitral regurgitation: decreased survival despite a low frequency of left ventricular thrombus. *Am Heart J*. 1991 Sep;122(3 Pt 1):763-71.
68. Carabello BA. The current therapy for mitral regurgitation. *J Am Coll Cardiol*. 2008 Jul;52(5):319-26.
69. Olsson AG, Istad H, Luurila O, Ose L, Stender S, Tuomilehto J, et al. Effects of rosuvastatin and atorvastatin compared over 52 weeks of treatment in patients with hypercholesterolemia. *Am Heart J*. 2002 Dec;144(6):1044-51.
70. Brown WV, Bays HE, Hassman DR, McKenney J, Chitra R, Hutchinson H, et al. Efficacy and safety of rosuvastatin compared with pravastatin and simvastatin in patients with hypercholesterolemia: a randomized, double-blind, 52-week trial. *Am Heart J*. 2002 Dec;144(6):1036-43.
71. Liao JK, Laufs U. Pleiotropic effects of statins. *Annu Rev Pharmacol Toxicol*. 2005;45:89-118.
72. Sola S, Mir MQ, Lerakis S, Tandon N, Khan BV. Atorvastatin improves left ventricular systolic function and serum markers of inflammation in nonischemic heart failure. *J Am Coll Cardiol*. 2006 Jan;47(2):332-7.

73. Horwich TB, MacLellan WR, Fonarow GC. Statin therapy is associated with improved survival in ischemic and non-ischemic heart failure. *J Am Coll Cardiol*. 2004 Feb;43(4):642-8.
74. Antonini-Canterin F, Hîrșu M, Popescu BA, Leiballi E, Piazza R, Pavan D, et al. Stage-related effect of statin treatment on the progression of aortic valve sclerosis and stenosis. *Am J Cardiol*. 2008 Sep;102(6):738-42.
75. Rupérez M, Rodrigues-Díez R, Blanco-Colio LM, Sánchez-López E, Rodríguez-Vita J, Esteban V, et al. HMG-CoA reductase inhibitors decrease angiotensin II-induced vascular fibrosis: role of RhoA/ROCK and MAPK pathways. *Hypertension*. 2007 Aug;50(2):377-83.
76. Enriquez-Sarano M, Akins CW, Vahanian A. Mitral regurgitation. *Lancet*. 2009 Apr;373(9672):1382-94.
77. Hernández-Perera O, Pérez-Sala D, Navarro-Antolín J, Sánchez-Pascuala R, Hernández G, Díaz C, et al. Effects of the 3-hydroxy-3-methylglutaryl-CoA reductase inhibitors, atorvastatin and simvastatin, on the expression of endothelin-1 and endothelial nitric oxide synthase in vascular endothelial cells. *J Clin Invest*. 1998 Jun;101(12):2711-9.
78. Benton JA, Kern HB, Leinwand LA, Mariner PD, Anseth KS. Statins block calcific nodule formation of valvular interstitial cells by inhibiting alpha-smooth muscle actin expression. *Arterioscler Thromb Vasc Biol*. 2009 Nov;29(11):1950-7.
79. Moravec CS, Schluchter MD, Paranandi L, Czerska B, Stewart RW, Rosenkranz E, et al. Inotropic effects of angiotensin II on human cardiac muscle in vitro. *Circulation*. 1990 Dec;82(6):1973-84.
80. Ramton AMSr. Stability of angiotensin II and bradykinin solutions investigated by capillary liquid chromatography. Oslo: The University of Oslo; 2006.
81. Jemal M, Ouyang Z, Powell ML. Direct-injection LC-MS-MS method for high-throughput simultaneous quantitation of simvastatin and simvastatin acid in human plasma. *J Pharm Biomed Anal*. 2000 Aug;23(2-3):323-40.
82. O'Brien KD, Shavelle DM, Caulfield MT, McDonald TO, Olin-Lewis K, Otto CM, et al. Association of angiotensin-converting enzyme with low-density lipoprotein in aortic valvular lesions and in human plasma. *Circulation*. 2002 Oct;106(17):2224-30.

83. Rabkin E, Aikawa M, Stone JR, Fukumoto Y, Libby P, Schoen FJ. Activated interstitial myofibroblasts express catabolic enzymes and mediate matrix remodeling in myxomatous heart valves. *Circulation*. 2001 Nov;104(21):2525-32.
84. Lee AA, Dillmann WH, McCulloch AD, Villarreal FJ. Angiotensin II stimulates the autocrine production of transforming growth factor-beta 1 in adult rat cardiac fibroblasts. *J Mol Cell Cardiol*. 1995 Oct;27(10):2347-57.
85. Jian B, Xu J, Connolly J, Savani RC, Narula N, Liang B, et al. Serotonin mechanisms in heart valve disease I: serotonin-induced up-regulation of transforming growth factor-beta1 via G-protein signal transduction in aortic valve interstitial cells. *Am J Pathol*. 2002 Dec;161(6):2111-21.
86. Booth BA, Uitto J. Collagen biosynthesis by human skin fibroblasts. III. The effects of ascorbic acid on procollagen production and prolyl hydroxylase activity. *Biochim Biophys Acta*. 1981 Jun;675(1):117-22.
87. Latif N, Sarathchandra P, Taylor PM, Antoniw J, Yacoub MH. Localization and pattern of expression of extracellular matrix components in human heart valves. *J Heart Valve Dis*. 2005 Mar;14(2):218-27.
88. Ferdous Z, Lazaro LD, Iozzo RV, Höök M, Grande-Allen KJ. Influence of cyclic strain and decorin deficiency on 3D cellularized collagen matrices. *Biomaterials*. 2008 Jun;29(18):2740-8.
89. Ferdous Z, Wei VM, Iozzo R, Höök M, Grande-Allen KJ. Decorin-transforming growth factor- interaction regulates matrix organization and mechanical characteristics of three-dimensional collagen matrices. *J Biol Chem*. 2007 Dec;282(49):35887-98.
90. Gupta V, Barzilla JE, Mendez JS, Stephens EH, Lee EL, Collard CD, et al. Abundance and location of proteoglycans and hyaluronan within normal and myxomatous mitral valves. *Cardiovasc Pathol*. 2009 Jul-Aug;18(4):191-7.
91. O'Tierney PF, Chattergoon NN, Louey S, Giraud GD, Thornburg KL. Atrial natriuretic peptide inhibits angiotensin II-stimulated proliferation in fetal cardiomyocytes. *J Physiol*. 2010 Aug;588(Pt 15):2879-89.
92. Cheng TH, Leung YM, Cheung CW, Chen CH, Chen YL, Wong KL. Propofol depresses angiotensin II-induced cell proliferation in rat cardiac fibroblasts. *Anesthesiology*. 2010 Jan;112(1):108-18.

93. Fujisaki H, Ito H, Hirata Y, Tanaka M, Hata M, Lin M, et al. Natriuretic peptides inhibit angiotensin II-induced proliferation of rat cardiac fibroblasts by blocking endothelin-1 gene expression. *J Clin Invest.* 1995 Aug;96(2):1059-65.
94. Tiede K, Stöter K, Petrik C, Chen WB, Ungefroren H, Kruse ML, et al. Angiotensin II AT(1)-receptor induces biglycan in neonatal cardiac fibroblasts via autocrine release of TGFbeta in vitro. *Cardiovasc Res.* 2003 Dec;60(3):538-46.
95. Brilla CG, Zhou G, Matsubara L, Weber KT. Collagen metabolism in cultured adult rat cardiac fibroblasts: response to angiotensin II and aldosterone. *J Mol Cell Cardiol.* 1994 Jul;26(7):809-20.
96. Tedder ME, Simionescu A, Chen J, Liao J, Simionescu DT. Assembly and Testing of Stem Cell-Seeded Layered Collagen Constructs for Heart Valve Tissue Engineering. *Tissue Eng Part A.* 2010 Sep.
97. Ruel J, Lachance G. A New Bioreactor for the Development of Tissue-Engineered Heart Valves. *Ann Biomed Eng.* 2009 Jan.
98. Warnock J, Konduri S, He Z, Yoganathan A. Design of a sterile organ culture system for the ex vivo study of aortic heart valves. *J Biomech Eng.* 2005 Oct;127(5):857-61.
99. Sucusky P, Padala M, Elhammali A, Balachandran K, Jo H, Yoganathan AP. Design of an ex vivo culture system to investigate the effects of shear stress on cardiovascular tissue. *J Biomech Eng.* 2008 Jun;130(3):035001.